UNIVERSITÀ DEGLI STUDI DI PARMA

Dottorato di ricerca in Scienze Chimiche

Ciclo XXVII (2012-2014)

Innovative mass spectrometry-based analytical strategies in proteomics

Coordinator: **Prof. R. Cammi**

Supervisor: **Prof. M. Careri**

Ph.D. Candidate:
Marco Milioli

2015

To my family

Science never solves a problem without creating ten more

George Bernard Shaw

INDEX

Chapter 3: Into the platelet derived microparticle membrane PTM-ome

Chapter 4: The targeted way

INTRODUCTION

The name "mass spectrometry" is a misnomer of sorts. The mass is not what is measured; instead, mass spectrometry determines the mass-to-charge (m/z) ratio or a property related to m/z. A mass spectrum is a plot of ion abundance *versus* m/z, although in many cases the x-axis is labelled 'mass' rather than m/z [1]. Basically, these few rows depicts mass spectrometry (MS) as a highly simple and intuitive tool for all kinds of users. However, for mass spectrometry users this discipline is still full of daily challenges. In particular, mass spectrometry was born in the 19th century during studies focused on gas discharges. Moreover, a key chapter in the mass spectrometry story was the introduction of electrospray ionization (ESI), which allowed the analysis of proteins, biomolecules and large organic molecules, impraticable with the previously conventional ionization techniques. Fenn and Tanaka were awarded with the Nobel Prize in the 2002 for ESI development. ESI is also the ion source used in this manuscript.

The ability of mass spectrometry to efficiently generate intact biomolecular ions in the gas phase has led to its widespread application in metabolomics, proteomics, biological imaging, biomarker discovery and clinical assays. Advances in MS technologies, high resolution liquid phase separations, and informatics/bioinformatics for large scale data analysis have made MS-based proteomics an indispensable research tool with the potential to broadly impact biology and laboratory medicine, attesting the importance of mass spectrometry in everyday life. As a result, high accuracy mass measurements coupled with improved sample preparation and multi-dimensional liquid separation methods are enabling to accomplish the task of determining structures of biomolecules and structure/function relationships at sensitivity levels adequate for proteins and peptides [2].

In addition, several data shown in this manuscript have been a part of a collaboration between the University of Parma and the University of Southern Denmark under the supervision of Prof. M. Careri and Prof. M. R. Larsen. (Project Title: "Quantitative comparison of proteome and PTM-ome of platelet derived microparicles using different agonist stimulations").

This PhD thesis has been divided in four main sections. In particular, the first section is composed by fourth chapters showing an overview of the main components of a mass spectrometer such as ion sources, mass analyzers, fragmentation techniques, bottom up strategies, focus on a mass spectrometer used for our proteomics experiments as first chapter. An introduction of mass spectrometry-based proteomics was therefore summarized in the first chapter. In the second chapter of the first section, key aspects of phosphoproteomics were discussed starting from enrichment-based protocols as TiO_2, IMAC (employed in our phospoproteins investigation), SAX, SCX and

ERLIC. Fragmentation strategies and mass spectra interpretation in phosphopeptide experiments were shown. Phosphoproteomics was discovered to be implicated in relevant signaling pathways. Phosphoproteins were reported in this thesis as known and mostly studied PTM (post-translational modifications) as well as glycoproteomics, described in the third chapter of the first section. Glycosylation is deeply implicated in several physiological and pathological process. In particular, protein sialylation, which was analyzed in a specific type of cells in this work, was found to be involved in cancer metastasis. Furthermore, typical enrichment methods such as HILIC (used in our glycoproteomics experiments) were reviewed. MS is a challenge in glycoproteomics due to the heterogenous structures of glycans linked to peptides; this aspect was specifically investigated in this study. In the fourth chapter main quantitative proteomics approaches were presented. Protein quantitation was found to be very useful in order to compare different biological condition, different time points especially in organ development, cancer progression and cell stimulation. In addition, iTRAQ-based proteomics was demonstrated to be widely used as quantitative tool in comparative analysis.

In the second section, an iTRAQ-based quantitative proteomics experiment was performed in order to compare the protein content of platelet derived microparticles (PMPs) obtained by differentially activated platelet samples. PMPs are a population of vesicles generated upon platelet activation by various stimuli known to be involved in several physiological and pathological processes. In particular, platelet activation was carried out using known physiological platelet stimulants as ADP, thrombin and collagen. Our proteomics analysis allowed the quantification of 3383 proteins, of which 428 membrane and 131 soluble proteins were found as significantly different in at least one of the analyzed conditions chosing thrombin, which is mostly used to generate PMPs in vitro, as control. Our findings suggest a biological link between agonist strength and proteins associated to platelet mediated processes such as activation and degranulation. These data may provide new insights for understanding PMPs biological role and formation. In the appendix, the datasets of the significantly changed membrane and soluble proteins after cluster analysis were reported.

Moreover, in the third section the same approach was used to study the phosphoproteome and the glycoproteome of PMPs. In addition, glycoproteome was divided into N-sialiome and N-glycoproteome by performing two different enrichment strategies as TiO_2 and HILIC. Phosphopeptides were separated into monophosphorylated and multiply phosphorylated peptides using SIMAC. Furthermore, our pipeline allowed the identitification of 1225 unique phosphopeptides assigned to 614 phosphoproteins and 1245 unique glycosylated peptides assigned to 533 unique glycoproteins. Our proteomics approach unveiled that glycosylation on focal adhesion related protein, in particular on integrins such as $\alpha_{IIb}\beta_3$, was directly related to the

physiological agonist strength used for platelet activation. Collectively, our MS-based quantitative study provided an overview of the PTM-ome of PMPs, which can be of high interest to reveal biological insights about platelet response to stimuli. In the fourth chapter, MS-based proteomics was applied to the analysis of allergenic proteins in wine samples: for this purpose, different sample treatment protocols for the liquid chromatography (LC)-ESI-MS/MS analysis of potential residuals of ovalbumin and caseins added to red wines were investigated. In particular, attention was paid to the simultaneous detection and quantitation of fining agent residues such as ovalbumin, α- and β-casein, in wine samples. The different sample treatment methods were compared in terms of protein recovery. Finally, the chosen method was applied for the analysis of 20 commercial red wine samples.

This PhD. thesis has shown that mass spectrometry has evolved to become an irreplaceable technique to investigate biological and food samples.

REFERENCES

[1] Glish GL, Vachet RW. The basics of mass spectrometry in the twenty-first century. Nat Rev Drug Discov. 2003;2:140-50.

[2] Careri M., Mangia A., Trends in analytical atomic and molecular mass spectrometry in biology and the life sciences. Special Issue of Anal Bioanal Chem "Advances in analytical mass spectrometry", Guest Editor: Careri M., 2011; 399:2585-95

1. MS-based proteomics

1. MASS SPECTROMETRY

Mass spectrometry (MS) has become the technology of choice in several disciplines including proteomics. MS allows the determination of accurate mass of ionized compounds. The analytes are ionized into an ion source, mainly electrospray and matrix assisted-ionization, accelerated and deflected by electric and magnetic fields which provide their mass to charge ratio (m/z). Every kind of mass spectrometer is formed by three different components: ion source, mass analyzer and detector. Ion sources are able to create gas phase-ions from the investigated compounds. Gas phase ions, which are separated by mass-to-charge ratio into the mass analyzer, are finally revealed by the detector and the output is then computationally processed enabling the generation of a mass spectrum based on the acquired signals.

Ion sources - The most commonly used ion sources in proteomics are matrix-assisted laser desorption ionization (MALDI) and electrospray ionization (ESI) [1]. Due to its ability of preserving the main structure of compounds without any possibility of fragmentation, MS has raised great interest as a tool for analyzing large bio-molecules such as proteins. In the MALDI ionization process, laser radiation hits the matrix, which is co-crystalized with samples. The matrix donates a charge to the analyte by inducing the sublimation of matrix-analytes sample [2]. Ions are mostly present as singly charged species. Sample preparation and not homogeneous deposition may affect the reproducibility, so that scarce precision is the main disadvantage of this technique; despite that, MALDI is very useful because it allows the analysis of compounds with very high MW (300.000 Da). In the ESI strategy, a strong electric field allows the evaporation of the sample solution into gas phase giving highly charged droplet. During this evaporation step, the analyte is transferred to the gas phase and attracted by opposite charges MS lenses [3]. ESI process is suitable for the analysis of large biomolecules giving multiply charged species. In addition, ESI can be coupled to separation and fractionation techniques such as liquid chromatography (LC). This configuration is very proficient in analyzing different sizes of molecules with various polarities in a complex sample mixture such as whole cell lysates.

Mass analyzers - Mass analyzer is responsible to separate gas phase ions according to their mass-to-charge ratio. Mass analyzer can be used in scanning and selecting mode; in scanning mode, it analyzes a determined mass-to-charge ratio range providing a "full scan" spectrum, whereas in selecting mode, it allows the isolation of a specific analyte, filtering it out from the rest of the ions. There are several types of mass analyzers: 1. quadrupole; 2. ion trap (linear or 3-dimensional); 3. time of flight (TOF); 4. Fourier transform-based mass analyzer (orbitrap). Those mass analyzers separate mass-to-charge ratio signals based on different mechanisms. Fourier transform-based mass

analyzers have the highest mass resolution (up to 1,000,000). However, quadrupoles and ion traps are the fastest and most sensitive analyzers, but their mass accuracy and resolution is quite low (~1,000).

1. Quadrupole mass analyzer is composed of four parallel metal rods in which a radio frequency voltage is applied between one pair of rods and the other, generating an oscillating electric field. Only ions of a certain m/z ratio have a stable oscillating trajectory and will reach the detector, the other ions have unstable trajectories and will hit the rods without any possibility of being detected.

2.Ion trap mass analyzers. Ion trap is similar to the quadrupole mass filter, but the ions are trapped before their ejection into a zone defined by a ring electrode (usually connected to the radio frequency potential) and two endcap electrodes (typically connected to direct current or auxiliary alternating current potentials).

3. Time of flight (TOF) mass analyzer that separates ions on the bases of their masses, by accelerating them in an electric field. TOF mass analyzer can be in a linear or in a reflectron mode, and this affects its mass resolution.

4. Fourier transform ion cyclotron resonance (FTICR) and orbitrap mass analyzer. These types of mass analyzers are the ones capable of achieving the highest resolutions. They resolve the m/z of the analytes based on their frequency of oscillation. The orbitrap is the most recent mass analyser developed.

Detectors - The ions separated by the mass analyzer are directed to the detector and converted into a detectable signal. There are different types of detectors, the choice of which depends on the experimental application. The role of detector is to produce signals from incident ions by producing secondary electrons and their amplification or inducing the present ones (produced by moving charges). The preferable properties of a detector are 1. high amplification 2. fast time response, 3. narrow distribution of responses, 4. same response for all masses, 5.low noise, 6. high collection efficiency, 7. large dynamic range, 8. long term stability, 9. long life, and 10. low cost. There are mainly two groups of ion detectors; a) point detectors: ions are temporary resolved and will be detected sequentially, b) array detectors: ions are spatially resolved and detected simultaneously [4].

Tandem MS/MS - The application of tandem mass spectrometry (MS/MS) is one of the most used approaches for peptide sequencing [5]. In a tandem mass spectrometry experiment, the combination of a couple of mass analyzers is exploited in a single instrument. Due to the recent advances in mass spectrometry and the integration of the collision cell, new instruments are now suitable to perform peptide fragmentation. The fragmentation of the precursor ions in the collision cell will provide the respective MS/MS spectra of the precursor ions, sequence information of the peptides, and the information about PTMs identification and localization. The role of the precursor ions fragmentation in MS/MS proteomics studies is crucial for improving identification in complex samples and investigating PTMs. Tandem mass spectrometry provides a good platform for structure elucidation, selective detection of target compound, reducing interferences.

Fragmentation techniques - To obtain information about the amino acid sequence of peptides from digested proteins using MS, the precursor peptide ion has to be fragmented into a combination of consecutively smaller fragment ions, each having lost one or more amino acids. Collision-induced dissociation (CID), which is the most common peptide fragmentation technique in MS, leads to N- and C-terminal fragment ions resulting from a cleavage of the C-N bond in the peptide backbone, yielding y- and b-ions [6,7]. The other relevant type of fragmentation methods in proteomics is electron transfer dissociation (ETD), which produces N- and C-terminal fragments of a backbone bond between the nitrogen and alpha carbon atom, generating c- and z-ions modifications, allowing their analysis and peptide sequencing [8]. The use of both ECD/ETD and CID increases the amount of information derived from peptide fragmentation (Fig. 1).
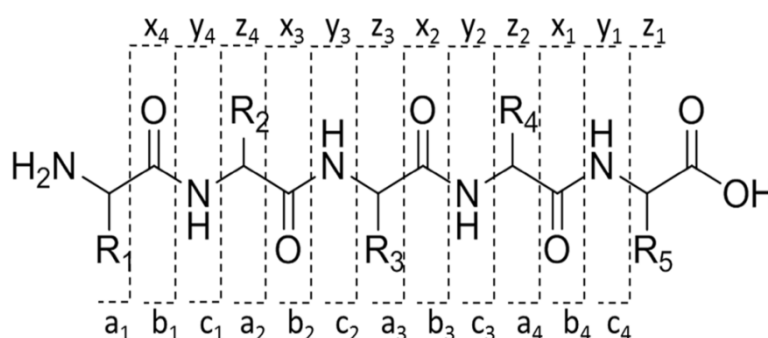

Fig. 1 Scheme of peptide fragmentation proposed (Adapted from I)

Applicability - Different approaches can be used for the analysis of protein sequencing by MS/MS. The first is a *bottom-up* protein sequencing, in which the fragmentation of peptides derived from protein digestion occurs, whereas the second is the *top-down* sequencing, which is based on the direct fragmentation of intact proteins. For complex samples and large scale analysis, the bottom-up approach is more adopted and it is well suited for the study of peptide modifications. This is because analysis of short peptides is simpler, as peptides are more efficiently separated by techniques such as liquid chromatography and they are detected with higher mass accuracy due to their smaller mass. The most common enzyme used for protein digestion is trypsin, which specifically cleaves on the C-terminal side of Lys and Arg, providing each peptide with at least a basic amino acid, which increases the possibility of positive ionization. Several methods are present for the interpretation of tandem MS data such as *de novo* sequencing, in which spectra are investigated using amino acid masses table. The second strategy is based on database searching/matching with bioinformatics search engines, in which experimental fragmentation spectra are compared with *in silico* predicted peptide fragmentation of known protein sequences. The algorithm recognizes all of the peptides in the database with the same mass as the precursor ion, and it makes a comparison between predicted and observed fragments matching the most probable sequence.

Bottom-up proteomics strategies - For MS analysis, proteins have to be pulled out efficiently from the biological sample to preserve the cellular environment of the system to be characterized. Residual enzymatic activities from proteases, phosphatases and other enzymes may result in unexpected and unnatural modifications of proteins and the cellular state. A common guideline for samples that do not require extensive tissue disruption is to dissolve and denature proteins by boiling them in a detergent such as SDS or chaotropic agents such as urea, thiourea and guanidinium hydrochloride. Detergent-based protocols can offer better recovery of membrane proteins compared to chaotropic salts- or organic solvents-based approaches. However, the majority of detergents are not utilizable in LC-MS and they have to be removed completely before analysis using purification techniques. Sample treatments mostly exploits steps to chemically protect cysteines by reduction, followed by irreversible alkylation, to cleave existing disulfide bonds and prevent them from forming again. Proteins are mainly cleaved into peptides by sequence-specific proteases such as trypsin. After digestion, peptide mixtures are cleaned, purified and concentrated, commonly in pipette-based devices filled with particular resins. A key challenge in shotgun proteomics remains the analysis and detection of peptides in very complex mixtures, such as whole cell lysates and tissues. To reach this goal, a combination of high performance liquid chromatography and high-resolution mass spectrometry with very high sequencing speed have

proven most successful. During chromatography, peptides are fractionated in a gradient of aqueous to organic solvent based on their interaction with the hydrophobic stationary phase. Efficiency of peptide separation on the column enhances with decreasing bead size and inner column diameter (normally 2 mm) as well as with increasing column length (usually up to 50 cm). Eluted peptides are ionized by electrospray at the tip of the column and transferred into the vacuum of the mass spectrometer for direct analysis (Fig. 2).
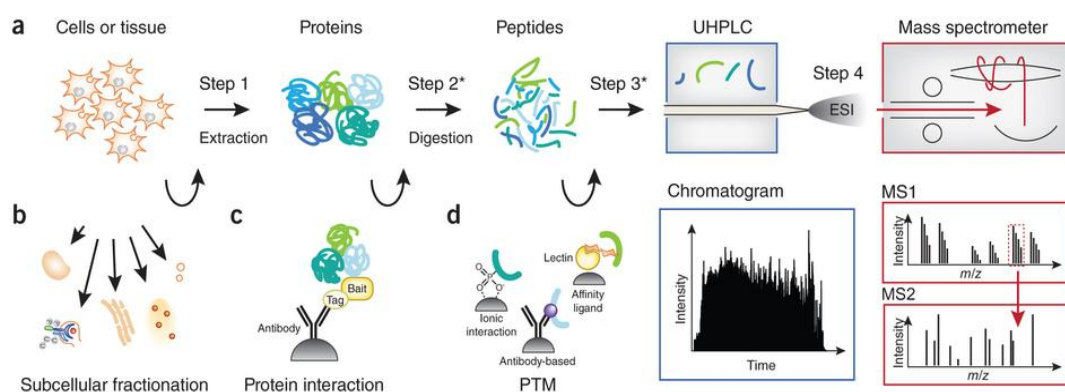
Fig. 2 Scheme of a typical shotgun proteomics experiment showing protein extraction, digestion, purification and LC-MS/MS analysis (Adapted from II)

Q-Exactive Plus mass spectrometer - The Q-Exactive Plus consists in four main components: 1. Ion source 2. Intermediate storage device (C-Trap) for short pulse injection 3. HCD collision cell 4. Orbitrap analyzer for Fourier transform mass analysis (Fig. 3). Basically, samples can be introduced into the ion source and gas phase ions are transferred into the C-Trap through four stages of differential pumping. In the C-Trap, ions are stored and their energy dampened using a bath gas (nitrogen). Ions are then injected through three further stages of differential pumping using a lens system (Z-lens) into the Orbitrap analyzer where mass spectra are acquired via image current detection. The HCD cell adds a higher energy collision induced dissociation capability to the instrument. After the ions fragmentation into the HCD cell, its voltages are ramped up and ions are moved back into the C-Trap from where they are injected into the Orbitrap. In particular, this instrument offers advanced ion transfer guides, enhanced mass resolution and high sensitivity providing a perfect platform for protein analysis [9].
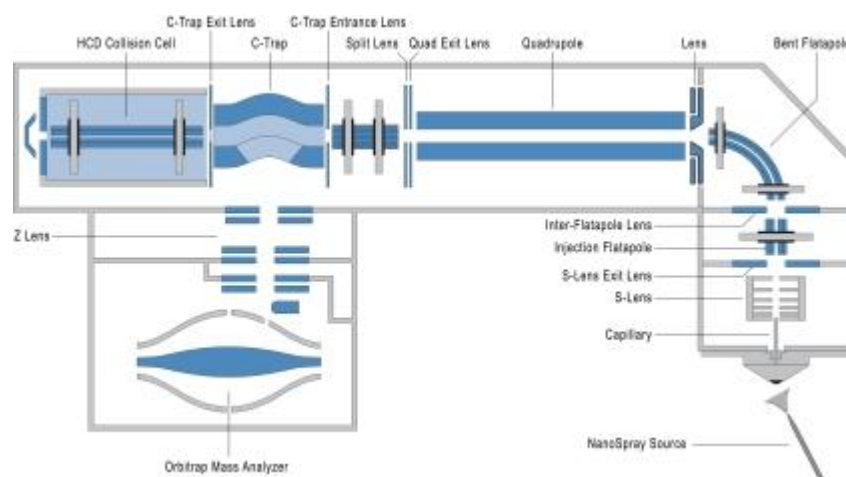
Fig. 3 Scheme of Q-Exactive plus mass spectrometer (Adapted from III)

PTMs - The term PTM describes alterations in the polypeptide chain through addition or removal of distinct chemical groups to amino acid residues, proteolytic processing of the protein termini, or the introduction of covalent crosslinks between domains of the protein. PTMs participate in several cellular processes such as the control of protein structure and integrity, regulation of metabolism and defense mechanism, cellular recognition events and morphology modifications. A wide range of modifications are known (more than 200) [10]. Phosphorylation and glycosylation are the most important and studied PTMs (Fig. 4). Correct localization and quantification are key elements in investigating a PTM. PTMs have been recognized by using Edman degradation, amino acid analysis, isotopic labeling, or immunochemistry but recently MS has been successfully applied in the PTM discovery. MS has shown many advantages for PTM investigation such as 1. high sensitivity; 2. capability to identify the site of PTM; 3. discovery of novel PTMs; 4. capability to pinpoint PTMs in complex mixtures of proteins; and 4. capability to quantify relative changes in PTM occupancy at distinct sites.
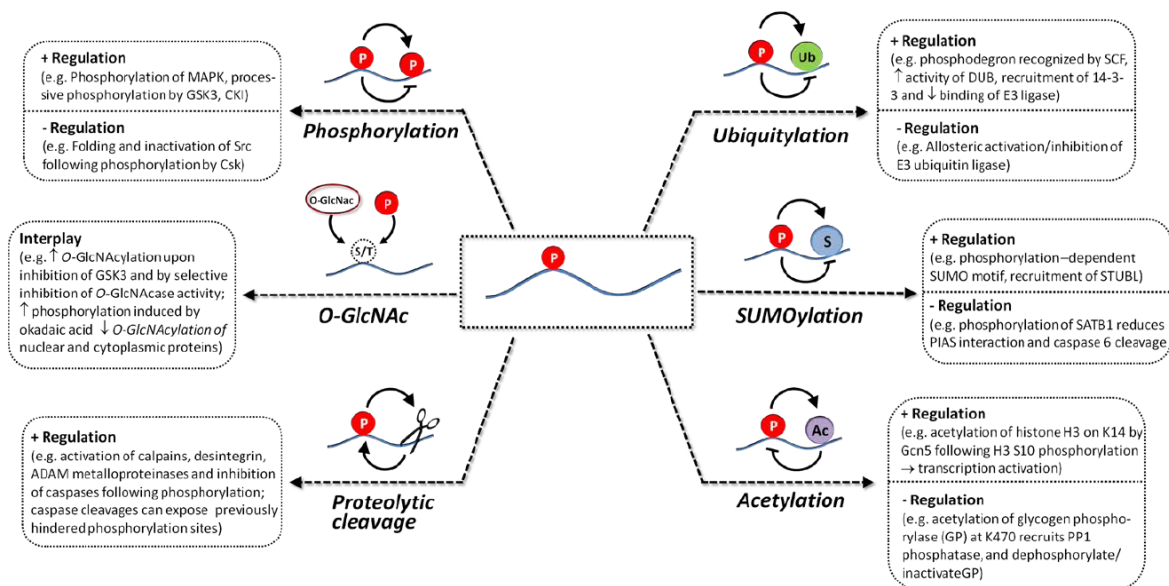
Fig. 4 Crosstalk between protein PTMs. Examples of positive and negative regulation of protein phosphorylation on different modifications ar highlighted in rounded rectangles. Interplay between phosphorylation and O-GlcNAcylation o specific Ser/Thr residues is also shown. (Adapted from IV).

2. PHOSPHOPROTEOMICS

Addition of a phosphate group to a protein may affect several protein properties such as folding, activity, capability to interact with other proteins, localization or degradation. Phosphorylation plays key roles in regulation of diverse cellular mechanism, including proliferation, differentiation, apoptosis, and cellular communication [11,12]. Alterations in reversible phosphorylation regulated by protein kinases/phosphatases may be the starting point of several pathological conditions including cancer, diabetes, chronic inflammatory and neurodegenerative diseases. Prior to MS, the principal techniques for identification of phosphorylation sites in proteins were ^{32}P labeling [13], sequencing by Edman degradation [14], and site-directed mutagenesis. Despite of being very sensitive and specific, ^{32}P labeling has common disadvantages such as the high levels of radioactivity involved, and a very low throughput. Cytotoxicity of the radioactive emission represents a limit of *in vitro* labeling. However, specificity of the phosphorylation is a challenge because of the promiscuous behavior in reactions occurring in an artificial, non-cellular context with abnormal concentrations of the reactions species [15]. Recently, substantial improvements in sample preparation, purification, enrichment, instrumentation, and bioinformatic tools, have facilitated the growth of the phosphoproteomics field allowing a more confident identification and quantification of phosphorylation sites.

Phosphopeptide enrichment – Immobilized metal ion affinity chromatography (IMAC) with different metal ions including Fe(III), Ga(III), Al(III), and Zr(III) has been employed for enriching phosphopeptides in large-scale proteomics experiments [16-18]. IMAC efficiency can be affected by several factors such as binding, washing, and elution [19]. In order to avoid the binding of non-phosphorylated peptides, acidic conditions for loading and washing were used, eluting phosphopeptides using alkaline conditions [20]. Titanium dioxide (TiO_2), which is also widely used for enriching phosphopeptides, offers high capacity and selectivity [21]. TiO_2 precolumns, TiO_2-based HPLC chips, TiO_2 tips were employed for purification of those peptides [22]. In order to increase the recovery of phosphopeptides, multiple step of incubation with the optimized amount of TiO_2 beads were also applied [23]. Diverse strategies for the elution of bound phosphopeptides including ammonium bicarbonate with 50 mM ammonium phosphate (pH 10.5), ammonia solution (pH 10.5-11), or step gradients from pH 8.5 (100 mM triethylammonium bicarbonate) to pH 11.5 (3% ammonium hydroxide) were also tested [24,25]. A composed method for the simultaneous enrichment of monophosphorylated and multiphosphorylated peptides exploiting sequentially elution of IMAC (SIMAC) and TiO_2 was also developed [26]. Monophosphorylated peptides are eluted during acidic condition from IMAC and multiphosphorylated peptides by basic elution, leading to an increased sensitivity of detection and reduced sample complexity. Recently, polymer-based metal ion affinity capture (PolyMAC) based on polyamidoamine dendrimers with titanium ions and aldehyde groups were also presented, showing high selectivity, fast chelation times, and high phosphopeptide recovery [27]. Fractionation of protein samples is still recommended even if the method exploits both IMAC and TiO_2 for enriching phosphopeptides. Many chromatographic methods such as SCX [28], SAX [29], HILIC [30], and ERLIC [31] were used in order to increase the identification of phosphorylation site (Fig. 5).

Chromatography
- SCX
- HILIC
- ERLIC
- RP-RP
- etc.

Enrichment
- IMAC
- MOAC
- HAP
- Aptamers

Quant. Strategy
- iTRAQ
- TMT
- SILAC
- Dimethylation
- Label free

nLC–MS/MS
- HCD
- CID
- ETD
- etc.

Data Analysis
- Sequest
- Mascot
- Max Quant
- Discoverer
- Spectrum Mill
- etc.
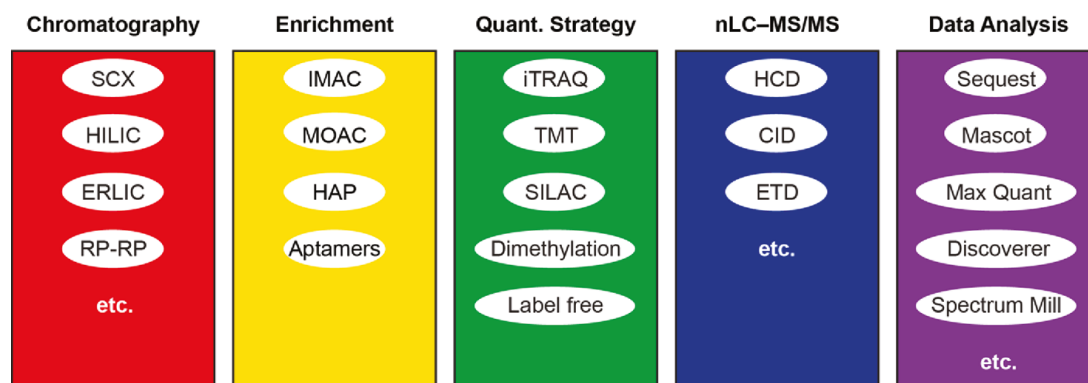
Fig. 5 Scheme of quantitative phosphoproteomics experiments including the choice of chromatography, enrichment, fragmentation type, data analysis tools (Adapted from V)

Phosphopeptide fragmentation – A challenge in phosphopeptide analysis is to obtain sequence information using the correct fragmentation strategy in MS/MS. The phosphoryl group on serine and threonine residues is a labile post-translational modification, especially in CID and is normally β-eliminated as phosphoric acid after fragmentation leading to an energetically favorable α,β-unsaturated carbonyl group on the peptide [32]. This β-elimination from serines and threonines leads to increase dehydroalanine and dehydro-2-aminobuturic acid, respectively, which highlights the presence of a phosphorylation site. The 69 Da loss characteristic of phosphoserine-to-dehydroalanine conversion can be used to discriminate β-eliminated phosphoserine and phosphothreonine. However, 98 Da neutral loss of phosphoric acid is usually the well-known fragmentation reaction. The neutral loss is related to several aspects including charge state (higher charged peptides often experience lower neutral loss), and the collision energy used during fragmentation step. The slowest fragmentation by using lower collision energy in ion trap instruments leads to generate more neutral loss of phosphoric acid compared to the faster high-energy CID fragmentation mainly used in "tandem-in-space" instruments (quadropoles, Q-TOFs, etc.) [33]. This mechanism can be linked to the slowest resonant excitation (i.e. ion traps) leading to fragmentation through the pathways of lowest energy such as neutral loss of phosphoric acid. MS-based phosphopeptide methods were then developed: 1. on triple quadropole instruments exploiting a neutral loss scanning method for the detection of the loss of H_3PO_4 by scanning the whole mass range with a fixed offset between precursor and fragment ion of 98 Da [34] and 2. on an ion trap instruments for serine and threonine phosphopeptide detection and sequencing by using the data-dependent neutral-loss-triggered MS/MS/MS (MS^3) scan [28]. In this case the loss of 98 Da from the precursor ion in the MS/MS spectrum causes the selection and fragmentation of the neutral loss ion. Due to an additional isolation and fragmentation step of the neutral loss, extra time spent and

loss of sensitivity are major disadvantages of this solution. Recently, MultiStage Activation (MSA), introduced on ion trap instruments, was shown able of removing the ion isolation round between the MS/MS and MS^3 scan [35]. It provides a collisional activation in the mass-to-charge region of the potential neutral loss ion, while the fragments are stored in the ion trap, obtaining a spectrum which includes product ions from both the precursor and the neutral loss. By not exploiting extra time and isolation step, MSA offers shorter duty cycles and higher sensitivity compared to MS^3. Negative ion mode is also applied for discovering phosphosites. In particular, m/z -79 related to PO_3^- loss can be found in CID fragmentation [36,37]. In this case, development of a precursor ion scanning method, using a single quadrupole with in-source CID or a triple quadropole instrument in which the entire precursor mass range is explored detecting only mass to charge -79, are required. Relevant advantages are high specificity and sensitivity, but it allows only limited peptide sequence information. Modern instrument, which are capable of fast polarity switching between negative and positive ion mode, can improve identification of phosphopeptides. In the case of tyrosine-phosphorylated peptides, the neutral loss of their phosphoryl group (a 80 Da loss of HPO_3) in CID is rarely observed [38]. An additional indicator of the presence of these species is the finding of a phosphotyrosine-specific immonium ion. This ion, which results from another fragmentation N- and C-terminally to the phosphotyrosine, has a mass of 216.043 Da [39].

3. GLYCOPROTEOMICS

A protein is glycosylated when its amide or alcohol group is covalently linked to a glycan. A N-linked glycan is bound to the amide group of asparagines residue in an amino acid sequence motif of Asn-X-Ser/Thr, where X represents all amino acids except proline [40]. An O-linked glycosylation links the glycan to the hydroxyl group of serine or threonine. Several studies have explained that glycosylation, which can be mainly found on membrane and secreted proteins, affects diverse biological functions such as protein folding, protein turnover, and immunity. Glycan analysis, or glycomics, is normally focused to explore only glycan modifications in glycoproteins. On the other hand, glycoproteomics aims to fully study glycoproteins and glycopeptides. Glycomics approaches investigate glycan structures, but lose the information on localization sites because of the release of glycan moieties from the glycosylated proteins. N-linked glycans (Fig. 6, 7) are normally removed by using an amidase, such as peptide N-glycosidase F (PNGase F), which releases linked sugars. Due to many forms of linkage structure, an universal enzyme is not available for cleaving O-linked glycans. This are normally cleaved by chemical methods including

hydrazinolysis [41] and alkaline β-elimination [42]. Removed glycans can be analyzed with or without derivatization by mass spectrometry or nuclear magnetic resonance (NMR).
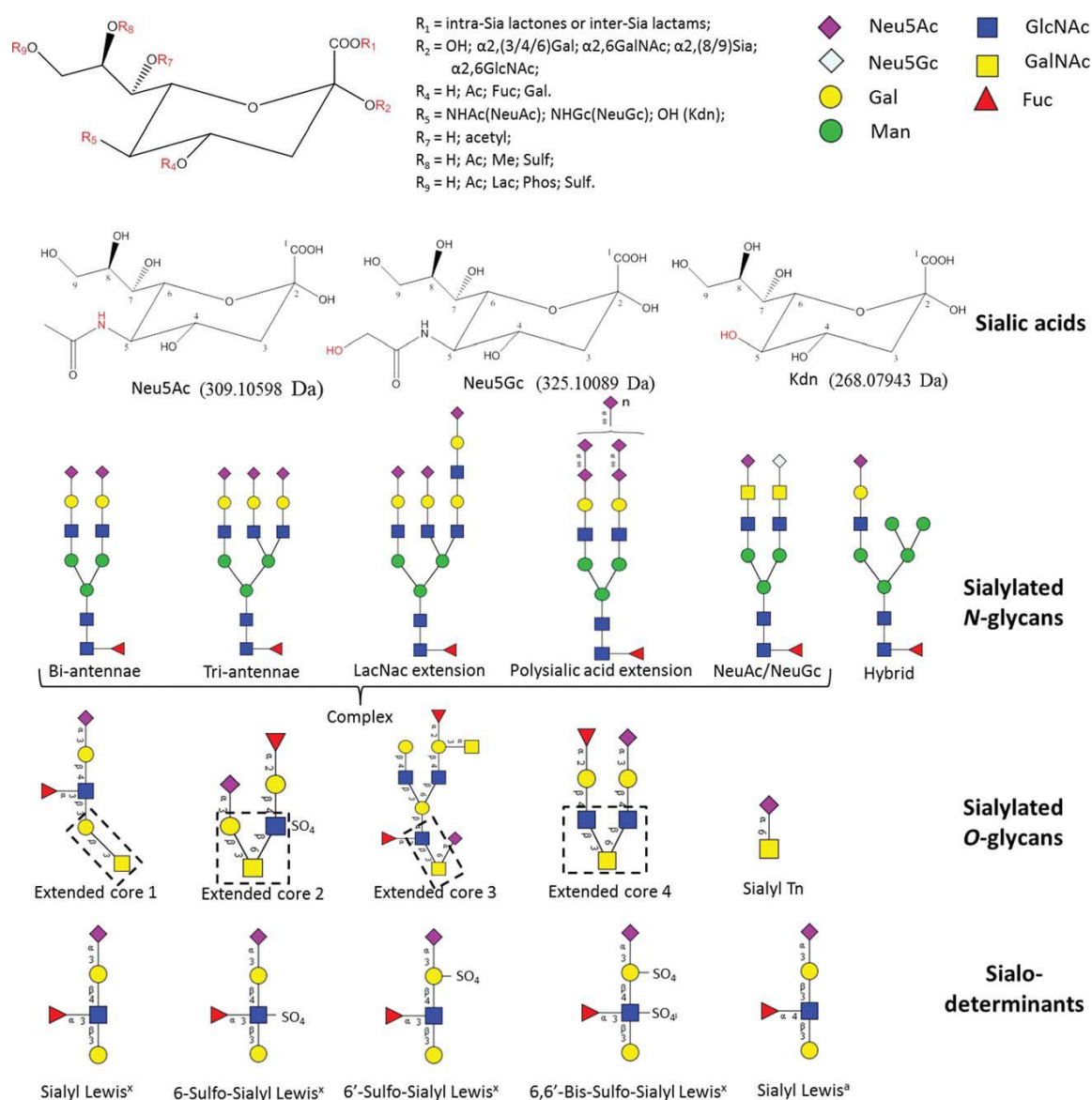

Fig. 6 Scheme of chemical structures and masses (in hydrolysed form) of the most common mammalian sialic acids (i.e. Neu5Ac, Neu5Gc and Kdn) and some examples of common mammalian sialylated N- and O-linked glycans and determinants. The core structures for the four main O-linked core types (core 1–4) have been highlighted (broken lines). (Adapted from VI)

Glycopeptides enrichment – Enrichment steps are typically used in order to improve sensitivity of glycosylation sites detection due to the low abundance of glycopeptides. However, a several number of enrichment strategies have been introduced such as including lectin affinity [43,44], hydrazide coupling [45], HILIC [46,47], and boronic acid affinity [48,49]. Due to its high specificity, lectin-based affinity strategy is the most widely performed. Lectins are carbohydrate binding proteins, which can specifically bind to sugar moieties. Many different lectins can be used for enriching glycopeptides such as concanavalin A and wheat germ agglutinin (WGA), which binds respectively to mannose glycan and N-acetylglucosamine. Ulex europaeus agglutinin (UEA) and aleuria aurantia lectin (AAL) are lectins specific for fucose recognition. Maackia amurensis leukoagglutinin (MAL) and hemoagglutinin (MAH) can be used for enriching N-Acetylneuraminic acid [50].

Glycopeptides MS analysis – There are two different strategies for the analysis of glycopeptides using mass spectrometry. The first method exploits the detection of the intact glycopeptides with glycan; using this approach the amino acid sequence and glycosylation site can be found by the spectrum interpretation. This method could be ideal because glycans and peptides are detected at the same time, but it has some limits in large scale analysis such as glycan heterogeneity which it makes spectral interpretation difficult for glycopeptides, and the sugar group makes peptide fragmentation challenging. In addition to widely used CID method for peptide fragmentation, new ion dissociation methods were implemented such as infrared multiphoton dissociation (IRMPD) [51], electon-capture dissociation (ECD) [52], and electron-transfer disassociation (ETD) [53] in order to obtain more fragment ions derived from peptide backbone with no loss of the glycans. Different complementary dissociation approaches can be employed to fully characterize glycopeptide and glycan. Glycan structure details can be generated by CID fragmentation, which normally cleaves the glycopeptide at glycosidic bonds. In order to create more peptide backbone fragments for improving peptide sequence identification, ETD fragmentation can also be used. Another common method is to cleave glycan by using an amidase. Deglycosylated peptides are then analyzed by shotgun proteomics. This protocol allows only the identification of peptides which were glycosylated. PNGase F, which removes N-linked glycans from glycoproteins by deaminating asparagine to aspartic acid, results in a 1 Da mass increase. Useful targeted database can be used to assist N-linked glycosylation sites due to the fixed motif sequence of Asn-X-Ser/Thr increasing sensitivity of glycopeptides identification and reducing the false discovery rate [54].
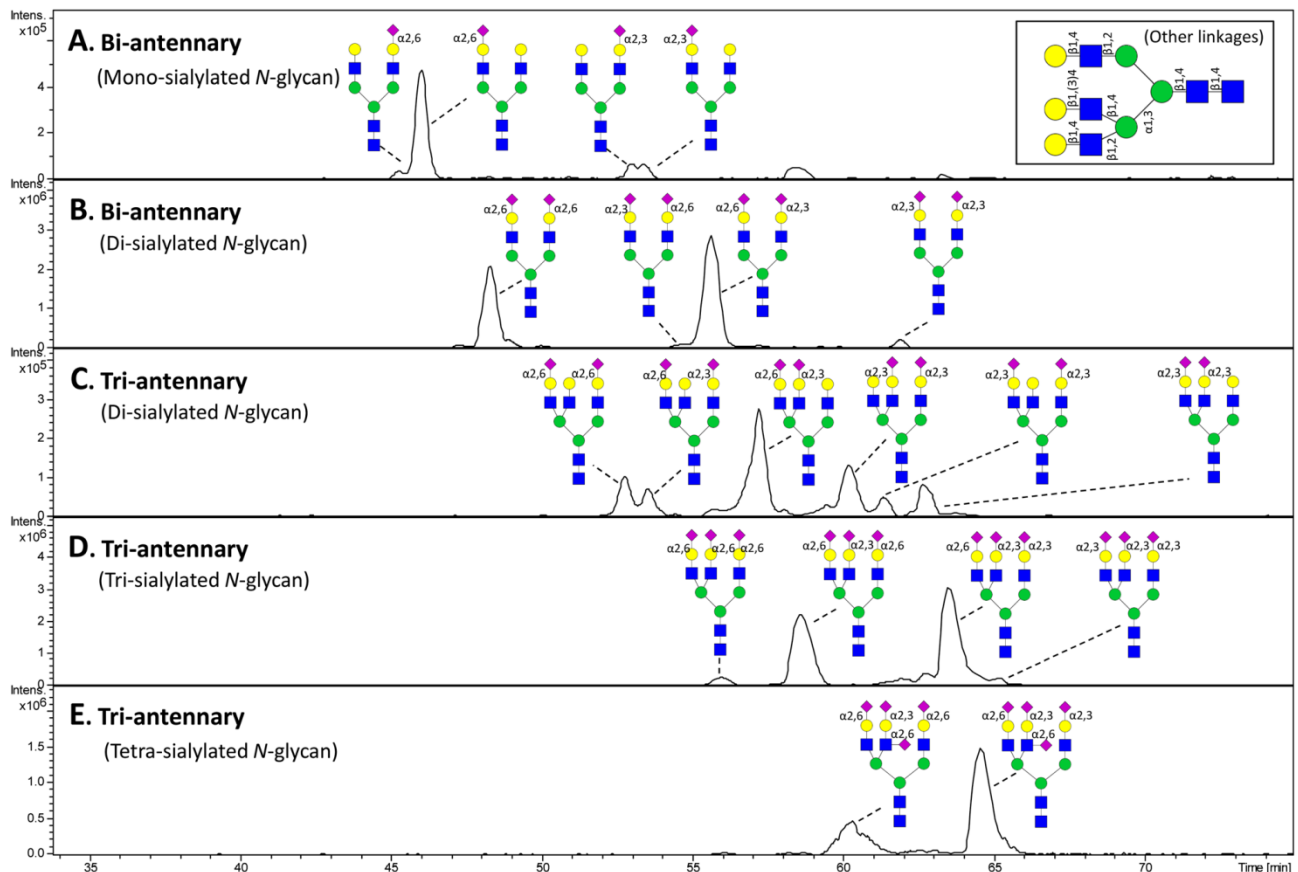
Fig. 7 Overview of LC separation and detection of sialylated N-linked glycans released from bovine fetuin by treating with PNGaseF. (Adapted from VII)

4. QUANTITATIVE PROTEOMICS

The most common proteomic approach, 2-DE, was the first tool introduced for protein quantification. Quantification can be easily performed by comparing the staining densities of proteins on different gels, obtaining a measure of relative quantification. However, 2-DE has still some limits such as limited resolution for a large number of proteins and entire proteomes, protein spots coappearance not allowing accurate quantification, incompatibility for hydrophobic and membrane proteins, incapability of detecting low abundant proteins. 2-DE based quantification can unveil only substantial differences and inaccurately estimates quantity changes. Due to these limitations, several strategies were developed to quantify proteomes based on the mass spectrometry data. MS-based quantitative data can be obtained by using stable isotope labeling or label-free strategies. The label-free strategy analyzes samples individually, comparing the MS ion intensity [55-57] of peptides or using the number of acquired spectra [58,59] matching a peptide/protein as an indicator for their respective amounts in a given sample. The isotope labeling

18

approach exploits the mixing of multiple samples of different biological conditions. The absolute or relative protein abundance can be achieved by measuring the intensities of different isotope coded peaks discriminated by MS. Furthermore, different methods can be mainly used to obtain quantitative information from mass spectrometry data such as determination of peptide precursor ion abundance in the MS^1 scan and measuring the isotope coded reporter ions (which reflect peptide quantity) in peptide fragmentation in the MS^2 scan (Fig. 9).
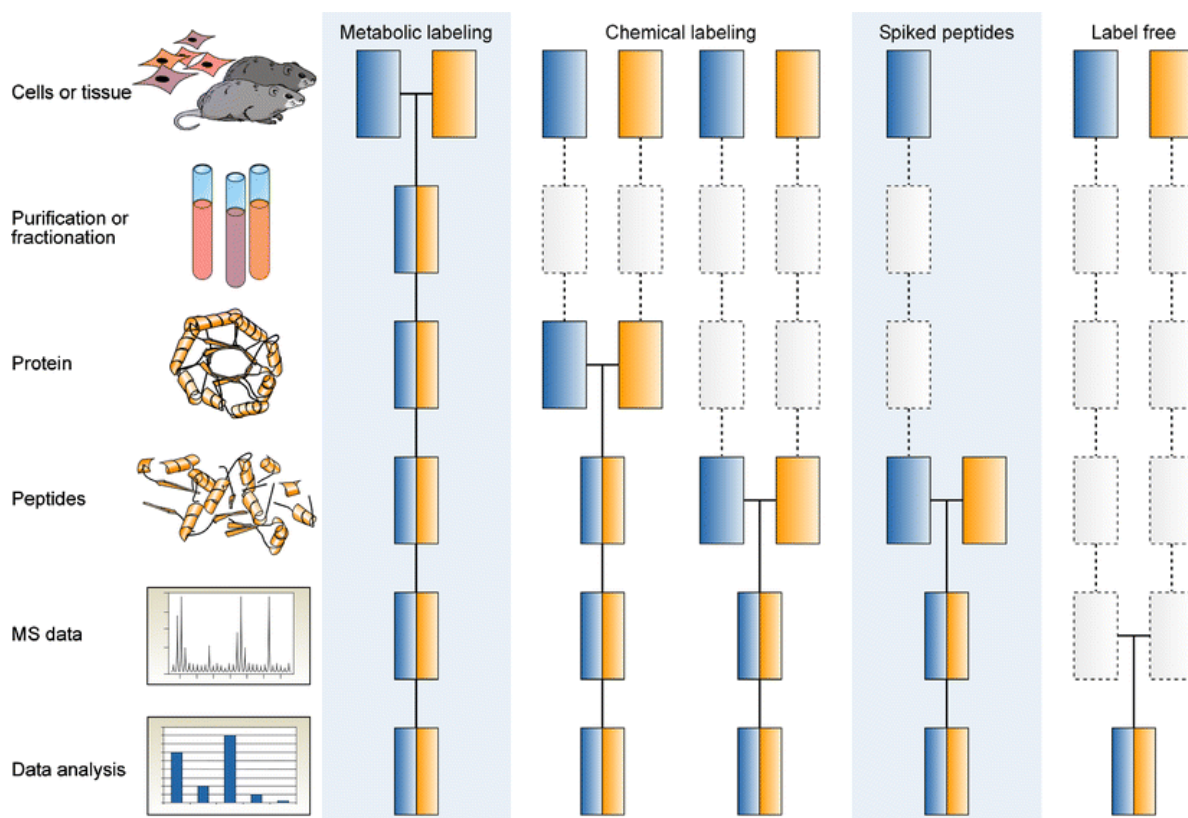
Fig. 8 Overview of quantitative strategies in proteomics showing metabolic labeling as SILAC, chemical labeling as iTRAQ, spiked peptides and label free. (Adapted from VIII)

MS^1 based strategies – MS-based quantification methods use chemical labeling in order to add isotope-coded reagents to reactive groups on the side chains of amino acids or to the peptide termini. Isotope coded affinity tag (ICAT) [60,61], which exploits the reaction between the thiol side chain of cysteine and the tag, was the first chemical labeling method developed. The ICAT reagent is formed by three units: a biotin affinity tag, a thiol specific reactive group, and the light or heavy isotopes included into a linker. In this case, cysteine residues are functionalized with an ICAT reagent containing either eight ^1H or eight ^2H atoms, and the protein mixture is then purified by avidin affinity chromatography. Protein mixture is then digested using trypsin and analyzed by

LC-MS. However, ICAT technique can greatly reduce the complexity of the peptide mixture, but it is not suitable for comprehensive large-scale analysis because it excludes all non-cysteine-containing peptides. Deuterium-based tag gives a shift in the retention time between light and heavy peptides in reversed phase (RP) chromatography, which complicates data analysis [62]. Other ICAT reagents include a ^{13}C-labeled linker instead of deuterium [63,64]. Another labeling strategy exploits the use of formaldehyde in order to introduce dimethyl labels to mark the N-terminus and amino group of Lys residues [65,66]. In this case, the light form of formaldehyde is combined with cyanoborohydride to include double chemical groups of CH_3 to each primary amine in a peptide. The medium and heavy labeled chemicals generate two sets of CHD_2 and $^{13}CD_3$, respectively, giving a 4 Da mass difference between three groups during MS analysis. However, dimethyl labeling presents a chromatographic retention time shift due to deuterium labeling as well as the ICAT method.

MS^2 based strategies - Isobaric tags for relative and absolute quantification (iTRAQ) [67] and tandem mass tags (TMT) [68] are formed by three main parts: a unique mass reporter, a cleavable linker as a mass balancer, and an amine-reactive group. All labeling group in a set of multiplex tags have the same total mass weight and these labeling parts increases co-elution of peptides during LC and co-isolation for fragmentation during MS/MS. Peptide mixtures obtained by different biological samples are then labeled with different types of the tag employing the reaction between the amine-reactive group of the tag with the peptide N-termini and lysine residues of the peptide. During MS/MS the linker is fragmented, releasing the mass reporter, where the intensity evidences the relative abundance of the original peptide. There are several types of isobaric labeling which are capable of analyzing multiple labeled pools of peptides such as TMT (up to 10 samples) and iTRAQ (up to 8 samples) [69] in a single analysis, reducing instrument time. This strategies have several advantages such as not increasing the complexity of the MS1 scan and not decreasing the precursor signal sensitivity due to the fact that all the tags lead to the same mass increase for each labeled peptide. Higher-energy collisional dissociation (HCD) is typically exploited in iTRAQ and TMT analysis [70]. HCD offers better MS^2 data quality because all the MS^2 data are acquired with high mass accuracy, but it uses more ions and time to obtain a MS^2 spectrum compared with that from normal CID. HCD-based experiment leads to lower proteome coverage. Isobaric tags has still also some restrictions, especially in the quantification accuracy [71,72], which is affected by co-fragmentation of co-eluting peptides with similar m/z. During the selection of the peptide precursor, MS isolates the precursor in a wide m/z window, which could contain target peptide and co-eluting peptides. In this case, the reporter ions are obtained from a mixture leading to an unaccurate

quantifications. However, modified strategies were introduced to overcome this limits, such as the introduction of an additional MS stage to increase ion selection specificity [73,74]. In this approach, the most intense MS^2 fragment ion is selected for the fragmentation, and the reporter ions generated during the second fragmentation are exploited for quantification. In order to not selecting non-labeled fragments in MS^2, Lys-C is introduced to digest proteins. After digestion, all of the peptides contains Lys and are labeled with isobaric tags at both termini.

Label Free – Isotope labeling has still drawbacks such as the cost of labeling reagents, labeling efficiency, difficult detection of low abundance peptides and limitation of sample number. In order to overcome these drawbacks, label free can be performed instead of labeling methods. There are two different methods for quantifying proteins in label free such as 1. spectral counting, which uses the frequency of peptide identification of a particular protein as a measure of relative abundance or 2. ion intensity, which exploits the MS chromatographic signal intensity of peptide peaks belonging to a particular protein [75]. In the first case, the frequency of peptide spectral matches of a specific protein can be related with the amount of a protein. This method can be used with low and moderate mass resolution (0.1-1 Da) MS data. Moreover, the spectral counting employs simpler normalization and statistical analysis compared to the ion intensity method. In order to calculate the protein abundance, protein abundance index (PAI), which is the number of identified peptides divided by the number of observable peptides for each protein, can be used [76]. PAI can be converted into emPAI (exponentially modified), which reflects protein abundance in a sample [77]. This parameter can be employed for searching databases and search engines such as Mascot and SEQUEST. However, peptides with different physicochemical properties can produce bias in MS results. In order to overcome this disadvantage, a modified spectral counting method, called the absolute protein expression (APEX), was proposed for measuring the protein concentration per cell, based on the number of observed peptides for a protein and the probability of MS detection of peptides [78]. The ion intensity method exploits the integration of all chromatographic peak areas of a given protein, the area under the curve (AUC) being related to the concentration of peptides in the range of 10 fmol to 100 pmol. This AUC-based protein quantification method, which is called "the ion count", is performed by measuring the ion abundance at specific retention times for given ionized peptides. It can be useful for quantification within the given detection limits of the instrument [79]. This strategy can be affected by several factors such as peptide co-elution, multiple signals for the same peptide due to technical or biological variation in retention time, MS speed and sensitivity, and background noise due to chemical interference. In order to improve these drawbacks, computational methods that include

mass accuracy and alignment of retention times of peptides across various sets, background noise, and peak abundance normalization have been developed [80]. A combination of both spectral counting- and ion intensity-based label-free quantification further improved accuracy [81].

CHAPTER FIGURE REFERENCES

[I] Zhang Y, Fonslow BR, Shan B, Baek MC, Yates JR 3rd. Protein Analysis by Shotgun/Bottom-up Proteomics. Chem Rev. 2013;113:2343-94

[II] Meissner F, Mann M. Quantitative shotgun proteomics: considerations for a high-quality workflow in immunology. Nat Immunol 2014;15:112-17.

[III] Michalski A, Damoc E, Hauschild JP, Lange O, Wieghaus A, Makarov A et al. Mass spectrometry-based proteomics using Q Exactive, a high-performance benchtop quadrupole Orbitrap mass spectrometer. Mol Cell Proteomics 2011;10:M111-011015.

[IV] Roux PP, Thibault P. The Coming of Age of Phosphoproteomics—from Large Data Sets to Inference of Protein Functions. Mol Cell Proteomics 2013;12:3453-64.

[V] Nilsson CL. Advances in quantitative phosphoproteomics. Anal Chem 2011;84:735-46.

[VI] Thaysen-Andersen M, Larsen MR, Packer NH, Palmisano G. Structural analysis of glycoprotein sialylation–Part I: pre-LC-MS analytical strategies. RSC Advances 2013;3:22683-705.

[VII] Palmisano G, Larsen MR, Packer NH, Thaysen-Andersen M. Structural analysis of glycoprotein sialylation–part II: LC-MS based detection. RSC Advances 2013;3:22706-26.

[VIII] Bantscheff M, Schirle M, Sweetman G, Rick J, Kuster B. Quantitative mass spectrometry in proteomics: a critical review. Anal Bioanal Chem 2007;389:1017-31.

CHAPTER REFERENCES

[1] El-Aneed A, Cohen A, Banoub J. Mass spectrometry, review of the basics: Electrospray, MALDI, and commonly used mass analyzers. Applied Spectroscopy Reviews 2009;44:210-30.

[2] Hillenkamp F, Karas M, Holtkamp D, Klüsener P. Energy deposition in ultraviolet laser desorption mass spectrometry of biomolecules. International journal of mass spectrometry and ion processes 1986:69;265-76.

[3] Fenn JB, Mann M, Meng CK, Wong SF, Whitehouse CM. Electrospray ionization for mass spectrometry of large biomolecules. Science 1989;246:64-71.

[4] Horning EC, Carroll DI, Dzidic I, Haegele KD, Horning MG, Stillwell RN. Liquid chromatography - mass spectrometer - computer analytical systems: A continuous-flow system based on atmospheric pressure ionization mass spectrometry. J Chromatogr A 1974;99:13-21.

[5] Hunt DF, Yates JR, Shabanowitz, J, Winston S, Hauer CR. Protein sequencing by tandem mass spectrometry. Proc Nat Acad Sci USA 1986; 83:6233-37.

[6] Roepstorff P, Fohlman J. Proposal for a common nomenclature for sequence ions in mass spectra of peptides. Biomed Mass Spectrom 1984;11:601.

[7] Biemann, K. Appendix 5. Nomenclature for peptide fragment ions (positive ions). Methods Enzymol 1990;193:886-7.

[8] Wiesner J, Premsler T, Sickmann A. Application of electron transfer dissociation (ETD) for the analysis of posttranslational modifications. Proteomics 2008;8:4466-83.

[9] Q-Exactive Plus User Manual, Thermo Fischer Scientific

[10] Temporini C, Calleri E, Massolini G, Caccialanza G. Integrated analytical strategies for the study of phosphorylation and glycosylation in proteins. Mass spectrom rev 2008;27:207-36.

[11] Blume-Jensen P, Hunter T. Oncogenic kinase signaling. Nature 2001;411:355-65.

[12] Hunter, T. Signaling-2000 and beyond. Cell 2000;100:113-27.

[13] MacDonald JA, Mackey AJ, Pearson WR, Haystead, TA. A strategy for the rapid identification of phosphorylation sites in the phosphoproteome. Mol Cell Proteomics 2002;1:314-22.

[14] Roepstorff P, Kristiansen K. The use of Edman degradation in peptide mixture analysis by mass spectrometry. Biomed Mass Spectrom 1974;1:231-36.

[15] Graham ME, Anggono V, Bache N, Larsen MR, Craft GE, Robinson PJ. The in vivo phosphorylation sites of rat brain dynamin I. J Biol Chem 2007;282:14695-707.

[16] Andersson L, Porath J. Isolation of phosphoproteins by immobilized metal (Fe3+) affinity chromatography. Anal Biochem. 1986;154:250-4.

[17] Posewitz MC, Tempst P. Immobilized gallium (III) affinity chromatography of phosphopeptides. Anal Chem 1999;71:2883-92.

[18] Michel H, Hunt DF, Shabanowitz, J, Bennett J. Tandem mass spectrometry reveals that three photosystem II proteins of spinach chloroplasts contain N-acetyl-O-phosphothreonine at their NH2 termini. J Bioll Chem 1988;263:1123-30.

[19] Trojer L, Stecher G, Feuerstein I, Lubbad S, Bonn GK. Characterisation and evaluation of metal-loaded iminodiacetic acid–silica of different porosity for the selective enrichment of phosphopeptides. J Chromatogr A 2005;1079:197-207.

[20] Haydon CE, Eyers PA, Aveline-Wolf LD, Resing KA, Maller JL, Ahn NG. Identification of novel phosphorylation sites on Xenopus laevis Aurora A and analysis of phosphopeptide enrichment by immobilized metal-affinity chromatography. Mol Cell Proteomics 2003;2:1055-67.

[21] Larsen MR, Thingholm TE, Jensen ON, Roepstorff P, Jørgensen TJ. Highly selective enrichment of phosphorylated peptides from peptide mixtures using titanium dioxide microcolumns. Mol Cell Proteomics 2005;4:873-886.

[22] Thingholm TE, Jørgensen TJ, Jensen ON, Larsen MR. Highly selective enrichment of phosphorylated peptides using titanium dioxide. Nat Prot 2006;1:1929-35.

[23] Li QR, Ning ZB, Tang JS, Nie S, Zeng R. Effect of peptide-to-TiO2 beads ratio on phosphopeptide enrichment selectivity. J Proteome Res 2009;8: 5375-81.

[24] Mazanek M, Mituloviæ G, Herzog F, Stingl C, Hutchins JR, Peters JM, Mechtler K. Titanium dioxide as a chemo-affinity solid phase in offline phosphopeptide chromatography prior to HPLC-MS/MS analysis. Nat Prot 2006;2:1059-69.

[25] Simon ES, Young M, Chan A, Bao ZQ, Andrews PC. Improved enrichment strategies for phosphorylated peptides on titanium dioxide using methyl esterification and pH gradient elution. Anal Biochem 2008;377:234-42.

[26] Thingholm TE, Jensen ON, Robinson PJ, Larsen MR. SIMAC (sequential elution from IMAC), a phosphoproteomics strategy for the rapid separation of monophosphorylated from multiply phosphorylated peptides. Mol Cell Proteomics 2008;7:661-671.

[27] Iliuk AB, Martin VA, Alicie BM, Geahlen RL, Tao WA. In-depth analyses of kinase-dependent tyrosine phosphoproteomes based on metal ion-functionalized soluble nanopolymers. Mol Cell Proteomics 2010;9:2162-72.

[28] Beausoleil SA, Jedrychowski M, Schwartz D, Elias JE, Villén J, Li J et al. Large-scale characterization of HeLa cell nuclear phosphoproteins. Proc Nat Acad Sci USA 2004;101:12130-5.

[29] Han G, Ye M, Zhou H, Jiang X, Feng S, Tian R et al. Large-scale phosphoproteome analysis of human liver tissue by enrichment and fractionation of phosphopeptides with strong anion exchange chromatography. Proteomics 2008;8:1346-61.

[30] Alpert A. Hydrophilic-interaction chromatography for the separation of peptides, nucleic acids and other polar compounds. J Chromatogr 1990;499:177-96.

[31] Alpert A. Electrostatic repulsion hydrophilic interaction chromatography for isocratic separation of charged solutes and selective isolation of phosphopeptides. Anal Chem 2008;80:62-76.

[32] Boersema PJ, Mohammed S, Heck AJ. Phosphopeptide fragmentation and analysis by mass spectrometry. J Mass Spectrom 2009;44:861-78.

[33] Lehmann WD, Krüger R, Salek M, Hung CW, Wolschin F, Weckwerth W. Neutral loss-based phosphopeptide recognition: a collection of caveats. J Proteome Res 2007;6:2866-73.

[34] Steen H, Küster B, Mann M. Quadrupole time-of-flight versus triple-quadrupole mass spectrometry for the determination of phosphopeptides by precursor ion scanning. J Mass Spectrom. 2001;36:782-90.

[35] Schroeder MJ, Shabanowitz J, Schwartz JC, Hunt DF, Coon JJ. A neutral loss activation method for improved phosphopeptide sequence analysis by quadrupole ion trap mass spectrometry. Anal Chem 2004;76:3590-98.

[36] Wilm M, Neubauer G, Mann M, Parent ion scans of unseparated peptide mixtures. Anal Chem 1996;68:527-33.

[37] Carr SA, Huddleston MJ, Annan RS. Selective detection and sequencing of phosphopeptides at the femtomole level by mass spectrometry. Anal Biochem 1996;239:180-92.

[38] Le Blanc JC, Hager JW, Ilisiu AM, Hunter C, Zhong F, Chu I. Unique scanning capabilities of a new hybrid linear ion trap mass spectrometer (Q TRAP) used for high sensitivity proteomics applications. Proteomics 2003;3:859-69.

[39] Steen H, Küster B, Fernandez M, Pandey A, Mann M. Detection of tyrosine phosphorylated peptides by precursor ion scanning quadrupole TOF mass spectrometry in positive ion mode. Anal Chem 2001;73:1440-8.

[40] Bause E. Structural requirements of N-glycosylation of proteins. Studies with proline peptides as conformational probes. Biochem. J. 1983;209:331-6.

[41] Gerken TA, Gupta R, Jentoft N. A novel approach for chemically deglycosylating O-linked glycoproteins. The deglycosylation of submaxillary and respiratory mucins. Biochemistry 1992;31:639-48.

[42] Greis KD, Hayes BK, Comer FI, Kirk M, Barnes S, Lowary TL, Hart GW. Selective detection and site-analysis of O-GlcNAc-modified glycopeptides by beta-elimination and tandem electrospray mass spectrometry. Anal Biochem 1996;234:38-48.

[43] Gonzalez-Begne M, Lu B, Liao L, Xu T, Bedi G, Melvin JE, Yates JR 3rd. Characterization of the human submandibular/sublingual saliva glycoproteome using lectin affinity chromatography coupled to multidimensional protein identification technology. J Proteome Res. 2011;10:5031-46.

[44] Mechref Y, Madera M, Novotny MV. Glycoprotein enrichment through lectin affinity techniques. Methods Mol Biol 2008;424:373-96.

[45] Zhang H, Li XJ, Martin DB, Aebersold R. Identification and quantification of N-linked glycoproteins using hydrazide chemistry, stable isotope labeling and mass spectrometry. Nat. Biotechnol 2003;21:660-6.

[46] Hagglund P, Bunkenborg J, Elortza F, Jensen ON, Roepstorff P. A new strategy for identification of N-glycosylated proteins and unambiguous assignment of their glycosylation sites using HILIC enrichment and partial deglycosylation. J Proteome Res. 2004;3:556-66.

[47] Yeh CH, Chen SH, Li DT, Lin HP, Huang HJ, Chang CI et al. Magnetic bead-based hydrophilic interaction liquid chromatography for glycopeptide enrichments. J Chromatogr A 2012; 1224:70-8.

[48] Monzo A, Bonn GK, Guttman A. Boronic acid–lectin affinity chromatography. 1. Simultaneous glycoprotein binding with selective or combined elution. Anal Bioanal Chem 2007;389:2097-102.

[49] Krisp C, Kubutat C, Kyas A, Steinstrasser L, Jacobsen F, Wolters D. Boric acid gel enrichment of glycosylated proteins in human wound fluids . J Proteomics 2011;74:502-9.

[50] Zhang Y, Fonslow BR, Shan B, Baek MC, Yates JR 3rd. Protein Analysis by Shotgun/Bottom-up Proteomics. Chem Rev. 2013;113:2343-94

[51] Hakansson K, Cooper HJ, Emmett MR, Costello CE, Marshall AG, Nilsson CL. Electron capture dissociation and infrared multiphoton dissociation MS/MS of an N-glycosylated tryptic peptic to yield complementary sequence information. Anal Chem. 2001;73:4530-6.

[52] Hakansson K, Chalmers MJ, Quinn JP, McFarland MA, Hendrickson CL, Marshall AG. Combined electron capture and infrared multiphoton dissociation for multistage MS/MS in a Fourier transform ion cyclotron resonance mass spectrometer. Anal Chem. 2003;75:3256-62.

[53] Catalina MI, Koeleman CA, Deelder AM, Wuhrer M. Electron transfer dissociation of N-glycopeptides: loss of the entire N-glycosylated asparagine side chain. Rapid Commun. Mass Spectrom. 2007;21:1053-61.

[54] Atwood JA 3rd, Sahoo SS, Alvarez-Manilla G, Weatherly DB, Kolli K, Orlando R, York WS. Simple modification of a protein database for mass spectral identification of N-linked glycopeptides. Rapid Commun. Mass Spectrom. 2005;19:3002-6.

[55] Bondarenko PV, Chelius D, Shaler TA. Identification and relative quantitation of protein mixtures by enzymatic digestion followed by capillary reversed-phase liquid chromatography-tandem mass spectrometry. Anal Chem. 2002;74:4741-9.

[56] Chelius D, Bondarenko PV. Quantitative profiling of proteins in complex mixtures using liquid chromatography and mass spectrometry. J Proteome Res. 2002;1:317-23.

[57] Wang W, Zhou H, Lin H, Roy S, Shaler TA, Hill LR et al. Quantification of proteins and metabolites by mass spectrometry without isotopic labeling or spiked standards. Anal. Chem. 2003;75:4818-26.

[58] Liu H, Sadygov RG, Yates JR 3rd, A model for random sampling and estimation of relative protein abundance in shotgun proteomics. Anal. Chem. 2004, 76,4193.

[59] Gilchrist A, Au CE, Hiding J, Bell AW, Fernandez-Rodriguez J, Lesimple S, Nagaya H et al. Quantitative proteomics analysis of the secretory pathway. Cell 2006;127:1265-81.

[60] Gygi SP, Rist B, Gerber SA, Turecek F, Gelb MH, Aebersold R. Quantitative analysis of complex protein mixtures using isotope-coded affinity tags. Nat. Biotechnol. 1999;17:994-9.

[61] Smolka MB, Zhou H, Purkayastha S, Aebersold R. Optimization of the isotope-coded affinity tag-labeling procedure for quantitative proteome analysis. Anal Biochem. 2001;297:25-31.

[62] Regnier FE, Riggs L, Zhang R, Xiong L, Liu P, Chakraborty A et al. Comparative proteomics based on stable isotope labeling and affinity selection. J Mass Spectrom. 2002;37:133-45.

[63] Oda, Y.; Owa, T.; Sato, T.; Boucher, B.; Daniels, S.; Yamanaka, H.; et al. Quantitative chemical proteomics for identifying candidate drug targets. Anal. Chem.2003;75:2159-65.

[64] Hansen KC, Schmitt-Ulms G, Chalkley RJ, Hirsch J, Baldwin MA, Burlingame AL. Mass spectrometric analysis of protein mixtures at low levels using cleavable 13C-isotope-coded affinity tag and multidimensional chromatography. Mol Cell Proteomics 2003;2:299-314.

[65] Hsu JL, Huang SY, Chow NH, Chen SH. Stable-isotope dimethyl labeling for quantitative proteomics. Anal. Chem. 2003;75:6843-52.

[66] Boersema PJ, Raijmakers R, Lemeer S, Mohammed S, Heck AJ. Multiplex peptide stable isotope dimethyl labeling for quantitative proteomics. Nat. Protoc. 2009;4:484-94.

[67] Ross PL, Huang YN, Marchese JN, Williamson B, Parker K, Hattan S et al. Multiplexed protein quantitation in Saccharomyces cerevisiae using amine-reactive isobaric tagging reagents. Mol. Cell. Proteomics 2004;3:1154-69.

[68] Thompson A, Schafer J, Kuhn K, Kienle S, Schwarz J, Schmidt G. Tandem mass tags: a novel quantification strategy for comparative analysis of complex protein mixtures by MS/MS. Anal. Chem. 2003;75:1895-904.

[69] Ow SY, Cardona T, Taton A, Magnuson A, Lindblad P, Stensjo K, Wright PC. Quantitative shotgun proteomics of enriched heterocysts from Nostoc sp. PCC 7120 using 8-plex isobaric peptide tags. J. Proteome Res 2008;7:1615-28.

[70] Kocher T, Pichler P, Schutzbier M, Stingl C, Kaul A, Teucher N, High precision quantitative proteomics using iTRAQ on an LTQ Orbitrap: a new mass spectrometric method combining the benefits of all. J. Proteome Res. 2009;8:4743-52.

[71] Ow SY, Salim M, Noirel J, Evans C, Rehman I, Wright PC. iTRAQ underestimation in simple and complex mixtures: "the good, the bad and the ugly". J. Proteome Res. 2009;8:5347-55.

[72] Karp NA, Huber W, Sadowski PG, Charles PD, Hester SV, Lilley KS. Addressing accuracy and precision issues in iTRAQ quantitation. Mol. Cell. Proteomics 2010;9:1885-97.

[73] Ting L, Rad R, Gygi SP, Haas W. MS3 eliminates ratio distortion in isobaric multiplexed quantitative proteomics. Nat. Methods 2011;8:937-40.

[74] Wenger CD, Lee MV, Hebert AS, McAlister GC, Phanstiel DH, Westphall MS, Coon JJ. Gas-phase purification enables accurate, multiplexed proteome quantification with isobaric tagging. Nat. Methods 2011;8:933-5.

[75] Bantscheff M, Schirle M, Sweetman G, Rick J, Kuster B. Quantitative mass spectrometry in proteomics: a critical review. Anal. Bioanal. Chem. 2007;389:1017-31.

[76] Cutillas PR, Vanhaesebroeck B. Quantitative profile of five murine core proteomes using label-free functional proteomics. Mol. Cell. Proteomics 2007;6:1560-73.

[77] Ishihama Y, Oda Y, Tabata T, Sato T, Nagasu T, Rappsilber J, Mann M. Exponentially modified protein abundance index (emPAI) for estimation of absolute protein amount in proteomics by the number of sequenced peptides per protein. Mol. Cell. Proteomics 2005;4:1265-72.

[78] Braisted JC, Kuntumalla S, Vogel C, Marcotte EM, Rodrigues AR, The APEX Quantitative Proteomics Tool: generating protein quantitation estimates from LC-MS/MS proteomics results. BMC Bioinf. 2008;9:529.

[79] Podwojski K, Eisenacher M, Kohl M, Turewicz M, Meyer HE, Rahnenfuhrer J, Stephan, C. Peek a peak: a glance at statistics for quantitative label-free proteomics. Expert Rev. Proteomics 2010;7:249-61.

[80] Listgarten J, Emili A. Statistical and computational methods for comparative proteomic profiling using liquid chromatography-tandem mass spectrometry. Mol. Cell. Proteomics 2005;4: 419-34.

[81] Griffin NM, Yu J, Long F, Oh P, Shore S, Li Y et al.. Label-free, normalized quantification of complex mass spectrometry data for proteomic analysis. Nat. Biotechnol. 2010;28:83-9.

2. Into the platelet derived microparticle proteome

ABSTRACT

Platelet-derived MPs (PMPs) are a heterogeneous population of microvesicles released from platelets upon activation and apoptosis. Different platelet activations may affect PMP protein profiles and roles in intercellular communication. Here, we performed a quantitative proteomics study to characterize the protein content of PMPs generated by four differentially activated platelet samples. We selected known physiological agonists for platelet activation such as ADP, thrombin and collagen. Thrombin, which is mostly used to generate PMPs *in vitro*, was set as control. Platelets were activated by following a known agonist strength scale in which ADP was the weakest activation and thrombin and collagen stimulations were the strongest ones. Our proteomics analysis allowed the quantification of 3383 proteins, of which 428 membrane and 131 soluble proteins were found as significantly different in at least one of the analyzed conditions. Activation with stronger agonists led to the enrichment of proteins related to platelet activation in PMPs. In addition, proteins involved in platelet degranulation and proteins from the electron transport chain were less abundant in PMPs when stronger activation was used. Collectively, our data describe the most detailed characterization of PMPs after platelet physiological activation. Furthermore, we show that PMP protein content is highly dependent on the type of physiological agonist involved in platelet stimulation.

1. INTRODUCTION

Platelet-derived microparticles, first identified by Wolf in 1967 as "platelet dust"[1], are submicrometer wide (0.1-1µm) membrane vesicles, resulting from the reorganization of the platelet membrane in response to several conditions such as platelet activation and apoptosis [2]. In addition to microparticles, platelets are known to generate exosomes from the exocytosis of multivesicular bodies (MVBs) and alpha-granules [3]. MPs from different cell types can be found in human plasma, and PMPs represent the major population of circulating MPs [4,5]. It was recently shown that megakaryocytes, progenitor of platelets, also release MPs [6]. PMPs are crucial for several physiological functions, including regulation of hemostasis, and their importance has been demonstrated by the bleeding disposition with a diminished formation of PMPs in patients with Castaman disease [7]. Changes in the MP population have been detected in many pathological disorders such as cardiovascular (e.g. coronary heart disease and acute coronary syndrome [8]), infections (e.g. sepsis [9]), autoimmune diseases (e.g. multiple sclerosis [10] and rheumatoid arthritis [11]) and cancer (e.g. gastric and breast cancer [12,13]). However, little information is available about the mechanism of MP formation, in particular regarding the biological process that controls the distribution of proteins between the MPs that are being released and the remaining

platelet [14]. During activation and apoptosis, signalling starts from specific receptors followed by common vesiculation processes such as Ca^{2+} entry, cytoskeletal remodelling, calpain/caspase activity and mitochondrial depolarization [15]. However, PMP formation-related events, such as phosphatidylserine (PS) exposure and precoagulant activity, are different in the case of activation and apoptosis. [16]. Platelet activation can be performed by both biochemical and mechanical stimuli. Disruption of the contact between platelet glycoprotein Ib beta chain and cytoskeleton is a key event in mechanical platelet stimulation [17] as well as integrin α_{IIb}-β_3 receptor activity in biochemical activation [18]. In particular, platelet activation promoted by biochemical agonist is also called sustained calcium induced platelet morphology (SCIP), due to the role of intracellular Ca^{2+} concentration for the MP generation.

Currently, the most common approaches to inspect MPs are flow cytometry, imaging by microscopy, ELISA and mass spectrometry-based proteomics [19]. The high mass accuracy, high speed and the possibility to perform high throughput analyses have made MS-based proteomics the preferred strategy to analyze complex protein mixtures [20-22]. This is also due to recent developments in the proteomics workflow, including sample preparation, liquid chromatography and bioinformatics tools for data processing. Recently, a shotgun proteomics approach was successfully applied to investigate the proteomic profile of ADP induced MPs [23]. By using gel filtration chromatography, Dean *et al.* separated PMPs into four size classes ranging from greater than 500 nm to approximately 100 nm and analyzed each fraction by LC-MS/MS showing that PMPs size classes contain proteins of different subcellular origin with mitochondrial proteins highly represented in the largest MPs and α-granule proteins predominating in the smallest fraction [24]. By using flow cytometry analysis, Pérez-Pujol *et al.* revealed that the PMP composition is highly dependent on the activation mechanism, showing substantial differences between thrombin receptor activated peptide (TRAP) and calcium ionophore-stimulated MPs [25]. Comparative proteomics was also performed to characterize PMPs generated in response to biomechanical (high shear) and biochemical (thrombin) stimulations, revealing 26 differentially expressed proteins, 21 of which were part of a common network related to cell assembly, organization and cell morphology [26]. Recently, Aatonen *et al.* studied the protein content of extracellular vesicles generated from differentially activated platelet samples using both physiological and not-physiological agonist leading the identification of only 267 proteins in the MPs [27]. However, a comprehensive and detailed comparison between PMPs protein content, composition and abundance after platelet stimulation with different physiological agonists has not yet been performed.

In this work, we used MS-based quantitative proteomics to investigate changes in protein content and abundance in PMPs generated by differentially activated platelets. Two studies investigated the physiological strength of different agonists for platelet activation; i.e. C5b-9 > thrombin and collagen > thrombin > collagen > ADP > epinephrine [27,28]. Therefore, we selected for platelet stimulation ADP, collagen, thrombin and collagen/thrombin, where thrombin was used as control due to its frequent use to generate MPs *in vitro* [26]. Moreover, thrombin plays a key role in myocardial infarction [29], ischemic stroke [30] and peripheral arterial vascular disease [31]. Understanding how platelet interacts with thrombin has raised great interest also for the development of anti-platelet drugs [32]. In addition, we tested the action of thrombin and collagen together in order to study a stronger platelet activation effect as compared to individual agonists [33]. Results highlighted a sustained increase of cytosolic Ca^{2+} concentration during thrombin and collagen co-stimulation [34]. After clustering and protein-protein interaction studies of the quantified proteins we found biological links between agonist strength and PMP composition such as platelet activation and degranulation proteins, energy related proteins important for the electron transport chain, glycolysis, pentose phosphate pathway and the proteasome.

2. MATERIALS AND METHODS

All chemicals were purchased from Sigma (St. Louis, MO, USA) unless otherwise stated. Ultrapure water was from an ELGA Purelab Ultra water system (Bucks, U.K.).

Platelet isolation and MP generation – PMPs were obtained from fresh apheresis platelets provided by three healthy volunteers in accordance with the guidelines of the University of Southern Denmark (SDU) and the Odense University Hospital (OUH). Platelets ($7x10^7$ cells) were isolated and activated to obtain PMPs as previously described with minor modifications [14,23]. Briefly, platelets were pelleted by centrifugation at 700 x g for 20 min at 20°C. The pellet was washed twice with 137 mmol l^{-1} NaCl, 2.6 mmol l^{-1} KCl, 1 mmol l^{-1} $MgCl_2$, 11.9 mmol l^{-1} $NaHCO_3$, 5.6 mmol l^{-1} D-Glucose and 1 mmol l^{-1} EDTA (Buffer A, pH = 6.5), and resuspended in buffer A without EDTA (Buffer B, pH = 6). Platelet suspensions were divided in four aliquots of 5 ml each and stimulated in presence of a) 10 μmol l^{-1} ADP [23], b) 1 U ml^{-1} thrombin, c) 20 μg ml^{-1} collagen and d) 1 U ml^{-1} thrombin plus 20 μg ml^{-1} collagen. The mixtures were incubated for 10 min at 37°C for ADP stimulation and for 30 min at 37°C for the other treatments. Finally, the activations were stopped by adding 2.5 mmol l^{-1} final concentration of EDTA or 2 mmol l^{-1} EGTA in the case of the ADP stimulation. Activated platelets were removed by centrifugation at 700 x g and 1,000 x g for 20 min at 20°C and the supernatants containing platelet derived MPs suspensions

were collected. Platelet derived MPs were then pelleted by centrifugation at 130,000 x g for 60 min at 4°C.

MP lysis and protein digestion – PMPs pellets were resuspended in ice-cold Na_2CO_3 buffer (0.1 M, pH = 11) containing protease inhibitor (Roche complete EDTA free, Meylan, France), PhosSTOP phosphatase inhibitor cocktail (Roche, Meylan, France) and 10 mM sodium pervanadate on ice. The suspension was tip probe sonicated for 20 sec (amplitude = 50%) twice and incubated on ice for 60 min to lyse the microparticles. The lysate was then centrifuged at 100,000 x g for 90 min at 4°C to enrich membrane proteins (pellet). The supernatant (soluble proteins) was concentrated using 10 kDa cutoff Amicon ultra centrifugal filters units (Millipore, Billerica, MA,USA), whereas membrane fraction was redissolved directly in urea 6 M, thiourea 2 M and tip probe sonicated for 20 sec (amplitude = 20%). Both fractions were reduced in 10 mM dithiothreitol (DTT) for 30 min and then alkylated in 20 mM iodoacetamide (IAA) for 30 min at room temperature in the dark. Lysyl Endopeptidase C (Wako, Osaka, Japan) was added for 3 h (1:100 w/w) and then the samples were diluted 8 times with 50 mM triethylammonia bicarbonate (TEAB, pH = 8). Trypsin was added at a ratio of 1:50 (w/w) and left overnight at 37°C to digest. Following incubation, samples were acidified with formic acid (2% final concentration) and centrifuged at 14,000 x g for 10 min to stop trypsin digestion and precipitate insoluble material such as lipids. The supernatant was purified using in-house packed staged tips with Poros R2 and Oligo R3 reversed phase resins (Applied Biosystem, Foster City, CA, USA). Briefly, a small plug of C_{18} material (3M Empore) was inserted in the constricted end of a P200 tips, followed by packing of the stage tip with the resin (resuspended in 100% ACN) by applying gentle air pressure. The acidified sample was loaded onto the micro-column, after equilibration of the column with 0.1% trifluoroacetic acid (TFA), washed twice with 0.1% TFA and peptides were eluted with 60% ACN/0.1% TFA. A small amount of purified peptides (6 µl) was dried down and subjected to amino acid composition analysis to determine the concentration, while the remaining sample was lyophilized prior to iTRAQ labeling.

iTRAQ labeling and peptide fractionation – Equal amount of peptides from each condition were iTRAQ 4-plex™ labeled according to manufacturer's instructions (Applied Biosystem, Foster City, CA, USA). Labeled peptides were combined in 1:1:1:1 proportion based on the quantification achieved from the amino acid composition analysis and MALDI-MS/MS analysis (Bruker Daltonics, Billerica, CA, USA, in lift mode). The samples were labeled as follow: ADP, iTRAQ-114; thrombin (control), iTRAQ-115; collagen, iTRAQ-116; thrombin plus collagen, iTRAQ-117. All peptide samples were fractionated by using hydrophilic interaction chromatography (HILIC) on

an Agilent 1200 HPLC system [35]. Samples were loaded onto a 450 μm OD x 320 μm ID x 17 cm micro-capillary column packed with TSK-gel Amide 80 (3 μm, Tosoh Bioscience, Japan). Peptides were resuspended in solvent B (90% ACN/0.1% TFA) and eluted over a gradient of 100% to 60% solvent B (solvent A = 0.1% TFA) over 35 min, followed by 60% to 0% over 7 min at a flow rate of 6 μl/min. HILIC fractions were combined into eleven samples and lyophilized.

Reversed-phase nanoLC-ESI-MS/MS – Dried fractions were resuspended in 0.1% formic acid (FA) (solvent A) and loaded onto an Ultimate 3000 RSLC nanoLC system (Thermo Fisher Scientific) coupled to a Q-Exactive Plus mass spectrometer (Thermo Fisher Scientific, Bremen, Germany). The peptides were loaded onto a two-column setup employing an Acclaim PepMap 100 precolumn (100 μm x 2 cm, C_{18}, 5 μm, 100A, nanoViper) and a 20 cm fused silica capillary column (75 μm ID) packed with Reprosil – Pur C_{18} AQ 3 μm reversed-phase material (Dr. Maisch, Ammerbuch-Entrigen, Germany). The HPLC gradient was 1-35% solvent B (95% ACN/0.1% FA) in 60 min at a flow-rate of 250 nl/min. The mass spectrometer was operated in positive mode with a data dependent acquisition method (Top N, N = 12). A falcon tube with 5% v/v ammonia solution was placed below the needle tip of the chromatographic column, located next to the orifice of the mass spectrometer to decrease the charge state of the ions and increase the HCD fragmentation [36]. Briefly, MS scans (400-1400 m/z) were recorded at a resolution of 70,000. The automatic gain control (AGC) target for MS acquisitions was set to 1×10^{6} with a maximum ion injection time of 120 msec. Microscans were set to 1 for both the MS and MS/MS. Dynamic exclusion was set to 15 sec. Singly charged species were rejected. Peptides of two and higher charges were fragmented into the HCD collision cell with a normalized collision energy (NCE) set to 32. Subsequent MS/MS scans with a target value of 2×10^{4} ions were collected with a maximum injection time of 100 msec and a resolution of 17,500. All MS and MS/MS spectra were acquired in profile mode.

Data Analysis – The Proteome Discoverer software (v.1.4.0.288, Thermo Fisher Scientific) was used to perform database searching and peptide/protein relative quantification. MS/MS spectra were searched using MASCOT (v2.3, Matrix Science, London, UK) and Sequest HT (Thermo Fisher Scientific) as database searching engines with a Swiss-Prot v.3.53 human database (20, 243 entries) and the Uniprot human reference database (updated April 2014). Methionine oxidation, peptide N-terminal iTRAQ labeling and lysine iTRAQ labeling were set as variable modifications, while cysteine carbamidomethylation was set as fixed modification. Precursor mass tolerance was set to 10 ppm and MS/MS tolerance to 0.05 Da. Trypsin was selected as digestion enzyme, and up to two missed cleavages were allowed. Data were filtered to a 1% false discovery rate using Proteome Discoverer's Percolator function [37]. Protein iTRAQ ratios were log2 transformed and

normalized for the average to compensate for unequal amounts of digested and labeled protein samples in the sample mixture. One tail heteroscedastic Student's t-test (p-value < 5%) was used to assess statistical differences in protein amount between conditions. Annotation and classification of the identified proteins were performed by using Protein Center (Thermo Fischer Scientific). Clustering analysis was performed by using Perseus (v. 1.5.0.15, tool of MaxQuant package). Literature mining of protein-protein interactions was performed using STRING (v. 9.1) in action view at high settings (0.7) [38]. Membrane protein which did not have clear sequence signatures that characterize them as membrane proteins, were subjected to KohGPI analysis (http://gpi.unibe.ch/) in order to identify possible GPI-anchor signals.

3. RESULTS

In this study we investigated the composition of PMPs by pursuing a comprehensive comparative study of the proteome of such particles produced by differentially activated platelets from healthy subjects. Thrombin, which is mostly used to generate PMPs *in vitro*, was chosen as control [26]. Activation was also performed by using ADP, collagen and thrombin plus collagen, as all are known to play a role in nature as physiological agonists. PMPs were first generated from platelet, lysed, and partitioned into membrane and soluble fractions by treatment with Na_2CO_3, which linearizes membranes and releases loosely bound proteins from membrane [39] and subsequent ultracentrafugation. After trypsin digestion and purification, peptides from each condition were labeled with iTRAQ and merged to reduce variability of the analysis for quantitative proteomics. Samples were mixed, fractionated by hydrophilic interaction liquid chromatography (HILIC) and analyzed by nano liquid chromatography (nLC)-MS/MS (Fig. 1). All experiments were performed in biological triplicates.
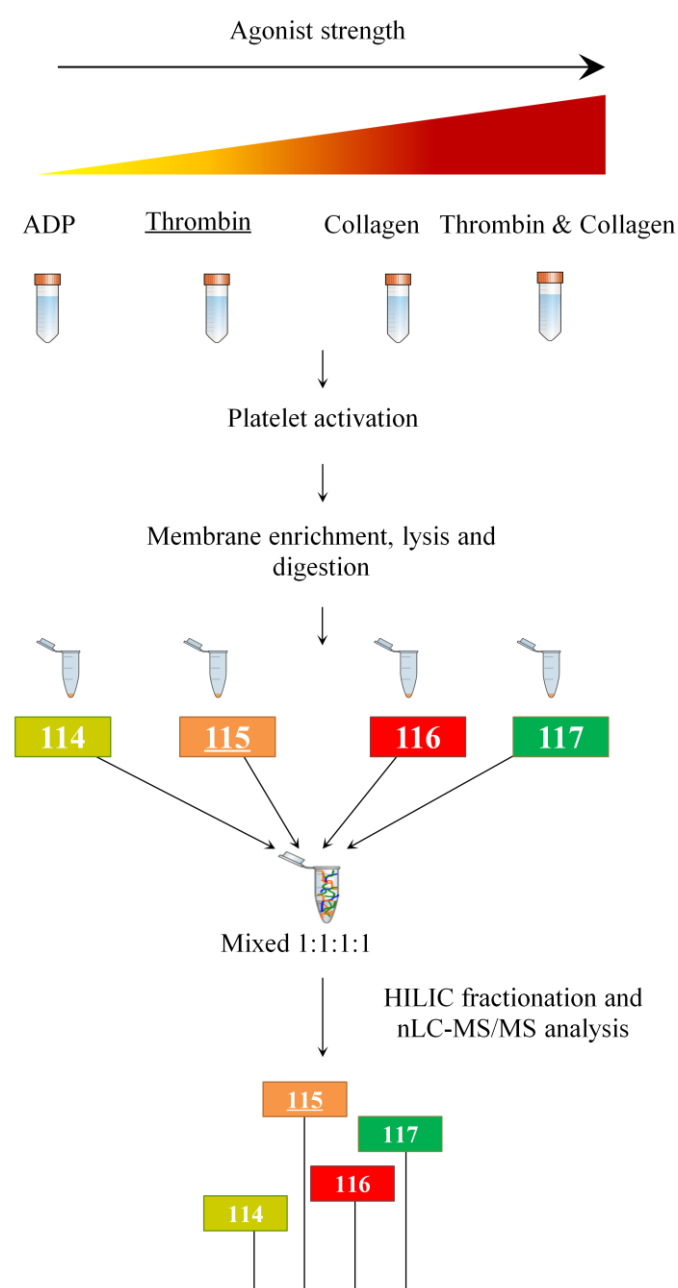
Fig. 1 Experimental scheme for the quantitative analysis of platelet-derived microparticles proteome by using different agonist stimulations.

Protein identification and comparison analysis − Using the nLC-MS/MS analysis we identified a total of 2380 proteins in the membrane fraction, 1476 of which showed a transmembrane (TM) domain or a signal peptide characteristic for membrane proteins. A total of 1109 proteins were found in all three biological replicates (46.6%). On the other hand, 2399 proteins were identified in the soluble fraction, 1109 (46.2%) of which were found in all three biological replicates. Such data evidenced the high reproducibility between biological replicates. After removing redundancy, a total of 3383 proteins were identified in our study, 984 were found

only in the membrane fraction and 1003 were found only in the soluble fraction (Fig. 2A). The large number of proteins identified in both fractions indicated that the purification of the membrane fraction from the soluble has still its limitations most likely due to large protein complex formation. However, by determining the presence of TM domains and signal peptides we could determine which proteins contain amino acid sequence signature that characterize them as membrane associated with high confidence. In addition, by using KohGPI on proteins which did not show clear sequence signatures that characterize them as membrane proteins (904 proteins), we found 5 proteinshaving both C- and N-terminal signal sequences (GPI-anchored). By performing iTRAQ-based relative quantification, we determined the ratio of the identified proteins in PMPs in the analyzed conditions. In the membrane fraction a total of 350 proteins (243 of which showed TM domain or signal peptide) were found to be significantly different in terms of relative abundance in the ADP induced MPs as compared to the control, which was thrombin stimulation. One hundred and sixty eight proteins (113 of which showed a TM domain or a signal peptide) were significantly different in collagen induced activation and 147 proteins (98 of which showed a TM domain or a signal peptide) in thrombin and collagen co-stimulated MPs (Fig. 2B). For the soluble fraction, 40 proteins were identified to be significantly different in ADP stimulated microparticles, 97 proteins in collagen induced activation and 49 proteins in thrombin and collagen co-stimulated MPs (Fig. 2C).
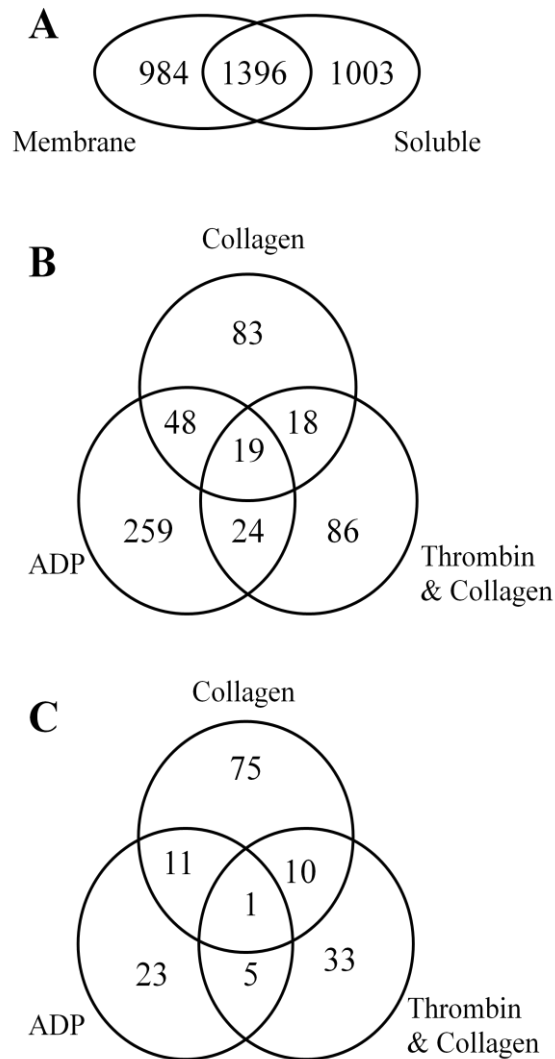
Fig. 2 A) Venn diagrams showing the overlaps between all of the identified proteins in this study. B) Overlaps between significantly different proteins in the membrane and C) the soluble fractions.

Gene ontology analysis of proteins with significantly different abundance between treatments – We next characterized the gene ontology of differentially expressed proteins during different stimulations. Regarding the membrane fractions (especially in ADP induced MPs), biological processes analysis showed that most of the proteins detected were involved in cell communication, metabolic process, response to stimulus and transport (Fig. 3A). Molecular functions analysis underlined that the majority of proteins played roles in catalytic activity and protein binding (Fig. 3B). Regarding all of the soluble fractions (especially in collagen induced MPs), biological processes analysis highlighted that proteins were mostly implicated in cell communication, cell organization and biogenesis, metabolic process, regulation of biological processes, development and response to stimulus (Fig. 3C). Molecular functions analysis displayed

(especially in collagen induced MPs) that proteins are involved in catalytic activity and protein binding (Fig. 3D).
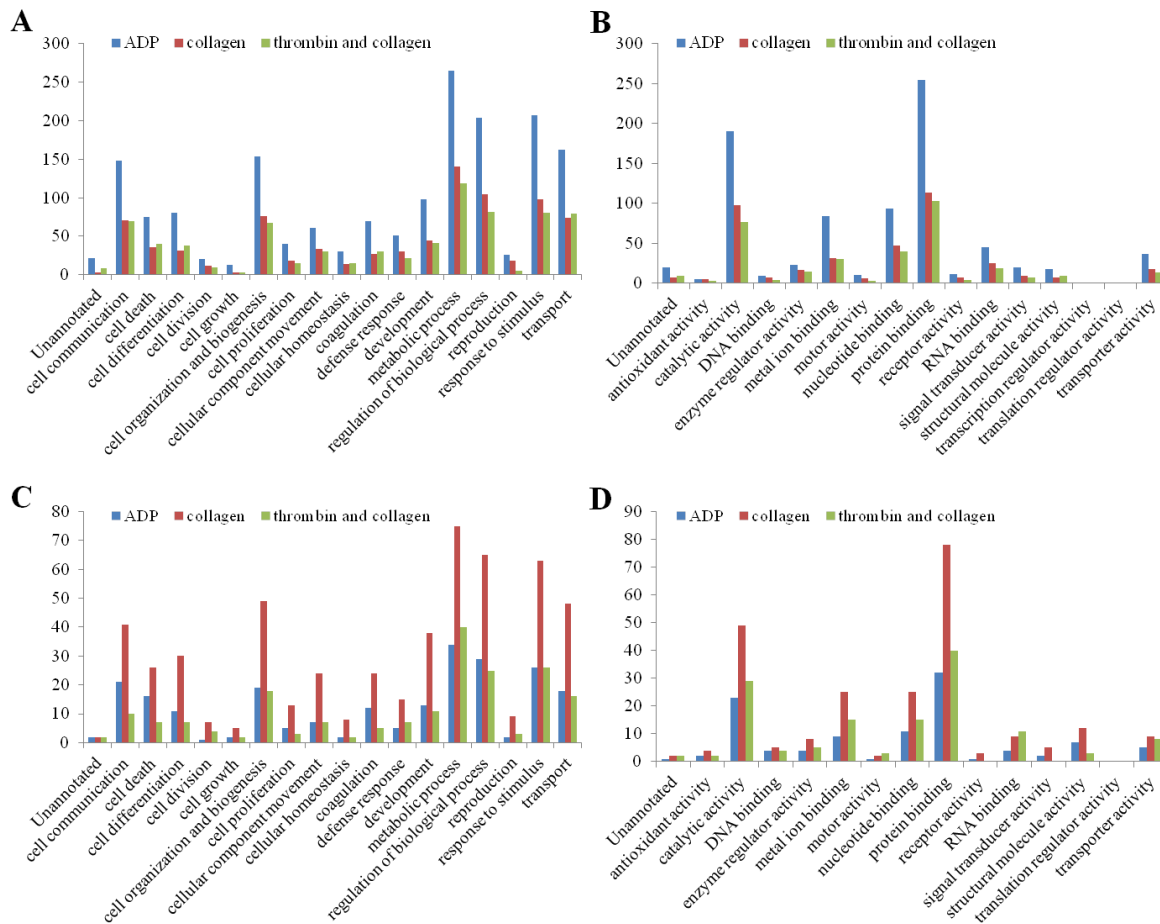
Fig. 3 Gene ontology graphs categorizing proteins for A) biological processes in the membrane fraction or C) soluble fraction, and B) molecular functions in the membrane fraction or D) soluble fraction. Blue, red and green bars indicate protein groups found as significantly more or less abundant in ADP, collagen, thrombin and collagen fractions as compared to control.

Next, we performed cluster analysis, considering the relative abundance of a protein in the three treatments as compared to control. We divided the trends of protein abundance into six clusters for the membrane and six for the soluble fraction. Proteins belonging to the same cluster were subjected to STRING analysis to perform literature mining of protein-protein interactions and protein networks. Regarding the membrane fraction, two major clusters were found to be associated to platelet mediated processes. A first cluster (Fig. 4A), containing 134 membrane proteins mostly abundant in ADP induced PMPs (Fig. 4B), grouped two different networks related to platelet degranulation and the electron transport chain (Fig. 4C). A second cluster, including 262 proteins that were mostly abundant in thrombin and collagen co-stimulated PMPs, was enriched in proteins

associated to regulation of the actin cytoskeleton, proteasome and glycolysis/pentose phosphate pathway (Fig. 5). Interestingly, in the soluble fraction one cluster (Fig. 6A), which contains 78 proteins that were mostly abundant in ADP induced PMPs (Fig. 6B), was found to be related to platelet degranulation (Fig. 6C). In particular, we found a general high enrichment in all treatments of proteins involved in cell communication, which suggests the role of PMPs in the intercellular communication network [28].

4. DISCUSSION

In this work, we carried out a proteomics study of PMPs obtained by differentially activated platelet samples. Apheresis platelets, which ensure very low RBCs and leukocytes contaminations, were used for microparticles generation. Activations were performed using relevant platelet physiological agonists following published procedures with minor modifications [14,23]. An additional centrifugation step (1000 x g) was introduced to further purify microparticles from platelets. However, despite the supernatant was formed mainly by PMPs, we cannot exclude possible exosome contaminations into our samples. The treatment with Na_2CO_3 was applied to fractionate soluble and membrane proteins, and thus increase sensitivity of the analysis. However, in the membrane fraction we found about 38% of proteins which did not have clear sequence signatures that characterize them as membrane proteins. HILIC fractionation also revealed as an efficient method to decrease sample complexity and increase sensitivity of the analysis (Fig. 7).

Platelet activation is known to be driven by the rearrangement of the actin cytoskeleton [40]. Our analysis revealed significant changes in proteins involved in this function in PMPs. Specifically, for these proteins we observed a decrease in the ADP and collagen induced MPs and an increase in the thrombin and collagen co-stimulated MPs. This also suggested a direct link between proteins related to platelet activation and physiological agonist strength. Agonists such as ADP or collagen alone were found to be weaker than thrombin and thrombin/collagen together in activating platelet, and proteins involved in cytoskeleton organization were found to be less abundant when the weakest activators were used. CD9 antigen is the third most abundant protein on the platelet surface and it is involved in the platelet activation mechanism [41] together with integrin $\alpha_{IIb}\beta_3$ [18]. The last two platelet integrin's were both identified to be less abundant in ADP induced activation than control. Interestingly, CD9 antigen, which was shown to be associated with integrin α_{IIb}-β_3 [42], was found to be increased in the same induced activation. Talin-1 was less abundant in the ADP induced stimulation and more abundant in thrombin and collagen co-stimulation; this protein was previously shown to be required for inside-out activation of platelet integrin's in hemostasis and thrombosis [43]. Actin-related protein 3, also found to be less abundant in ADP induced activation, was

41

previously shown to be involved in platelet activation by regulating actin cytoskeleton assembly [44]. We also observed lower amounts of profilin-1 in PMPs after ADP induced stimulation, which is a critical protein involved in building actin networks by promoting actin related protein 3 activation [45]. Finally, we found vinculin decreased in ADP induced activation, which was recently found to be a possible biomarker of atherosclerotic disease [46], in which platelet activation has a central role [47].
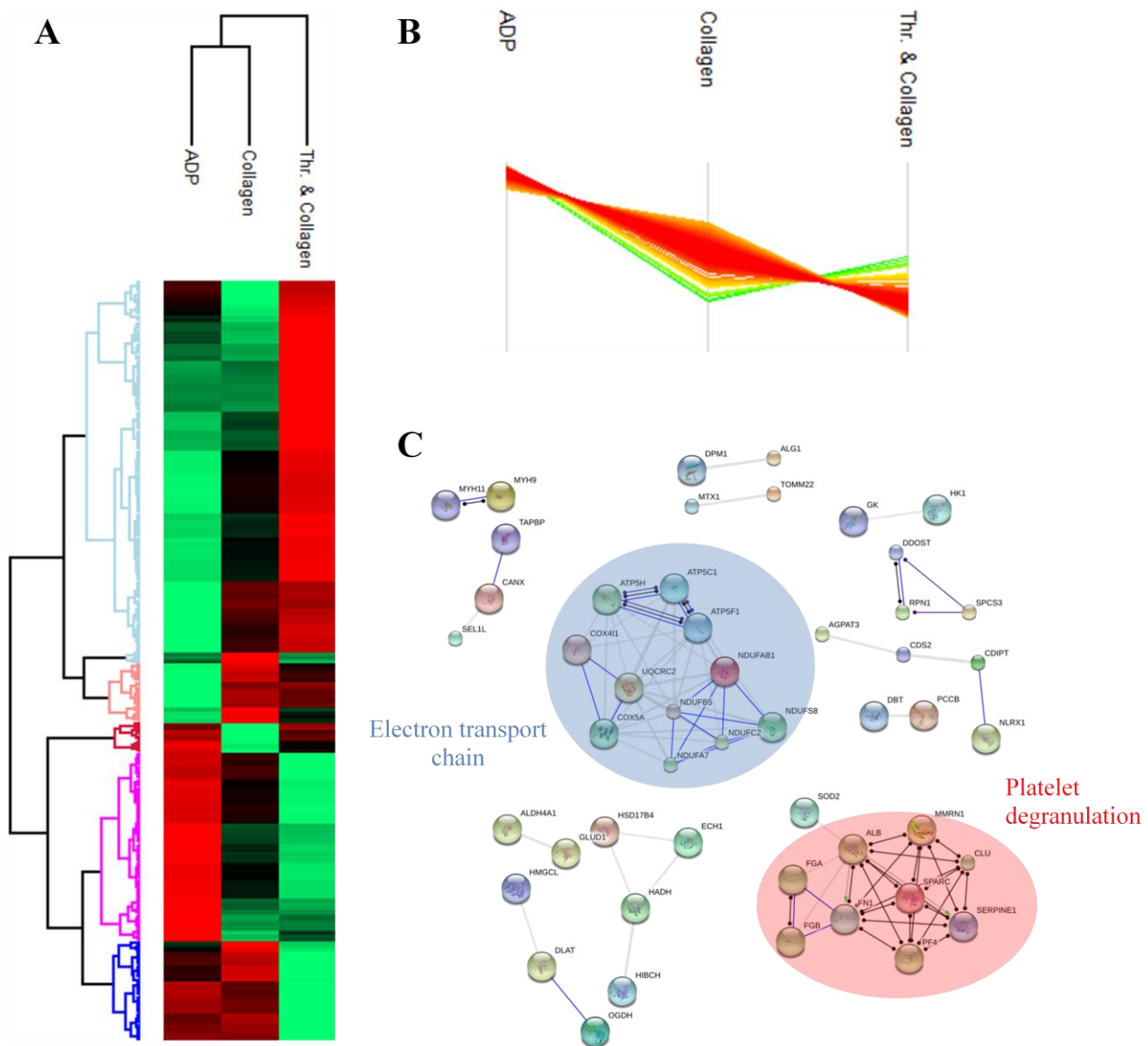
Fig. 4 A) Heat map representing log2 fold changes of the quantitative data (green-lowest abundance and red-highest abundance). B) Trends of the abundance of a specific cluster and C) protein-protein interaction analysis of the same cluster highlighting protein networks involved in electron transport

chain (blue) and platelet degranulation (red). Thicker, blue and black lines indicate more confident, binding and reaction associations, respectively.
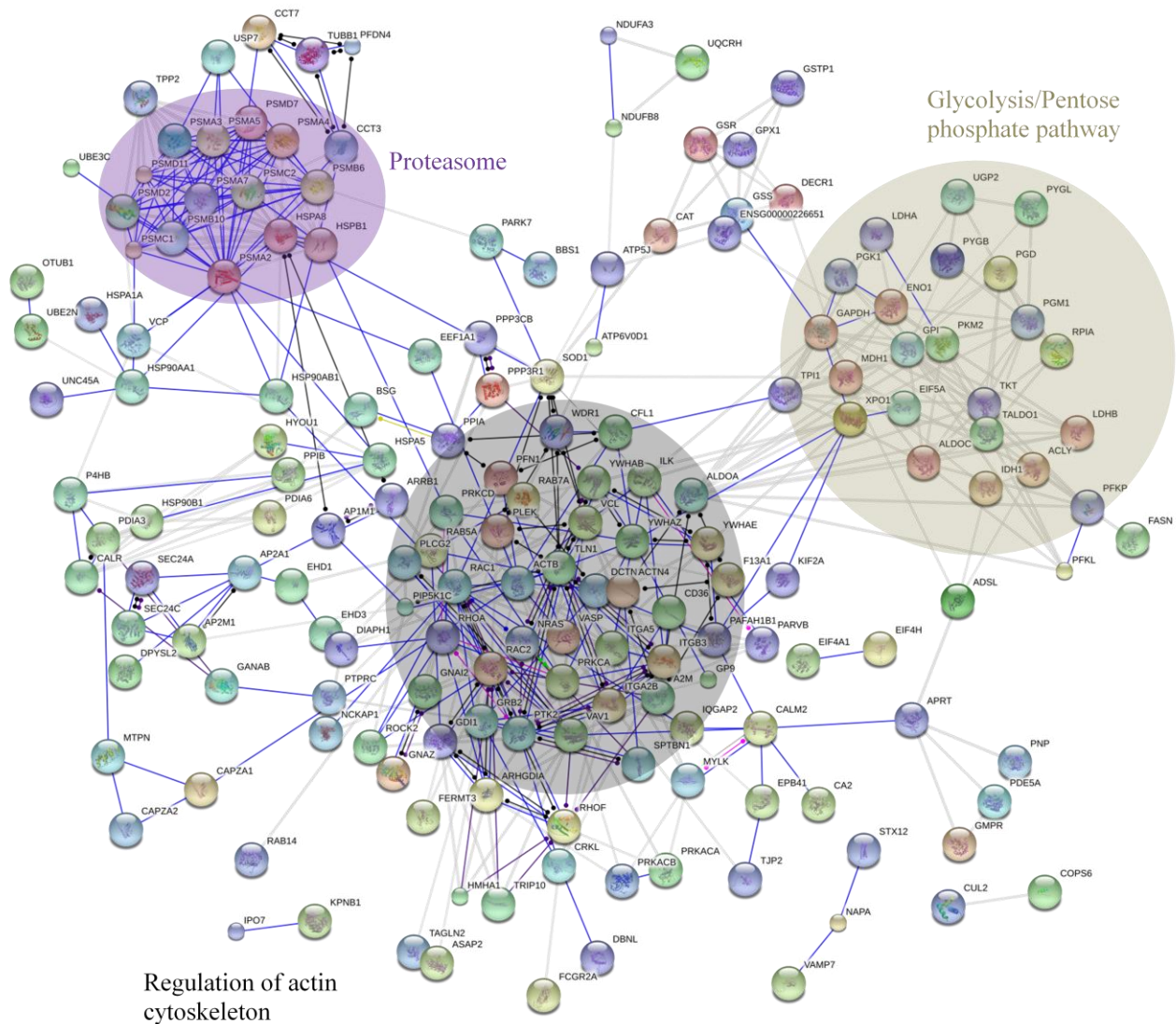
Fig. 5 Protein-protein interaction analysis of a membrane fraction cluster showing three different networks of protein related to regulation of actin cytoskeleton (black), proteasome (purple) and glycolysis/pentose phosphate pathway (brown). Thicker, blue and black lines indicate respectively more confident, binding and reaction associations.
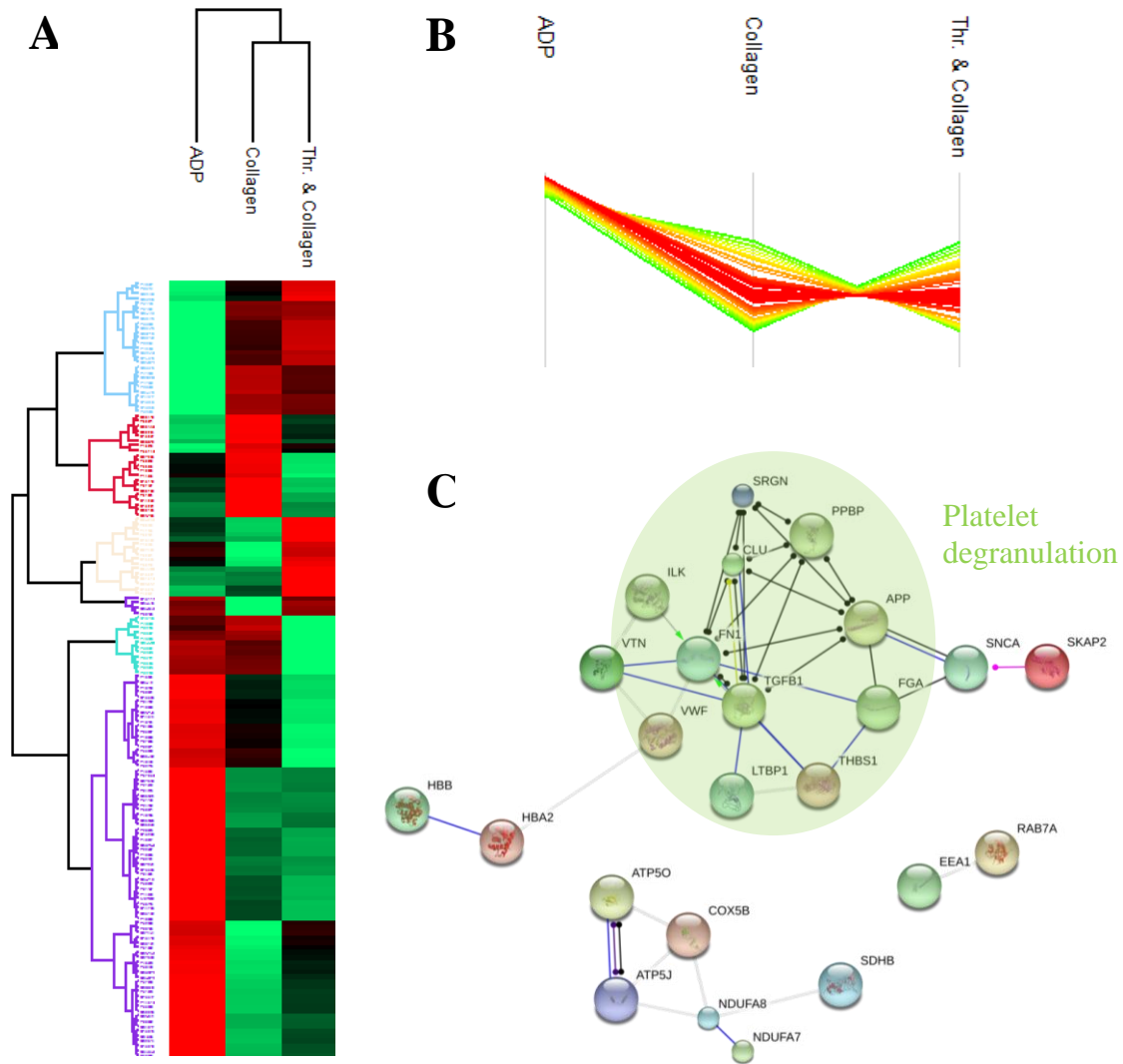
Fig. 6 A) Heat map representing log2 fold changes of the quantitative data (green-lowest abundance and red-highest abundance). B) Trends of the abundance of a specific cluster and C) protein-protein interaction analysis of the same cluster highlighting proteins network involved in platelet degranulation (green). Thicker, blue and black lines indicate more confident, binding and reaction associations, respectively.

As mentioned above, in the same cluster of proteins identified to be less abundant in ADP and collagen induced PMPs and more abundant in thrombin and collagen co-stimulated PMPs, a small subgroup of proteins involved in the glycolysis and pentose phosphate pathway was found. These pathways, together with oxidative phosphorylation, are important for platelet energy metabolism [48]. Interestingly, proteins related to ADP activation, which leads these bio-energetic processes together with ATP, were found to be decreased.
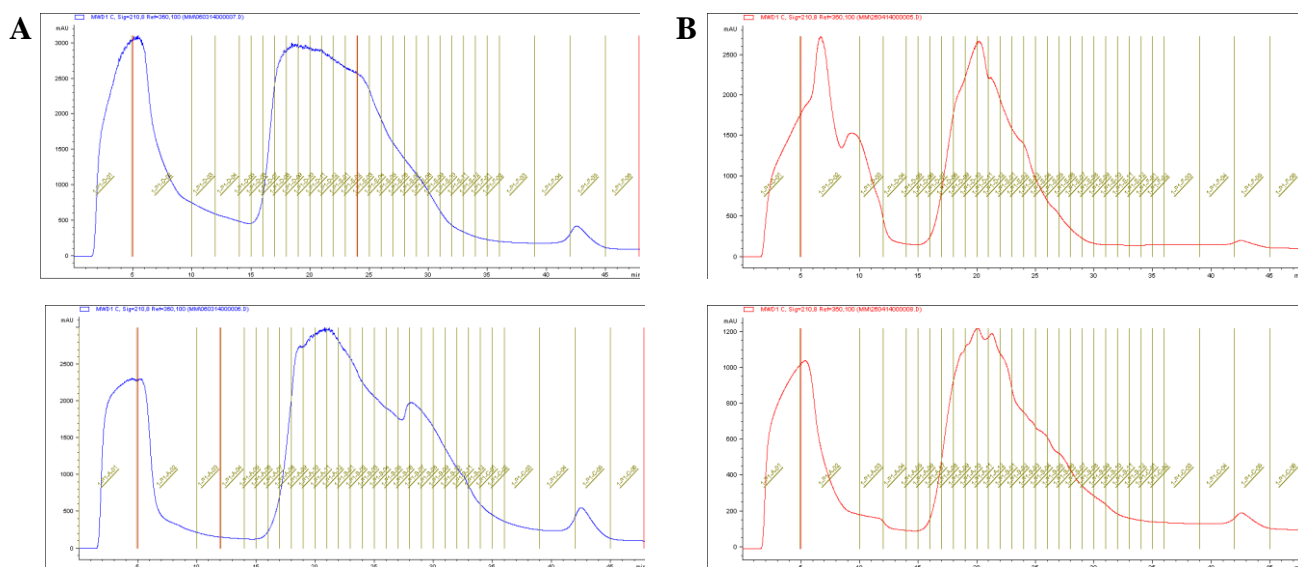
Fig 7. HILIC chromatograms showing the fractionation of the membrane and the soluble proteins respectively in the (A) first and in the (B) second replicates.

These results suggest a double role of ADP in platelets as agonist by triggering the activation process and as energetic molecule by probably inducing compensatory mechanisms, which affect the abundance of ATP-related proteins. Glyceraldehyde-3-phosphate dehydrogenase, decreased in ADP induced activation, was shown to be required for the transport of nitric oxide in platelets [49]. ATP-dependent 6-phosphofructokinase platelet type, also found to be less abundant in ADP induced PMPs, was shown to plays a critical role in cell proliferation in breast cancer cells [50]. A small group of proteins, included into the large protein complex proteasome, was also found to be changed. As shown, these proteins belong to a cluster which was identified to be decreased in ADP and collagen induced PMPs and increased in thrombin and collagen co-stimulated PMPs, thereby associated with activation strength. It is known that the activity of the proteasome in protein degradation is an ATP-dependent process [51]. Moreover, it was shown that stimulated platelet functions and thrombosis can be supported by proteasome proteolysis [52]. In this group we also found the proteasome subunit alpha type-3, which was shown to regulate thromboxane A2 receptor by inducing a multitude of downstream signaling events in platelets related to platelet shape change, aggregation and secretion [53,54]. We also found a group of proteins involved in the electron transport chain (Fig. 4C) more abundant in PMPs after ADP stimulation. Once again, ADP may activate platelet as an agonist and it may induce compensatory mechanisms by affecting the expression of ATP-related proteins such as ATP synthase subunit gamma mitochondrial and ATP

synthase subunit d, mitochondrial, found to be increased in ADP induced activation, which provide energy to the cells through the synthesis of ATP in the mitochondria. Active components of Complex I, involved in respiratory electron transport chain such as NADH dehydrogenase 1 subunit C2, NADH dehydrogenase iron-sulfur protein 8 mitochondrial, acyl carrier protein mitochondrial, NADH dehydrogenase 1 alpha subcomplex subunit 7 were found to be more abundant in ADP induced PMPs. Complex I inhibition, through accumulated damage caused by reactive oxygen and nitrogen species and by the binding of environmental toxins, plays a role in the development of neurodegenerative disorders such as Parkinson's [55], Alzheimer's and Huntington's diseases [56]. Taken together, these results suggest that activation could affect platelet mitochondria related processes such as the respiratory chain.

Finally, we investigated proteins involved in platelet degranulation. We grouped them into two different clusters, in which they were found to be increased in PMPs after ADP stimulation. These clusters were identified in both membrane and soluble fraction (Fig.4C, 5C). Platelets can work as an exocytotic cell releasing different types of useful molecules for the sites of vascular injury or for the storage such as alpha-granules, dense-granules and lysosomes [57]. Degranulation, which is also induced by physiological agonist through activation, was shown to be related to several pathologies [58,59]. Taken together, these results suggest a connection between proteins related to platelet degranulation and agonist strength. ADP, which was shown to induce partial degranulation [60], was considered to be weaker in activating platelet compared to the other agonists. Interestingly, we found proteins involved in degranulation more abundant in PMPs after ADP stimulation compared with thrombin stimulation. Moreover, we found SPARC, highly abundant in ADP induced activation, which is known to be involved in wound healing by facilitating the angiogenesis [61] and in acute coronary syndrome, which is a platelet activation related disease [62]. Interestingly, thrombospondin-1 and multimerin-1 were found to be increased during all of the activation performed in this study as compared to the control. In combination with von Willebrand factor, also found in our study, thrombospondin-1 was shown to mediate, platelet hemostasis by affecting the platelet adhesion to the sites of vascular injury [63]. Multimerin-1 was shown to promote platelet adhesion at sites of vascular injury as well by acting as adhesive ligand [64].

5. CONCLUSIONS

In conclusion, our proteomics approach revealed that the protein composition in PMPs was directly related to the agonist used for platelet stimulation. Platelet activation proteins were more abundant when using stronger agonists, while platelet degranulation proteins were lower. We observed a difference in expression of ATP-related proteins during MPs generation in ADP induced activation, suggesting the presence of compensatory mechanisms related to energy depletion. Collectively, our MS-based quantitative study provided an overview of the PMP proteome, which can be of high interest to reveal biological insights about platelet response to stimuli.

ACKNOWLEDGMENTS

CHAPTER REFERENCES

[1] Wolf P. The nature and significance of platelet products in human plasma. Br J Haematol 1967;13:269-88

[2] Zwaal RF, Comfurius P, Bevers EM. Platelet procoagulant activity and microvesicle formation. Its putative role in hemostasis and thrombosis. Biochim Biophys Acta 1992;1180:1-8.

[3] Heijnen HF, Schiel AE, Fijnheer R, Geuze HJ, Sixma JJ. Activated platelets release two types of membrane vesicles: microvesicles by surface shedding and exosomes derived from exocytosis of multivesicular bodies and alpha-granules. Blood 1999; 94:3791-9

[4] Daniel L, Fakhouri F, Joly D, Mouthon L, Nusbaum P, Grunfeld JP et al. Increase of circulating neutrophil and platelet microparticles during acute vasculitis and hemodialysis. Kidney Int 2006;69:1416-23.

[5] Lynch SF, Ludlam CA. Plasma microparticles and vascular disorders. Br J Haematol 2007;137: 36-48.

[6] Flaumenhaft R, Dilks JR, Richardson J, Alden E, Patel-Hett SR, Battinelli E et al. Megakaryocyte-derived microparticles: direct visualization and distinction from platelet-derived microparticles. Blood 2009;113:1112-21.

[7] Castaman G, Yu-Feng L, Rodeghiero F. A bleeding disorder characterised by isolated deficiency of platelet microvesicle generation. Lancet 1996;347:700–1

[8] Nomura S, Uehata S, Saito S, Osumi K, Ozeki Y, Kimura Y. Enzyme immunoassay detection of platelet-derived microparticles and RANTES in acute coronary syndrome. Thromb Haemost 2003;89:506-12.

[9] Joop K, Berckmans RJ, Nieuwland R, Berkhout J, Romijn FP, Hack CE et al. Microparticles from patients with multiple organ dysfunction syndrome and sepsis support coagulation through multiple mechanisms. Thromb Haemost 2001;85:810-20.

[10] Sheremata WA, Jy W, Horstman LL, Ahn YS, Alexander JS, Minagar A. Evidence of platelet activation in multiple sclerosis. J Neuroinflammation 2008;5:27

[11] Knijff-Dutmer EA, Koerts J, Nieuwland R, Kalsbeek-Batenburg EM, van de Laar MA. Elevated levels of platelet microparticles are associated with disease activity in rheumatoid arthritis. Arthritis Rheum 2002;46:1498-503.

[12] Janowska-Wieczorek A, Marquez-Curtis LA, Wysoczynski M, Ratajczak MZ. Enhancing effect of platelet-derived microvesicles on the invasive potential of breast cancer cells. Transfusion 2006;46:1199-209.

[13] Kim HK, Song KS, Park YS, Kang YH, Lee YJ, Lee KR et al. Elevated levels of circulating platelet microparticles, VEGF, IL-6 and RANTES in patients with gastric cancer: possible role of a metastasis predictor. Eur J Cancer 2003;39:184-91.

[14] Biró E, Akkerman JW, Hoek FJ, Gorter G, Pronk LM, Sturk A et al. The phospholipid composition and cholesterol content of platelet-derived microparticles: a comparison with platelet membrane fractions. J Thromb Haemost 2005;3:2754-63.

[15] Morel O, Jesel L, Freyssinet JM, Toti F. Cellular mechanisms underlying the formation of circulating microparticles. Arterioscler Thromb Vasc Biol 2011;31:15-26.

[16] Schoenwaelder SM, Yuan Y, Josefsson EC, White MJ, Yao Y, Mason KD et al. Two distinct pathways regulate platelet phosphatidylserine exposure and procoagulant function. Blood 2009;114:663-6.

[17] Cranmer SL, Ashworth KJ, Yao Y, Berndt MC, Ruggeri ZM, Andrews RK et al. High shear-dependent loss of membrane integrity and defective platelet adhesion following disruption of the GPIbα-filamin interaction. Blood 2011;117:2718-27.

[18] Gemmell CH, Sefton MV, Yeo EL. Platelet-derived microparticle formation involves glycoprotein IIb-IIIa. Inhibition by RGDS and a Glanzmann's thrombasthenia defect. J Biol Chem 1993;268:14586-9.

[19] Yuana Y, Bertina RM, Osanto S. Pre-analytical and analytical issues in the analysis of blood microparticles. Thromb Haemost 2011,105:396-408.

[20] Meissner F, Mann M. Quantitative shotgun proteomics: considerations for a high-quality workflow in immunology. Nature Immunology 2014,15:112-17.

[21] Han X, Aslanian A, Yates JR 3rd. Mass spectrometry for proteomics. Curr Opin Chem Biol 2008, 12:483-90.

[22] Aebersold R, Mann M. Mass spectrometry-based proteomics. Nature 2003,422:198-207.

[23] Capriotti AL, Caruso G, Cavaliere C, Piovesana S, Samperi R, Laganà A. Proteomic characterization of human platelet-derived microparticles. Anal Chim Acta 2013;776:57-63.

[24] Dean WL, LeeMJ, Cummins TD, Schultz DJ, Powell DW. Proteomic and functional characterisation of platelet microparticle size classes. Thromb Haemost 2009;102:711-18.

[25] Perez-Pujol S, Marker PH, Key NS. Platelet microparticles are heterogeneous and highly dependent on the activation mechanism: studies using a new digital flow cytometer. Cytometry A 2007;71:38-45.

[26] Shai E, Parguiña AF, Motahedeh S, Varon D, Garcia A. Comparative analysis of platelet-derived microparticles reveals differences in their amount and proteome depending on the platelet stimulus. J Proteomics 2012;76:287-96.

[27] Aatonen M, Öhman, T, Nyman TA, Laitinen, S, Grönholm, M, Siljander P. Isolation and characterization of platelet-derived extracellular vesicles. Journal Extracell vesicles doi: 10.3402/jev.v3.24692

[28] Aatonen M, Grönholm M, Siljander P, Platelet-Derived Microvesicles: Multitalented Participants in Intercellular Communication. Semin Thromb Hemost 2012;38:102-13.

[29] Smid M, Dielis AWJH, Winkens M, Spronk HMH, van Oerle R, Hamulya´ k K et al. Thrombin generation in patients with a first acute myocardial infarction. J Thromb Haemost 2011; 9:450–6.

[30] Carcaillon L, Alhenc-Gelas M, Bejot Y, Spaft C, Ducimetière P, Ritchie K et al. Increased thrombin generation is associated with acute ischemic stroke but not with coronary heart disease in the elderly: the Three-City cohort study. Arterioscler Thromb Vasc Biol 2011;31:1445-51.

[31] de Bruijne EL, Gils A, Rijken DC, de Maat MP, Guimarães AH, Poldermans D et al. High thrombin activatable fibrinolysis inhibitor levels are associated with an increased risk of premature peripheral arterial disease. Thromb Res 2011;127:254-8.

[32] De Candia E. Mechanisms of platelet activation by thrombin: A short history. Thromb Res 2012;129:250-6.

[33] Bevers EM, Comfurius P, Zwaal RF. Changes in membrane phospholipid distribution during platelet activation. Biochim Biophys Acta 1983;736:57-66.

[34] Keuren JF, Wielders SJ, Ulrichts H, Hackeng T, Heemskerk JW, Deckmyn H et al. Synergistic Effect of Thrombin on Collagen-Induced Platelet Procoagulant Activity Is Mediated Through Protease-Activated Receptor-1. Arterioscler Thromb Vasc Biol 2005;25:1499-505.

[35] Palmisano G, Lendal SE, Engholm-Keller K, Leth-Larsen R, Parker BL, Larsen MR. Selective enrichment of sialic acid-containing glycopeptides using titanium dioxide chromatography with analysis by HILIC and mass spectrometry. Nat Protoc 2010;5:1974-82.

[36] Thingholm TE, Palmisano G, Kjeldsen, F, Larsen MR. Undesirable charge-enhancement of isobaric tagged phosphopeptides leads to reduced identification efficiency. J Proteome Res 2010;9: 4045-52.

[37] Brosch M, Yu L, Hubbart T, Choudhary J. Accuarate and sensitive peptide identification with Mascot Percolator. J Proteome Res. 2009;8:3176-81.

 [38] Franceschini A, Szklarczyk D, Frankild S, Kuhn M, Simonovic M, Roth A et al. STRING v9. 1: protein-protein interaction networks, with increased coverage and integration. Nucleic Acids Res 2013;41:D808-15.

[39] Fujiki Y, Hubbard AL, Fowler S, Lazarow PB. Isolation of intracellular membranes by means of sodium carbonate treatment: application to endoplasmic reticulum. J Cell Biol 1982;93:97-102.

[40] Woronowicz K, Dilks JR, Rozenvayn N, Dowal L, Blair PS, Peters CG et al. The platelet actin cytoskeleton associates with SNAREs and participates in alpha-granule secretion. Biochemistry 2010;49:4533-42.

[41] Dale GL, Remenyi G, Friese P. Tetraspanin CD9 is required for microparticle release from coated-platelets. Platelets 2009;20:361-6.

[42] Slupsky JR, Seehafer JG, Tang SC, Masellis-Smith A, Shaw ARE. Evidence that monoclonal antibodies against CD9 antigen induce specific association between CD9 and the platelet glycoprotein IIb-IIIa complex. J Biol Chem. 1989;264:12289-12293

[43] Nieswandt B, Moser M, Pleines I, Varga-Szabo D, Monkley S, Critchley D et al. Loss of talin1 in platelets abrogates integrin activation, platelet aggregation, and thrombus formation in vitro and in vivo. J Exp Med. 2007;204:3113-8.

[44] Pollard TD. Regulation of actin filament assembly by Arp2/3 complex and formins. Annu Rev Biophys Biomol Struct 2007;36:451-77.

[45] Mouneimne G, Hansen SD, Selfors LM, Petrak L, Hickey MM, Gallegos LL et al. Differential remodeling of actin cytoskeleton architecture by profilin isoforms leads to distinct effects on cell migration and invasion. Cancer cell 2012;22:615-30.

[46] Kristensen LP, Larsen MR, Mickley H, Saaby L, Diederichsen AC, Lambrechtsen J et al. Plasma proteome profiling of atherosclerotic disease manifestations reveals elevated levels of the cytoskeletal protein vinculin. J Proteomics 2014;101:141-53.

[47] Bigalke B, Schuster A, Sopova K, Wurster T, Stellos K. Platelets in atherothrombosis-diagnostic and prognostic value of platelet activation in patients with atherosclerotic diseases. Curr vasc pharmacol 2012;10:589-96.

[48] Doery JC, Hirsh J, Cooper I. Energy metabolism in human platelets: interrelationship between glycolysis and oxidative metabolism. Blood 1970;36:159-68.

[49] McDonald B, Reep B, Lapetina EG, y Vedia LM. Glyceraldehyde-3-phosphate dehydrogenase is required for the transport of nitric oxide in platelets. Proc Nat Acad Sci USA 1993;90:11122-6.

[50] Moon JS, Kim HE, Koh E, Park SH, Jin WJ, Park BW et al. Krüppel-like factor 4 (KLF4) activates the transcription of the gene for the platelet isoform of phosphofructokinase (PFKP) in breast cancer. J Biol Chem 2011;286:23808-16.

[51] Lecker SH, Goldberg AL, Mitch WE. Protein degradation by the ubiquitin–proteasome pathway in normal and disease states. J Am Soc Nephrol 2006;17:1807-19.

[52] Gupta N, Li W, Willard B, Silverstein R L, McIntyre TM. Proteasome Proteolysis Supports Stimulated Platelet Function and Thrombosis. Arterioscler Thromb Vasc Biol 2014;34:160-8.

[53] Huang JS, Ramamurthy SK, Lin X, Le Breton GC. Cell signalling through thromboxane A2 receptors. Cell Signal 2004;16:521-33.

[54] Sasaki M, Sukegawa J, Miyosawa K, Yanagisawa T, Ohkubo S, Nakahata N. Low expression of cell-surface thromboxane A2 receptor β-isoform through the negative regulation of its membrane traffic by proteasomes. Prostaglandins Other Lipid Mediat 2007;83:237-49.

[55] Krige D, Carroll MT, Cooper JM, Marsden CD, Schapira AH. Platelet mitochondria function in Parkinson's disease. Ann Neurol 1992;32:782-88.

[56] Murray J, Taylor SW, Zhang B, Ghosh SS, Capaldi RA. Oxidative damage to mitochondrial complex I due to peroxynitrite: identification of reactive tyrosines by mass spectrometry. J Biol Chem 2003;278:37223-30.

[57] Coppinger, JA, Cagney G, Toomey S, Kislinger T, Belton O, McRedmond JP et al. Characterization of the proteins released from activated platelets leads to localization of novel platelet proteins in human atherosclerotic lesions. Blood 2004;103:2096-104.

[58] Kinlough-Rathbone RL, Perry DW, Guccione MA, Rand ML, Packham MA. Degranulation of human platelets by the thrombin receptor peptide SFLLRN: comparison with degranulation by thrombin. Thromb Haemost 1993;70:1019-23.

[59] Fateh-Moghadam S, Li Z, Ersel S, Reuter T, Htun P, Plöckinger U et al. Platelet degranulation is associated with progression of intima-media thickness of the common carotid artery in patients with diabetes mellitus type 2. Arterioscl Thromb Vasc Biol 2005;25:1299-303.

[60] Janes SL, Wilson DJ, Cox AD, Chronos NA, Goodall AH. ADP causes partial degranulation of platelets in the absence of aggregation. Br J Haematol 1994;86:568-73.

[61] Dobaczewski M, Gonzalez-Quesada C, Frangogiannis NG. The extracellular matrix as a modulator of the inflammatory and reparative response following myocardial infarction. J Mol Cell Cardiol 2010;48:504-11

[62] Parguiña AF, Grigorian-Shamajian L, Agra RM, Teijeira-Fernández E, Rosa I, Alonso J et al. Proteins involved in platelet signaling are differentially expressed in acute coronary syndrome: a proteomic study. PLoS One 2010;5:e13404

[63] Pimanda JE, Ganderton T, Maekawa A, Yap CL, Lawler J, Kershaw G et al. Role of Thrombospondin-1 in control of von Willebrand Factor Multimer size in mice. J Biol Chem 2004;279:21439-48

[64] Tasneem S, Adam F, Minullina I, Pawlikowska M, Hui SK, Zheng S et al. Platelet adhesion to multimerin 1 in vitro: influences of platelet membrane receptors, von Willebrand factor and shear. J Thromb Haemost 2009;7:685-92

6. APPENDIX

Table 1. Dataset of significantly changed membrane proteins after cluster analysis

ADP	Collagen	Thr. & Collagen	Cluster	Accession
0.2909437	-1.113208	0.8222646	Cluster 1	Q9UBM7
0.2763678	-1.109119	0.8327515	Cluster 1	Q562R1
0.2891396	-1.112712	0.8235721	Cluster 1	Q92619
0.2966776	-1.114769	0.8180912	Cluster 1	P21964
0.3123612	-1.118897	0.8065358	Cluster 1	Q9UNL2
0.3428897	-1.126338	0.7834478	Cluster 1	Q9UIA9
0.3116312	-1.118709	0.8070782	Cluster 1	P63000
0.3291564	-1.123088	0.7939321	Cluster 1	H7BZJ3
0.2254327	-1.093474	0.868041	Cluster 1	Q96DT5
0.2137515	-1.089593	0.8758413	Cluster 1	P63098
0.2150954	-1.090045	0.8749493	Cluster 1	M0R1L7
0.1979361	-1.084167	0.8862304	Cluster 1	Q16698
0.14688	-1.065317	0.9184368	Cluster 1	P00352
0.1449199	-1.064553	0.9196332	Cluster 1	P30101
0.1264514	-1.057211	0.93076	Cluster 1	Q99747
0.1328571	-1.059787	0.9269303	Cluster 1	Q9H8H3
0.1002016	-1.046329	0.946127	Cluster 1	O95169
0.114131	-1.052169	0.9380378	Cluster 1	P61586
-0.051087	-0.973477	1.024565	Cluster 1	Q93009
-0.036851	-0.981065	1.017916	Cluster 1	P17612
-0.015914	-0.991948	1.007862	Cluster 1	P35613
-0.068312	-0.964092	1.032405	Cluster 1	P50453
0.0036196	-1.001805	0.9981853	Cluster 1	Q15642
0.0534325	-1.025645	0.9722126	Cluster 1	O76074
-0.174239	-0.90143	1.075669	Cluster 1	O95858
-0.193375	-0.88919	1.082565	Cluster 1	P35813
-0.14996	-0.916551	1.066511	Cluster 1	P11021
-0.120405	-0.934346	1.054751	Cluster 1	P27797
-0.133262	-0.926687	1.059949	Cluster 1	P62258
-0.355698	-0.773524	1.129221	Cluster 1	P07237
-0.350508	-0.777562	1.12807	Cluster 1	Q86Y82
-0.36531	-0.765982	1.131292	Cluster 1	P49247
-0.362709	-0.768031	1.130739	Cluster 1	O60506
-0.372605	-0.760204	1.132809	Cluster 1	Q9BS40
-0.373027	-0.759868	1.132895	Cluster 1	Q9HBH0
-0.293642	-0.820304	1.113946	Cluster 1	P49368
-0.293661	-0.82029	1.113951	Cluster 1	P25787
-0.319711	-0.80105	1.120761	Cluster 1	P18859
-0.308277	-0.809565	1.117842	Cluster 1	P22314
-0.310915	-0.80761	1.118525	Cluster 1	P11171

-0.304986	-0.811996	1.116981	Cluster 1	P14618
-0.312007	-0.806799	1.118806	Cluster 1	Q9UDY2
-0.261543	-0.843239	1.104782	Cluster 1	P08575
-0.234511	-0.861904	1.096415	Cluster 1	Q9C0I1
-0.456046	-0.690681	1.146727	Cluster 1	P22061
-0.463947	-0.683758	1.147705	Cluster 1	P15170
-0.465071	-0.682769	1.14784	Cluster 1	P30740
-0.46715	-0.680935	1.148085	Cluster 1	Q9Y2A7
-0.48867	-0.661701	1.150371	Cluster 1	P00441
-0.47863	-0.670731	1.149362	Cluster 1	Q8N5J2
-0.481729	-0.667955	1.149684	Cluster 1	H3BPE1
-0.478201	-0.671116	1.149316	Cluster 1	P12318
-0.419862	-0.72162	1.141482	Cluster 1	P61088
-0.419145	-0.722221	1.141365	Cluster 1	O43707
-0.418814	-0.722498	1.141312	Cluster 1	Q05655
-0.416088	-0.724776	1.140864	Cluster 1	O94925
-0.694673	-0.451458	1.146131	Cluster 1	P61106
-0.683078	-0.46472	1.147798	Cluster 1	P50552
-0.686042	-0.461348	1.14739	Cluster 1	Q7L5N1
-0.687818	-0.459322	1.14714	Cluster 1	P09211
-0.686878	-0.460395	1.147273	Cluster 1	P47755
-0.659351	-0.491264	1.150615	Cluster 1	Q99832
-0.653953	-0.497195	1.151148	Cluster 1	P52907
-0.65596	-0.494995	1.150955	Cluster 1	P58546
-0.666774	-0.483044	1.149818	Cluster 1	Q8N9N7
-0.666194	-0.48369	1.149883	Cluster 1	P53396
-0.613427	-0.540506	1.153933	Cluster 1	O00139
-0.615427	-0.538417	1.153844	Cluster 1	P54920
-0.612643	-0.541323	1.153966	Cluster 1	P46109
-0.620472	-0.533127	1.153599	Cluster 1	Q9BXS5
-0.606616	-0.547582	1.154197	Cluster 1	P40306
-0.60372	-0.550573	1.154293	Cluster 1	P28072
-0.570166	-0.584505	1.154671	Cluster 1	Q9BUL8
-0.570322	-0.58435	1.154672	Cluster 1	P62993
-0.565137	-0.589478	1.154615	Cluster 1	P23528
-0.584597	-0.570073	1.15467	Cluster 1	P01023
-0.58382	-0.570856	1.154676	Cluster 1	Q14554
-0.584978	-0.569689	1.154667	Cluster 1	Q9Y4L1
-0.582368	-0.572318	1.154686	Cluster 1	P07203
-0.590786	-0.56381	1.154595	Cluster 1	Q01082
-0.589435	-0.565181	1.154616	Cluster 1	P49327
-0.589108	-0.565512	1.15462	Cluster 1	O75116
-0.595769	-0.558733	1.154503	Cluster 1	O14818
-0.596541	-0.557945	1.154485	Cluster 1	Q15019
-0.596444	-0.558044	1.154488	Cluster 1	P68104

-0.548221	-0.605997	1.154219	Cluster 1	P08238
-0.536429	-0.617327	1.153756	Cluster 1	Q12913
-0.542805	-0.61122	1.154025	Cluster 1	P35237
-0.508807	-0.64328	1.152088	Cluster 1	Q8WUM4
-0.529712	-0.623713	1.153424	Cluster 1	Q6P3W7
-0.518587	-0.634183	1.15277	Cluster 1	Q86TP1
-0.527902	-0.625425	1.153327	Cluster 1	Q96FW1
-0.814223	-0.301959	1.116182	Cluster 1	P09972
-0.806207	-0.312804	1.11901	Cluster 1	P08107
-0.807104	-0.311596	1.1187	Cluster 1	P51665
-0.831558	-0.278039	1.109597	Cluster 1	P48637
-0.824016	-0.288527	1.112542	Cluster 1	Q9UJ90
-0.821211	-0.292395	1.113606	Cluster 1	P23229-2
-0.826426	-0.285189	1.111615	Cluster 1	Q16851
-0.851597	-0.249544	1.101141	Cluster 1	O00231
-0.849761	-0.252194	1.101955	Cluster 1	P28676
-0.847474	-0.255484	1.102958	Cluster 1	Q16555
-0.844831	-0.25927	1.104101	Cluster 1	Q7KZF4
-0.842004	-0.263303	1.105306	Cluster 1	P01111
-0.844428	-0.259846	1.104274	Cluster 1	P53992
-0.74091	-0.396546	1.137455	Cluster 1	P60842
-0.728761	-0.4113	1.140061	Cluster 1	P40925
-0.744885	-0.391664	1.13655	Cluster 1	P29144
-0.746229	-0.390009	1.136238	Cluster 1	P25789
-0.7379	-0.400223	1.138123	Cluster 1	P28066
-0.746107	-0.390159	1.136266	Cluster 1	P00558
-0.729542	-0.410359	1.139901	Cluster 1	P60981
-0.770999	-0.358927	1.129926	Cluster 1	Q6IBS0
-0.774759	-0.354114	1.128872	Cluster 1	P30085
-0.778987	-0.34867	1.127656	Cluster 1	Q9NQP4
-0.779284	-0.348286	1.12757	Cluster 1	O00299
-0.785719	-0.339932	1.125651	Cluster 1	P36959
-0.760289	-0.372498	1.132787	Cluster 1	Q96CW1
-0.757937	-0.375451	1.133388	Cluster 1	Q99497
-0.758671	-0.374531	1.133201	Cluster 1	P22694
-1.001549	0.0031047	0.998444	Cluster 1	O75874
-1.000401	0.000802	0.9995987	Cluster 1	P04040
-1.00324	0.0065111	0.9967285	Cluster 1	P61421
-1.007533	0.0152409	0.9922925	Cluster 1	P41226
-1.009123	0.018502	0.9906207	Cluster 1	P51809
-1.011155	0.0226966	0.9884585	Cluster 1	Q9NYU2
-1.012339	0.0251529	0.9871863	Cluster 1	P55072
-1.013246	0.0270398	0.9862059	Cluster 1	Q6NXT6-2
-1.025588	0.0533076	0.97228	Cluster 1	Q7L1Q6
-1.02108	0.0435851	0.9774948	Cluster 1	P20339

-1.021529	0.044547	0.9769821	Cluster 1	P43034
-1.016672	0.0342228	0.9824493	Cluster 1	P16298
-1.018586	0.0382706	0.9803153	Cluster 1	Q13576
-1.017679	0.03635	0.9813294	Cluster 1	P06744
-1.017508	0.0359872	0.9815206	Cluster 1	P08567
-1.015335	0.0314108	0.9839245	Cluster 1	Q9HBI1
-1.048161	0.1045347	0.9436264	Cluster 1	Q9BZH6
-1.049532	0.1077976	0.9417341	Cluster 1	Q14697
-1.048297	0.1048577	0.9434395	Cluster 1	Q9Y3C5
-1.047361	0.1026399	0.9447216	Cluster 1	Q14974
-1.047113	0.1020528	0.9450604	Cluster 1	Q13418
-1.047903	0.1039214	0.9439812	Cluster 1	P63104
-1.047699	0.1034383	0.9442605	Cluster 1	P07195
-1.045538	0.0983435	0.9471948	Cluster 1	P60709
-1.053388	0.1170837	0.9363042	Cluster 1	K7EQ37
-1.051718	0.1130422	0.9386754	Cluster 1	Q14012
-1.055811	0.1230016	0.9328095	Cluster 1	P37802
-1.059072	0.1310709	0.9280013	Cluster 1	P23284
-1.058034	0.1284889	0.9295452	Cluster 1	Q3ZCW2
-1.063365	0.1418857	0.9214791	Cluster 1	Q8NG11
-1.036786	0.0781597	0.9586267	Cluster 1	P55209
-1.038699	0.0825103	0.9561886	Cluster 1	Q9Y490
-1.03716	0.079007	0.9581529	Cluster 1	P14770
-1.040707	0.0871144	0.9535929	Cluster 1	Q5JTZ9
-1.042088	0.0903	0.9517875	Cluster 1	B8ZZI0
-1.04007	0.0856499	0.9544203	Cluster 1	P05106
-1.040418	0.0864482	0.9539695	Cluster 1	Q15056
-1.029195	0.0612022	0.9679933	Cluster 1	Q96KP4
-1.030424	0.0639136	0.9665102	Cluster 1	Q15833
-1.030688	0.0644994	0.966189	Cluster 1	Q9UJU6
-1.031441	0.0661683	0.9652727	Cluster 1	Q8N9U0
-1.031518	0.0663404	0.965178	Cluster 1	P0C7P3
-1.033548	0.0708649	0.9626825	Cluster 1	P11216
-1.033808	0.0714476	0.9623601	Cluster 1	O00194
-0.881129	-0.20574	1.086869	Cluster 1	P37837
-0.883192	-0.202593	1.085785	Cluster 1	P48739
-0.880157	-0.207219	1.087375	Cluster 1	P04406
-0.883273	-0.202469	1.085742	Cluster 1	P51149
-0.914375	-0.1535	1.067875	Cluster 1	P15153
-0.913672	-0.15464	1.068312	Cluster 1	O95782
-0.916697	-0.149723	1.066419	Cluster 1	P52565
-0.928164	-0.1308	1.058964	Cluster 1	P36871
-0.927245	-0.132332	1.059578	Cluster 1	P00491
-0.928399	-0.130407	1.058806	Cluster 1	Q9H4M9
-0.923091	-0.139227	1.062318	Cluster 1	P62937

-0.903359	-0.171183	1.074542	Cluster 1	P16885
-0.90748	-0.164614	1.072093	Cluster 1	P62158
-0.908548	-0.162901	1.071449	Cluster 1	P06733
-0.909912	-0.16071	1.070622	Cluster 1	P49407
-0.899046	-0.178002	1.077048	Cluster 1	E7ESP4
-0.896878	-0.181408	1.078286	Cluster 1	Q15067-3
-0.990667	-0.018411	1.009079	Cluster 1	O60331
-0.988975	-0.021698	1.010672	Cluster 1	P61158
-0.989769	-0.020158	1.009926	Cluster 1	P30566
-0.992283	-0.015259	1.007542	Cluster 1	P63241
-0.96398	-0.068517	1.032496	Cluster 1	O00154
-0.965255	-0.0662	1.031455	Cluster 1	O75083
-0.96453	-0.067519	1.032048	Cluster 1	Q15762
-0.967165	-0.062719	1.029883	Cluster 1	Q9NQ75
-0.982178	-0.034738	1.016916	Cluster 1	P16671
-0.979314	-0.040161	1.019476	Cluster 1	Q13617
-0.971477	-0.054793	1.02627	Cluster 1	P18206
-0.972385	-0.053113	1.025498	Cluster 1	P06737
-0.974223	-0.049701	1.023924	Cluster 1	P07384
-0.975149	-0.047976	1.023124	Cluster 1	P07919
-0.977057	-0.044407	1.021464	Cluster 1	Q86UX7
-0.977074	-0.044375	1.021449	Cluster 1	P07741
-0.95801	-0.079263	1.037273	Cluster 1	P60174
-0.958389	-0.078585	1.036974	Cluster 1	Q14644
-0.956464	-0.08202	1.038484	Cluster 1	P68371
-0.956286	-0.082337	1.038623	Cluster 1	P08648
-0.954309	-0.085846	1.040156	Cluster 1	Q96FN4
-0.952145	-0.08967	1.041815	Cluster 1	P11142
-0.952905	-0.08833	1.041235	Cluster 1	Q9Y6D6
-0.950068	-0.093321	1.043389	Cluster 1	P07737
-0.951283	-0.091188	1.042471	Cluster 1	P00488
-0.948026	-0.096895	1.04492	Cluster 1	Q5HYI8
-0.942282	-0.106854	1.049136	Cluster 1	P08514
-0.943267	-0.105155	1.048422	Cluster 1	P25788
-0.935258	-0.11886	1.054118	Cluster 1	Q9UPU5
-0.938554	-0.113249	1.051803	Cluster 1	P29401
-0.939015	-0.112461	1.051476	Cluster 1	Q14203
-1.142234	0.4245728	0.7176617	Cluster 1	K7EM38
-1.142742	0.4278251	0.714917	Cluster 1	O75608
-1.142721	0.4276866	0.7150341	Cluster 1	P20020
-1.14304	0.4297654	0.7132748	Cluster 1	P14625
-1.142888	0.4287753	0.7141132	Cluster 1	O43150
-1.147079	0.4588379	0.6882415	Cluster 1	P04792
-1.14525	0.4449494	0.700301	Cluster 1	P19086
-1.140232	0.4123089	0.7279232	Cluster 1	P15498

-1.139638	0.4088237	0.730814	Cluster 1	P21333-2
-1.139037	0.4053638	0.7336729	Cluster 1	Q70IA8
-1.138003	0.3995579	0.7384455	Cluster 1	Q15084
-1.138201	0.4006563	0.737545	Cluster 1	Q8NFV4
-1.137765	0.3982412	0.7395236	Cluster 1	O60610
-1.148995	0.4752122	0.673783	Cluster 1	O95167
-1.149084	0.4760334	0.6730509	Cluster 1	E9PSI1
-1.149876	0.4836248	0.6662517	Cluster 1	O95486
-1.151334	0.4993666	0.6519679	Cluster 1	O95373
-1.151517	0.5015538	0.6499632	Cluster 1	Q15386
-1.152507	0.5146445	0.6378625	Cluster 1	Q9H4B7
-1.133605	0.3765259	0.7570789	Cluster 1	Q8NGA1
-1.128595	0.3528632	0.775732	Cluster 1	P07900
-1.126018	0.341509	0.7845092	Cluster 1	P00918
-1.130783	0.3629115	0.7678711	Cluster 1	Q13200
-1.129713	0.3579491	0.7717643	Cluster 1	P50995
-1.129984	0.359198	0.7707865	Cluster 1	Q9NY33
-1.110169	0.2800498	0.8301189	Cluster 1	P00390
-1.114906	0.2971852	0.8177203	Cluster 1	Q12974
-1.121918	0.3243682	0.7975497	Cluster 1	Q9H3U1
-1.118141	0.3094293	0.8087116	Cluster 1	Q01813
-1.119591	0.3150755	0.8045151	Cluster 1	P17858
-1.08725	0.2068525	0.8803974	Cluster 1	Q15746
-1.087493	0.2075626	0.8799302	Cluster 1	P30086
-1.079927	0.1859591	0.8939674	Cluster 1	P62191
-1.079814	0.1856458	0.8941683	Cluster 1	P31946
-1.082716	0.1938022	0.8889135	Cluster 1	P04075
-1.07229	0.1651395	0.9071507	Cluster 1	Q9NZN3
-1.071304	0.1625167	0.9087878	Cluster 1	O75954
-1.069341	0.1573335	0.9120071	Cluster 1	P06132
-1.075955	0.1750156	0.900939	Cluster 1	P00338
-1.095029	0.2302077	0.8648213	Cluster 1	O00442
-1.094679	0.2291289	0.8655503	Cluster 1	Q05397
-1.093105	0.2243092	0.868796	Cluster 1	P52209
-1.104733	0.2613802	0.8433532	Cluster 1	P04899
-1.105512	0.2639973	0.8415151	Cluster 1	O14980
-1.10571	0.2646627	0.8410469	Cluster 1	Q9UEY8
-1.100991	0.2490589	0.8519322	Cluster 1	P17252
-1.100278	0.2467554	0.8535224	Cluster 1	Q13976-2
-1.102479	0.2539103	0.8485689	Cluster 1	P31150
-1.099276	0.2435419	0.8557338	Cluster 1	P35998
-1.097353	0.2374485	0.8599042	Cluster 1	P50851
-0.505342	1.151822	-0.64648	Cluster 2	O94905
-0.556118	1.154443	-0.598325	Cluster 2	Q9UBQ0
-0.524711	1.153147	-0.628436	Cluster 2	O00159

-0.608515	1.154129	-0.545614	Cluster 2	B4DQH6
-0.609694	1.154085	-0.544391	Cluster 2	Q9BSJ8
-0.437108	1.144136	-0.707028	Cluster 2	P30626
-0.354253	1.128903	-0.77465	Cluster 2	Q10588
-0.290774	1.113162	-0.822387	Cluster 2	P17987
-1.034515	0.9614803	0.0730349	Cluster 3	Q13409
-1.031075	0.9657186	0.0653567	Cluster 3	Q8N0Y7
-1.030855	0.9659868	0.0648679	Cluster 3	Q14642
-1.049584	0.9416614	0.1079226	Cluster 3	Q8NF37
-1.043562	0.9498391	0.093723	Cluster 3	O75131
-1.099825	0.8545256	0.245299	Cluster 3	O43776
-1.09331	0.8683758	0.2249347	Cluster 3	O14579
-1.114082	0.8199413	0.2941402	Cluster 3	Q9NVM1
-1.106387	0.8394292	0.2669578	Cluster 3	Q01518-2
-1.104222	0.8445497	0.2596723	Cluster 3	Q06187
-1.114005	0.8201457	0.2938595	Cluster 3	P18031
-1.079038	0.89555	0.1834878	Cluster 3	Q9Y315
-1.077866	0.8976161	0.18025	Cluster 3	P68366
-1.153925	0.5403289	0.6135966	Cluster 3	P52333
-1.15456	0.5616607	0.592899	Cluster 3	Q9Y3A6
-1.154465	0.5570385	0.5974266	Cluster 3	P51148
-1.154673	0.5704717	0.5842016	Cluster 3	Q14432
-1.15385	0.6152891	0.5385614	Cluster 3	P62140
-1.153845	0.6154187	0.5384259	Cluster 3	P40616
-1.127678	0.7789136	0.3487642	Cluster 3	Q15049
-1.14308	0.7130542	0.4300256	Cluster 3	P50148
-1.142228	0.7176976	0.4245302	Cluster 3	Q9UHD2
-1.140687	0.7256673	0.4150193	Cluster 3	Q04759
-1.140471	0.7267432	0.4137276	Cluster 3	P43405
-1.141303	0.7225421	0.4187608	Cluster 3	P55160
-1.13711	0.7424371	0.3946733	Cluster 3	O15498
-1.135913	0.7476115	0.3883018	Cluster 3	O75915
-1.14613	0.6946788	0.4514509	Cluster 3	Q96P48
-1.148016	0.6814538	0.4665621	Cluster 3	Q9BT78
-1.149842	0.6665552	0.4832872	Cluster 3	Q9UJ68
-1.151876	0.6458439	0.5060318	Cluster 3	Q16539
-0.848363	1.10257	-0.254207	Cluster 3	O60234
-0.852816	1.100595	-0.24778	Cluster 3	Q63HN8
-0.785416	1.125744	-0.340327	Cluster 3	P20073
-0.949356	1.043925	-0.094569	Cluster 3	Q05209
-0.937869	1.052288	-0.114419	Cluster 3	Q9UPT5
-0.951807	1.042073	-0.090266	Cluster 3	Q9Y6W5
-0.971142	1.026554	-0.055412	Cluster 3	O15269
-1.000908	0.9990896	0.0018184	Cluster 3	Q01433
-0.921241	1.063519	-0.142277	Cluster 3	O60888

-0.919592	1.06458	-0.144988	Cluster 3	Q96RD7
-0.892435	1.080781	-0.188346	Cluster 3	P51153
0.5516566	-1.154325	0.6026683	Cluster 4	B1AK87
0.4878765	-1.150295	0.6624184	Cluster 4	Q9H0U4
0.5102391	-1.152194	0.6419545	Cluster 4	O75746
0.4432888	-1.145019	0.7017305	Cluster 4	Q96BY6
0.4245389	-1.142229	0.7176903	Cluster 4	Q969M1
0.8198218	-1.114126	0.2943043	Cluster 4	Q93050
0.8015267	-1.120601	0.3190742	Cluster 4	Q15843
0.7720492	-1.129634	0.3575848	Cluster 4	P60228
0.7420198	-1.137205	0.3951852	Cluster 4	Q9BQE3
0.7141064	-1.14289	0.4287833	Cluster 4	P20936
0.7123886	-1.143199	0.4308107	Cluster 4	Q92499
0.6857943	-1.147425	0.4616304	Cluster 4	Q9Y6A9
0.6920593	-1.146523	0.4544642	Cluster 4	I3L440
0.9650126	-1.031654	0.0666412	Cluster 4	Q8TF64
0.9625983	-1.033616	0.0710173	Cluster 4	Q00796
0.9825351	-1.016595	0.0340597	Cluster 4	P63096
1.022744	-0.975587	-0.047157	Cluster 4	Q6PL24
1.016817	-0.982289	-0.034528	Cluster 4	Q9Y2G8
0.9236832	-1.061931	0.1382475	Cluster 4	P43250
0.921083	-1.063621	0.1425378	Cluster 4	Q9P253
0.8942859	-1.079748	0.1854624	Cluster 4	Q16181
0.87511	0.2148536	-1.089964	Cluster 5	P51790
0.8762422	0.2131466	-1.089389	Cluster 5	Q86UT6
0.8698852	0.2226855	-1.092571	Cluster 5	O95563
0.8588995	0.2389204	-1.09782	Cluster 5	P49411
0.8571283	0.2415092	-1.098637	Cluster 5	Q8WVC6
0.8951395	0.1841294	-1.079269	Cluster 5	Q2TAA5
0.8866401	0.1973061	-1.083946	Cluster 5	P30038
0.887756	0.1955881	-1.083344	Cluster 5	A6NFX1
0.8957757	0.1831346	-1.07891	Cluster 5	P18054
0.8867411	0.1971508	-1.083892	Cluster 5	O94919
0.8105881	0.306893	-1.117481	Cluster 5	P22695
0.813715	0.3026501	-1.116365	Cluster 5	P50416
0.813476	0.302975	-1.116451	Cluster 5	O00400
0.8164232	0.2989588	-1.115382	Cluster 5	Q6PIU2
0.8187131	0.2958254	-1.114539	Cluster 5	Q15125
0.8298819	0.2803806	-1.110263	Cluster 5	P13987
0.8270578	0.2843117	-1.111369	Cluster 5	Q9P035
0.8352891	0.2728039	-1.108093	Cluster 5	Q86YW5
0.8414148	0.26414	-1.105555	Cluster 5	Q86VU5
0.986454	0.0265627	-1.013017	Cluster 5	O95298
0.9895095	0.0206608	-1.01017	Cluster 5	P35579
0.9905518	0.018636	-1.009188	Cluster 5	P20674

0.9811796	0.0366341	-1.017814	Cluster 5	Q8WZA9
0.9753326	0.0476325	-1.022965	Cluster 5	Q9BTZ2
0.975701	0.0469446	-1.022645	Cluster 5	Q9H061
0.9431745	0.1053152	-1.04849	Cluster 5	Q3KQZ1
0.9462281	0.1000257	-1.046254	Cluster 5	P08962
0.9643464	0.0678513	-1.032198	Cluster 5	Q9BS26
0.9598472	0.0759721	-1.035819	Cluster 5	Q13586
0.9541303	0.0861635	-1.040294	Cluster 5	P24557
0.9553556	0.083991	-1.039347	Cluster 5	Q9UJZ1
0.9558852	0.0830499	-1.038935	Cluster 5	P05121
0.9561858	0.0825154	-1.038701	Cluster 5	P51659
0.9559832	0.0828757	-1.038859	Cluster 5	Q14766
0.9519175	0.090071	-1.041989	Cluster 5	Q9H7M9
0.9491734	0.0948888	-1.044062	Cluster 5	O00151
0.9229825	0.1394061	-1.062389	Cluster 5	Q96A26
0.9200824	0.1441825	-1.064265	Cluster 5	P39656
0.9155231	0.1516341	-1.067157	Cluster 5	Q9H3N1
0.9179335	0.1477032	-1.065637	Cluster 5	Q92604
0.905049	0.1684947	-1.073544	Cluster 5	Q9C0E8
0.9014618	0.1741891	-1.075651	Cluster 5	Q9Y2Z4
0.9103149	0.160062	-1.070377	Cluster 5	P10515
0.9293803	0.1287652	-1.058145	Cluster 5	O75947
0.9249159	0.1362055	-1.061121	Cluster 5	Q9Y251
0.9327058	0.1231766	-1.055882	Cluster 5	P02671
0.9337073	0.1214855	-1.055193	Cluster 5	O14653
0.9359607	0.1176674	-1.053628	Cluster 5	Q9UBN7
0.936091	0.1174459	-1.053537	Cluster 5	Q8NE86
0.9388261	0.1127847	-1.051611	Cluster 5	P39210
1.124087	-0.333304	-0.790783	Cluster 5	Q9NRZ7
1.12849	-0.352391	-0.7761	Cluster 5	Q8TC12
1.125137	-0.337734	-0.787403	Cluster 5	P48449
1.113764	-0.292974	-0.82079	Cluster 5	Q9Y6C2
1.117537	-0.307106	-0.810431	Cluster 5	Q12846
1.116208	-0.302058	-0.81415	Cluster 5	P02776
1.117097	-0.305427	-0.81167	Cluster 5	P35914
1.110248	-0.28033	-0.829918	Cluster 5	P23368
1.110963	-0.282864	-0.8281	Cluster 5	Q9BT22
1.108521	-0.274287	-0.834235	Cluster 5	J3KN67
1.105187	-0.262903	-0.842285	Cluster 5	Q9HDC9
1.106748	-0.268187	-0.838561	Cluster 5	Q8WWA1
1.107189	-0.269694	-0.837495	Cluster 5	Q8IYS2
1.106421	-0.267074	-0.839347	Cluster 5	Q9NZC3
1.105899	-0.265302	-0.840596	Cluster 5	P13073
1.070383	-0.160079	-0.910305	Cluster 5	P02751
1.068995	-0.156426	-0.912568	Cluster 5	Q9Y274

1.065502	-0.147355	-0.918146	Cluster 5	O43674
1.066779	-0.150653	-0.916126	Cluster 5	Q16836
1.063431	-0.142054	-0.921377	Cluster 5	O00217
1.090229	-0.215645	-0.874584	Cluster 5	Q9BWM7
1.094706	-0.229211	-0.865495	Cluster 5	Q9Y2G3
1.080943	-0.188802	-0.892141	Cluster 5	P36551
1.079931	-0.185971	-0.89396	Cluster 5	Q96HV5
1.077022	-0.177932	-0.89909	Cluster 5	P27824
1.086054	-0.203373	-0.882681	Cluster 5	P51575
1.083769	-0.1968	-0.886969	Cluster 5	Q9P0L0
1.084279	-0.198258	-0.886021	Cluster 5	Q9Y6N5
1.028972	-0.06071	-0.968262	Cluster 5	Q13011
1.024646	-0.051263	-0.973383	Cluster 5	Q6YHK3
1.020252	-0.041815	-0.978436	Cluster 5	Q13642-1
1.014428	-0.02951	-0.984918	Cluster 5	P20933
1.009983	-0.020274	-0.989709	Cluster 5	O14561
1.014418	-0.029488	-0.98493	Cluster 5	Q04941
1.01113	-0.022644	-0.988486	Cluster 5	Q9BQA9
1.017682	-0.036355	-0.981327	Cluster 5	O95674
1.003062	-0.006152	-0.99691	Cluster 5	O14735
0.9979499	0.0040876	-1.002038	Cluster 5	Q13505
1.006279	-0.012678	-0.993601	Cluster 5	P36542
1.002746	-0.005515	-0.997231	Cluster 5	Q14BN4
1.037907	-0.080705	-0.957202	Cluster 5	O14523
1.039786	-0.084997	-0.954789	Cluster 5	Q13201
1.038826	-0.0828	-0.956026	Cluster 5	P35749
1.035895	-0.076143	-0.959752	Cluster 5	O95427
1.051194	-0.111782	-0.939412	Cluster 5	Q9H3P7
1.0497	-0.1082	-0.9415	Cluster 5	Q9H7J1
1.055023	-0.12107	-0.933953	Cluster 5	P24539
1.041789	-0.089609	-0.95218	Cluster 5	Q6NVY1
1.044118	-0.095018	-0.9491	Cluster 5	Q02218
1.046432	-0.100446	-0.945986	Cluster 5	Q13423
1.045934	-0.099272	-0.946661	Cluster 5	O15533
1.046236	-0.099983	-0.946253	Cluster 5	Q8IZ81
1.047288	-0.102467	-0.944821	Cluster 5	Q9UHQ9
1.142977	-0.42935	-0.713627	Cluster 5	Q96MH6
1.143569	-0.433269	-0.710301	Cluster 5	Q9HCE1
1.145433	-0.446276	-0.699157	Cluster 5	P61009
1.136308	-0.390383	-0.745926	Cluster 5	P02768
1.132528	-0.371237	-0.761291	Cluster 5	P05166
1.140925	-0.416455	-0.72447	Cluster 5	Q9UHQ4
1.14061	-0.414556	-0.726053	Cluster 5	O43865
1.13842	-0.401879	-0.736541	Cluster 5	P04843
1.149488	-0.479834	-0.669654	Cluster 5	P04179

1.15424	-0.548897	-0.605344	Cluster 5	P30405
1.153472	-0.530616	-0.622856	Cluster 5	P02675
1.153392	-0.529103	-0.624289	Cluster 5	Q96NB2
1.149222	-0.671903	-0.47732	Cluster 5	O60762
1.14783	-0.68284	-0.46499	Cluster 5	P09486
1.147228	-0.687194	-0.460034	Cluster 5	O95182
1.1513	-0.652335	-0.498965	Cluster 5	P11182
1.152536	-0.637474	-0.515062	Cluster 5	Q9BSF4
1.154607	-0.590039	-0.564568	Cluster 5	Q9NS69
1.154643	-0.58727	-0.567373	Cluster 5	Q96HD1
1.153831	-0.615716	-0.538115	Cluster 5	P07477
1.153363	-0.624809	-0.528554	Cluster 5	Q9Y3E5
1.153414	-0.623907	-0.529507	Cluster 5	P32189
1.154256	-0.604858	-0.549398	Cluster 5	Q9NZ45
1.100761	-0.852448	-0.248313	Cluster 5	Q9UBV2
1.089383	-0.876253	-0.213131	Cluster 5	O95140
1.090611	-0.873827	-0.216784	Cluster 5	Q5VY43
1.125486	-0.786263	-0.339223	Cluster 5	P10909
1.127935	-0.778029	-0.349906	Cluster 5	P00367
1.128875	-0.774748	-0.354128	Cluster 5	D6RIE3
1.121385	-0.799172	-0.322213	Cluster 5	Q8IWA5
1.118165	-0.808644	-0.309521	Cluster 5	P19367
-0.227321	1.094091	-0.86677	Cluster 6	P67812
-0.16435	1.071994	-0.907644	Cluster 6	Q86WI1
-0.193404	1.082575	-0.889171	Cluster 6	A1L0T0
-0.087448	1.040852	-0.953404	Cluster 6	P02656
-0.047344	1.022831	-0.975487	Cluster 6	Q9H845
-0.018344	1.009046	-0.990702	Cluster 6	Q9NXH8
0.0025953	0.9986998	-1.001295	Cluster 6	Q6ZRH9
0.3096433	0.808553	-1.118196	Cluster 6	O00264
0.3089626	0.8090572	-1.11802	Cluster 6	O75955
0.2729767	0.8351663	-1.108143	Cluster 6	Q14165
0.2798586	0.8302559	-1.110115	Cluster 6	Q5K4L6
0.3346477	0.7897593	-1.124407	Cluster 6	O60831
0.333151	0.7908992	-1.12405	Cluster 6	O43561
0.3438243	0.7827284	-1.126553	Cluster 6	Q05682
0.3439388	0.7826403	-1.126579	Cluster 6	Q6UXV4
0.3590273	0.7709203	-1.129948	Cluster 6	Q14677
0.3656352	0.7657251	-1.13136	Cluster 6	Q15526
0.1709799	0.9034865	-1.074466	Cluster 6	P49748
0.1959979	0.88749	-1.083488	Cluster 6	P02775
0.2003417	0.8846628	-1.085005	Cluster 6	P06753
0.1847758	0.8947257	-1.079502	Cluster 6	Q8TDM6
0.2553587	0.8475611	-1.10292	Cluster 6	Q93084-2
0.2395118	0.8584954	-1.098007	Cluster 6	O95573

0.2150426	0.8749844	-1.090027	Cluster 6	P01891
0.2215878	0.8706204	-1.092208	Cluster 6	O96008
0.221614	0.8706029	-1.092217	Cluster 6	Q15363
0.1173058	0.9361735	-1.053479	Cluster 6	P12236
0.1182741	0.9356033	-1.053877	Cluster 6	P12074
0.7821378	0.3445909	-1.126729	Cluster 6	P62341
0.7854814	0.3402424	-1.125724	Cluster 6	P30049
0.7731604	0.3561629	-1.129323	Cluster 6	P61073
0.7391602	0.3986853	-1.137845	Cluster 6	P27338
0.7347651	0.4040384	-1.138803	Cluster 6	P61619
0.7469215	0.389154	-1.136075	Cluster 6	P43304
0.7527217	0.3819646	-1.134686	Cluster 6	Q96G23
0.7575126	0.3759828	-1.133495	Cluster 6	Q9Y487
0.7614167	0.3710786	-1.132495	Cluster 6	Q969X5
0.7579426	0.3754439	-1.133386	Cluster 6	P09622
0.7203373	0.4213911	-1.141728	Cluster 6	P48047
0.7075265	0.4365245	-1.144051	Cluster 6	Q5VWC8
0.7127409	0.4303953	-1.143136	Cluster 6	P04844
0.707095	0.4370298	-1.144125	Cluster 6	P07996
0.6406387	0.5116581	-1.152297	Cluster 6	P15121
0.6501635	0.5013355	-1.151499	Cluster 6	P38117
0.6479989	0.503692	-1.151691	Cluster 6	Q7Z7H5
0.6726753	0.4764545	-1.14913	Cluster 6	Q96ER9
0.6720912	0.4771087	-1.1492	Cluster 6	O43306
0.6685157	0.4811041	-1.14962	Cluster 6	H7BYY1
0.6771619	0.4714121	-1.148574	Cluster 6	P35232
0.6859699	0.4614304	-1.1474	Cluster 6	Q9UFN0
0.6933592	0.4529702	-1.146329	Cluster 6	P08913
0.4198109	0.7216627	-1.141474	Cluster 6	P16615
0.4190405	0.7223079	-1.141348	Cluster 6	Q9UBF2
0.4120217	0.7281619	-1.140184	Cluster 6	Q96LW7-2
0.4124805	0.7277805	-1.140261	Cluster 6	O43169
0.45107	0.6950094	-1.146079	Cluster 6	Q9H444
0.4302529	0.7128617	-1.143114	Cluster 6	P02679
0.4380286	0.7062414	-1.14427	Cluster 6	Q9UIQ6
0.5150383	0.6374958	-1.152534	Cluster 6	P46977
0.5342592	0.6193947	-1.153654	Cluster 6	O60704
0.532912	0.6206762	-1.153588	Cluster 6	P48509
0.4831066	0.6667176	-1.149824	Cluster 6	Q96QS1
0.4809377	0.6686649	-1.149603	Cluster 6	P09669
0.5613524	0.5932016	-1.154554	Cluster 6	P40197
0.5582105	0.5962809	-1.154491	Cluster 6	Q9Y3B3
0.5723994	0.582287	-1.154686	Cluster 6	Q14643
0.5802211	0.5744746	-1.154696	Cluster 6	P21926
0.5882288	0.566403	-1.154632	Cluster 6	P43307

0.6012624	0.5531033	-1.154366	Cluster 6	Q9Y276
0.6197206	0.5339168	-1.153637	Cluster 6	Q7L1W4

Table 2. Dataset of significantly changed soluble proteins after cluster analysis

ADP	Collagen	Thr. & Collagen	Cluster	Accession
-1.053985	0.1185352	0.9354495	Cluster 1	P49327
-1.03846	0.0819644	0.9564953	Cluster 1	P06744
-1.002334	0.0046855	0.997649	Cluster 1	Q92499
-0.9447944	-0.1025138	1.047308	Cluster 1	O95295
-1.154282	0.5502121	0.6040697	Cluster 1	P51148
-1.15199	0.5075223	0.6444681	Cluster 1	P61224
-1.152938	0.5212321	0.6317056	Cluster 1	Q9UIA9
-1.146223	0.4521604	0.6940628	Cluster 1	Q684P5
-1.110773	0.2821889	0.8285844	Cluster 1	P55060
-1.109835	0.2788745	0.8309605	Cluster 1	Q86VP6
-1.104945	0.2620884	0.8428563	Cluster 1	Q9BT78
-1.099652	0.2447466	0.8549058	Cluster 1	Q08752
-1.097471	0.2378197	0.859651	Cluster 1	P22234
-1.08603	0.2033035	0.8827266	Cluster 1	P12429
-1.130738	0.3627031	0.768035	Cluster 1	Q32MZ4
-1.117356	0.3064151	0.810941	Cluster 1	Q7L576
-1.121113	0.3211222	0.799991	Cluster 1	Q8NBF2
-1.126833	0.781787	0.3450459	Cluster 1	O95373
-1.128526	0.775975	0.3525509	Cluster 1	P41250
-1.13287	0.7599642	0.3729062	Cluster 1	Q9C0C9
-1.131035	0.7669388	0.3640958	Cluster 1	P17252
-1.130082	0.7704344	0.3596473	Cluster 1	P20339
-1.116252	0.814029	0.3022228	Cluster 1	Q9UJ70
-1.15126	0.6527637	0.4984967	Cluster 1	O14617
-1.150159	0.663685	0.4864739	Cluster 1	Q13045
-1.149781	0.6671054	0.4826751	Cluster 1	Q15056
-1.145733	0.6972504	0.4484829	Cluster 1	P52333
-0.8686172	1.093193	-0.2245755	Cluster 2	O00410
-0.8355334	1.107993	-0.27246	Cluster 2	P68371
-0.9027758	1.074884	-0.1721078	Cluster 2	Q08AM6
-0.8992599	1.076925	-0.1776648	Cluster 2	O00264
-0.9268119	1.059866	-0.1330543	Cluster 2	Q13057
-0.777661	1.128041	-0.3503803	Cluster 2	Q9BSF0
-1.056427	0.9319108	0.1245163	Cluster 2	P16278
-0.9940099	1.005884	-0.0118744	Cluster 2	P35749-3
-0.0970316	1.044979	-0.9479473	Cluster 2	Q9Y265
-0.0863097	1.040357	-0.9540477	Cluster 2	P30048
-0.0354946	1.017275	-0.9817801	Cluster 2	P36543

-0.0398619	1.019335	-0.979473	Cluster 2	P18085
0.0817288	0.9566276	-1.038356	Cluster 2	P14543
-0.2705474	1.107438	-0.8368905	Cluster 2	Q15118
-0.3012677	1.115998	-0.8147305	Cluster 2	P07437
-0.2273059	1.094086	-0.8667802	Cluster 2	Q99798
-0.427606	1.142708	-0.7151022	Cluster 2	P61604
-0.4152507	1.140725	-0.7254744	Cluster 2	Q14258
-0.5723566	1.154686	-0.5823295	Cluster 2	Q13201
-0.5477464	1.154203	-0.6064565	Cluster 2	O00186
-0.5321098	1.153548	-0.6214384	Cluster 2	Q9NY65
-0.2229005	-0.8697411	1.092642	Cluster 3	Q9H2M9
-0.1878234	-0.8927705	1.080594	Cluster 3	P00488
-0.2039687	-0.8822908	1.086259	Cluster 3	P47755
-0.281084	-0.8293775	1.110461	Cluster 3	P62191
-0.4108858	-0.7291049	1.139991	Cluster 3	Q7Z460
0.1667686	-1.0729	0.9061314	Cluster 3	P18433
0.2418448	-1.098743	0.8568983	Cluster 3	Q9Y490
0.2603735	-1.104432	0.8440587	Cluster 3	P32321
0.0537566	-1.025794	0.9720375	Cluster 3	Q16363
-0.0503577	-0.9738697	1.024227	Cluster 3	P30740
-0.5311452	-0.622354	1.153499	Cluster 3	Q5VVQ6
-0.6426218	-0.5095188	1.152141	Cluster 3	O15327
-0.6047277	-0.549533	1.154261	Cluster 3	Q01518-2
-0.6226315	-0.5308526	1.153484	Cluster 3	Q8N5N7
-0.8331758	-0.2757729	1.108949	Cluster 3	Q13813
-0.8043911	-0.3152417	1.119633	Cluster 3	P49257
0.6977954	-1.145648	0.4478527	Cluster 4	O15117-2
0.4797578	-1.14948	0.6697223	Cluster 4	Q9UL46
0.53811	-1.153831	0.6157209	Cluster 4	Q9UBV8
0.5832486	-1.15468	0.5714318	Cluster 4	P68133
0.3746625	0.7585657	-1.133228	Cluster 5	Q16706
0.3779742	0.7559212	-1.133895	Cluster 5	P40939
0.2641683	0.8413948	-1.105563	Cluster 5	P02763
0.4736593	0.6751655	-1.148825	Cluster 5	P00387
0.5220804	0.6309093	-1.15299	Cluster 5	P46063
0.7716715	0.3580676	-1.129739	Cluster 5	Q9UHQ9
0.7282298	0.4119399	-1.14017	Cluster 5	P30084
0.7479907	0.387833	-1.135824	Cluster 5	P02679
0.6968491	0.4489467	-1.145796	Cluster 5	P05121
0.6697477	0.4797294	-1.149477	Cluster 5	P09486
0.6582366	0.492492	-1.150729	Cluster 5	P02675
0.631094	0.5218838	-1.152978	Cluster 5	P02768
1.077674	-0.1797212	-0.8979528	Cluster 6	P16284
1.055766	-0.1228921	-0.9328744	Cluster 6	Q9UII2
1.054848	-0.120642	-0.9342061	Cluster 6	P10720

1.065631	-0.1476876	-0.9179431	Cluster 6	P60891
1.063429	-0.1420497	-0.9213795	Cluster 6	Q15365
1.008932	-0.0181098	-0.9908221	Cluster 6	P04792
0.9998169	0.0003661	-1.000183	Cluster 6	P18859
1.018202	-0.0374572	-0.9807451	Cluster 6	Q9NTJ5
1.019166	-0.0395025	-0.9796634	Cluster 6	Q14344
1.026088	-0.054397	-0.9716913	Cluster 6	P10124
0.9481615	0.0966577	-1.044819	Cluster 6	P04003
0.9438235	0.104194	-1.048018	Cluster 6	P05067
0.9539104	0.0865528	-1.040463	Cluster 6	P10909
0.9756541	0.0470321	-1.022686	Cluster 6	P07996
0.9740278	0.0500638	-1.024092	Cluster 6	P02671
0.8619419	0.2344552	-1.096397	Cluster 6	P53990
0.8776724	0.2109856	-1.088658	Cluster 6	Q96J92
0.9104578	0.159832	-1.07029	Cluster 6	P48449
0.9192192	0.1455987	-1.064818	Cluster 6	P02775
1.153975	-0.6124327	-0.5415422	Cluster 6	P43034
1.154148	-0.6080086	-0.5461394	Cluster 6	P67936-2
1.154157	-0.6077498	-0.5464075	Cluster 6	Q9Y6C2
1.153454	-0.6231738	-0.5302805	Cluster 6	P21912
1.152896	-0.6323369	-0.5205588	Cluster 6	P04275
1.154341	-0.5522023	-0.6021382	Cluster 6	Q96C24
1.154514	-0.5592663	-0.5952474	Cluster 6	P51149
1.154695	-0.5742682	-0.5804269	Cluster 6	P24752
1.154587	-0.5913356	-0.5632511	Cluster 6	P68871
1.151199	-0.6534145	-0.4977848	Cluster 6	P49753
1.150242	-0.662917	-0.4873246	Cluster 6	Q96G03
1.149211	-0.672003	-0.4772076	Cluster 6	Q06830
1.14474	-0.4413062	-0.7034338	Cluster 6	P28676
1.145113	-0.4439611	-0.7011521	Cluster 6	Q15208
1.139054	-0.4054612	-0.7335925	Cluster 6	P48047
1.141561	-0.4203529	-0.7212083	Cluster 6	Q6ZRH9
1.142407	-0.425669	-0.7167377	Cluster 6	P22307
1.142098	-0.4237065	-0.7183911	Cluster 6	P10606
1.153676	-0.5347185	-0.6189573	Cluster 6	P02751
1.152828	-0.5194938	-0.6333347	Cluster 6	Q9Y251
1.149344	-0.478467	-0.6708775	Cluster 6	O75563
1.150488	-0.489907	-0.6605813	Cluster 6	P04004
1.127853	-0.3495432	-0.7783101	Cluster 6	Q5HYI8
1.128514	-0.3524962	-0.7760175	Cluster 6	P30042
1.125121	-0.3376674	-0.7874537	Cluster 6	P01137
1.126171	-0.3421667	-0.7840038	Cluster 6	P14649
1.131622	-0.3668786	-0.7647432	Cluster 6	M0R042
1.114237	-0.2947133	-0.8195239	Cluster 6	P36776
1.116423	-0.3028688	-0.8135541	Cluster 6	Q14766

1.115403	-0.299036	-0.8163666	Cluster 6	O95182
1.115428	-0.2991325	-0.8162959	Cluster 6	P10809
0.9156253	-1.067093	0.1514679	Cluster 6	P52209
0.8953103	-1.079173	0.1838625	Cluster 6	P08133
0.8828682	-1.085956	0.2030873	Cluster 6	Q9Y4L1
0.961387	-1.03459	0.0732029	Cluster 6	Q13418
0.9458901	-1.046503	0.1006132	Cluster 6	O00161
0.9912961	-1.008482	0.0171864	Cluster 6	P61952
1.025249	-0.9726772	-0.0525717	Cluster 6	Q9NYU2
1.033387	-0.9628813	-0.0705056	Cluster 6	Q9Y6E0
1.063331	-0.921532	-0.1417986	Cluster 6	P46379
1.056438	-0.931895	-0.1245428	Cluster 6	P50440
1.048262	-0.9434884	-0.1047732	Cluster 6	Q0ZGT2
1.07481	-0.9029018	-0.171908	Cluster 6	Q9UDY2
1.093024	-0.8689609	-0.2240637	Cluster 6	P37840
1.093358	-0.8682792	-0.2250785	Cluster 6	Q9BS40
1.104856	-0.843065	-0.261791	Cluster 6	P51970
1.100996	-0.8519216	-0.2490741	Cluster 6	O75347
1.101325	-0.8511834	-0.2501413	Cluster 6	P14618-2
1.098941	-0.856467	-0.2424738	Cluster 6	P33908
1.098796	-0.8567828	-0.2420132	Cluster 6	O60925
1.138163	-0.7377206	-0.4004422	Cluster 6	Q8N841
1.13717	-0.7421763	-0.3949933	Cluster 6	P09622
1.136183	-0.7464616	-0.3897216	Cluster 6	Q04917
1.118979	-0.8062969	-0.3126826	Cluster 6	Q15075
1.116122	-0.8143879	-0.3017343	Cluster 6	Q8IZ83
1.11227	-0.824727	-0.287543	Cluster 6	Q92614
1.124618	-0.78908	-0.3355384	Cluster 6	Q15819
1.126057	-0.7843807	-0.3416762	Cluster 6	Q5VZU9
1.129947	-0.7709207	-0.3590267	Cluster 6	P69905

3. Into the platelet derived microparticle membrane PTM-ome

ABSTRACT

As previously shown, platelet activation is mediated by different platelet membrane receptor and their activity in response to stimuli. These receptors are mainly phosphorylated and glycosylated. With the aim of investigating these receptors activity, in this study we also carried out a PTMs analysis of PMPs. Relevant platelet agonist such as ADP, thrombin and collagen were used for the activation. Thrombin, which is mostly used to generate PMPs *in vitro* was set as control. By using previously published protocols for the simultaneous enrichment of phosphorylated and glycosylated peptides, we identified 1225 unique phosphopeptides assigned to 614 phosphoproteins and 1245 unique glycosylated peptides assigned to 533 unique glycoproteins. By performing an iTRAQ-based quantitative experiment and following a known physiological agonist strength scale, our results revealed that glycosylation on focal adhesion related proteins as integrins is related to the agonist strength used for platelet activation.

1. INTRODUCTION

Platelet-derived microparticles (PMPs) are a heterogeneous population of vesicles (0.1-1 μm) generated from the plasma membrane upon platelet activation by various stimuli or apoptosis. Microparticles are released from several cell types such as leukocytes, erythrocytes, endothelial and cancer cells [1]. Recently, it was shown that adipocytes [2], megakaryocytes [3] and central nervous system related cells [4] are known to release microparticles. However, those generated from activated platelet represent the major population of circulating microparticles in the human plasma [5]. Exosomes, which are known to be secreted from activated platelet as well, are smaller on average than PMPs (0.04 and 0.1 μm) and stored within α-granules. [6]. Elevated PMP levels have been detected in several pathological conditions such as uremia [7], infectious diseases [8,9], acute coronary syndrome [10], ischemic attack [11], immune thrombocytopenic purpura [12], diabetes mellitus [13] and cancer [14,15]. PMPs were shown to bind to hematopoietic progenitors improving their engraftment [16] and endothelial cells protecting them from apoptosis [17]. Multiple pathways are involved in platelet activation, including those induced by biomechanical such as high shear stress [18] and biochemical agonist such as ADP, collagen, epinephrine, serotonin and thrombin [19-22]. Activations promoted by those agonists are also defined sustained calcium induced platelet (SCIP) morphology, due to the role of intracellular Ca^{2+} concentration for the microparticles generation. In particular, breakage of the contact between platelet glycoprotein Ib beta chain and cytoskeleton is the trigger event in mechanical platelet stimulation [23] as well as integrin $\alpha_{IIb}\beta_3$ receptor activity in biochemical activation [24]. However, microparticles shedding is known to be

driven by common steps such as signalling receptors recognition, cytoskeletal remodelling, calpain/caspase activity and mitochondrial depolarization [25]. Platelet membrane receptors play a central role during activation and primary hemostasis, interestingly most of these proteins are glycosylated and phosphorylated such as integrins [26]. However, platelet membrane glycoproteins were shown to mediate, by acting as receptors, several functions such as adhesion to the subendothelial matrix and platelet-platelet aggregation [27]. Platelet membrane glycoproteins were shown to be also involved in pathological conditions such as Bernard-Soulier syndrome [28], coronary artery [29] and renal diseases [30]. Platelet N-glycoproteome has been already elucidated [31,32] as well as platelet phosphoproteome has been intensely investigated [33-35]. However, phosporylated and glycosylated sites have, respectively, still to be elucidated in platelet derived microparticles. In this study, we performed a comprehensive proteomic analysis aimed to characterize the membrane phosphoproteome and glycoproteome of PMPs. In addition, by using iTRAQ-based quantitative proteomics we were able to quantify membrane-associated phosphoproteins and glycoproteins from differentially activated platelet samples. In particular, known physiological agonists were used for platelet activation; those agonists were chosen according to a previously reported agonist strength scale [36]. Thrombin, which is mostly used to generate PMPs *in vitro* was set as control [37]. Modified peptide enrichments were carried out using previously published method with minor modifications [38-41]. Our analysis revealed the membrane phosphoproteome and glycoproteome of PMPs showing also by using quantitative proteomics that glycosylation on focal adhesion associated proteins, mainly integrins, is related to the agonist strength used for platelet activation.

2. MATERIALS AND METHODS

All chemicals were purchased from Sigma (St. Louis, MO, USA) unless stated otherwise. Ultrapure water was from an ELGA Purelab Ultra water system (Bucks, U.K.).

Microparticles isolation - PMPs were obtained from fresh apheresis platelet provided by three healthy subject in accordance with the guidelines of the University of Southern Denmark (SDU) and the Odense University Hospital (OUH). Platelets were isolated and activated as previously described with minor modifications [42,43]. Briefly, platelets were pelleted by centrifugation at 700 x g for 20 min at 20°C. The pellet was washed twice with 137 mmol l^{-1} NaCl, 2.6 mmol l^{-1} KCl, 1 mmol l^{-1} MgCl$_2$, 11.9 mmol l^{-1} NaHCO$_3$, 5.6 mmol l^{-1} D-Glucose and 1 mmol l^{-1} EDTA (Buffer A, pH = 6.5), and resuspended in buffer A without EDTA (Buffer B, pH = 6). Platelet suspensions were divided in four aliquots of 5 ml each and stimulated in presence of a) 10 µmol l^{-1} ADP [42], b) 1 U ml^{-1} thrombin, c) 20 µg ml^{-1} collagen and d) 1 U ml^{-1} thrombin plus 20

μg ml^{-1} collagen. The mixtures were incubated for 10 min at 37°C for ADP stimulation and for 30 min at 37°C for the other treatments. Finally, the activations were stopped by adding 2.5 mmol l^{-1} final concentration of EDTA or 2 mmol l^{-1} EGTA in the case of the ADP stimulation. Activated platelets were removed by centrifugation at 700 x g and 1,000 x g for 20 min at 20°C and the supernatants containing platelet derived MPs suspensions were collected. Platelet derived MPs were then pelleted by centrifugation at 130,000 x g for 60 min at 4°C.

MP lysis and protein digestion – PMPs pellets were resuspended in ice-cold Na$_2$CO$_3$ buffer (0.1 M, pH = 11) containing protease inhibitor (Roche complete EDTA free, Meylan, France), PhosSTOP phosphatase inhibitor cocktail (Roche, Meylan, France) and 10 mM sodium pervanadate on ice. The suspension was tip probe sonicated for 20 sec (amplitude = 50%) twice and incubated on ice for 60 min to lyse the microparticles. The lysate was then centrifuged at 100,000 x g for 90 min at 4°C to enrich membrane proteins (pellet). The supernatant (soluble proteins) was concentrated using 10 kDa cutoff Amicon ultra centrifugal filters units (Millipore, Billerica, MA,USA) whereas membrane fraction was redissolved directly in urea 6 M, thiourea 2 M and tip probe sonicated for 20 sec (amplitude = 20%). Both fractions were reduced in 10 mM dithiothreitol (DTT) for 30 min and then alkylated in 20 mM iodoacetamide (IAA) for 30 min at room temperature in the dark. Lysyl Endopeptidase C (Wako, Osaka, Japan) was added for 3 h (1:100 w/w) and then the samples were diluted 8 times with 50 mM triethylammonia bicarbonate (TEAB, pH = 8). Trypsin was added at a ratio of 1:50 (w/w) and left overnight at 37°C to digest. Following incubation, samples were acidified with formic acid (2% final concentration) and centrifuged at 14,000 x g for 10 min to stop trypsin digestion and precipitate insoluble material such as lipids. The supernatant was purified using in-house packed staged tips with Poros R2 and Oligo R3 reversed phase resins (Applied Biosystem, Foster City, CA, USA). Briefly, a small plug of C$_{18}$ material (3M Empore) was inserted in the constricted end of a P200 tips, followed by packing of the stage tip with the resin (resuspended in 100% ACN) by applying gentle air pressure. The acidified sample was loaded onto the micro-column, after equilibration of the column with 0.1% trifluoroacetic acid (TFA), washed twice with 0.1% TFA and peptides were eluted with 60% ACN/0.1% TFA. A small amount of purified peptides (6 μl) was dried down and subjected to amino acid composition analysis to determine the concentration, while the remaining sample was lyophilized prior to iTRAQ labeling.

iTRAQ labeling and peptide fractionation – Equal amount of peptides from each condition were iTRAQ 4-plex^{TM} labeled according to manufacturer's instructions (Applied Biosystem, Foster City, CA, USA). Labeled peptides were combined in 1:1:1:1 proportion based on the quantification

achieved from the amino acid composition analysis and MALDI-MS/MS analysis (Bruker Daltonics, Billerica, CA, USA, in lift mode). The samples were labeled as follow: ADP, iTRAQ-114; thrombin (control), iTRAQ-115; collagen, iTRAQ-116; thrombin plus collagen, iTRAQ-117.

Simultaneous enrichment of phosphopeptides and formerly N-sialylated glycopeptides - The peptide mixture was resuspended in TiO_2 loading buffer (80% ACN, 5% TFA, 1 M glycolic acid). The optimal amount of TiO_2 beads (0.6 mg/100 µg peptide mixture) was added and the tube was mixed on a shaker at room temperature for 10 minutes. After incubation, the sample was centrifuged to pellet the beads. The supernatant was removed carefully without disturbing the beads. The beads were washed first with 100 µL of washing buffer 1 (80% ACN, 1% TFA) and with washing buffer 2 (20% ACN, 0.1% TFA), mixed for 15 s, centrifuged to pellet the beads, and the solvent was collected. This final step was performed in order to remove peptides that bind to TiO_2 due to hydrophilic interactions (mainly N-linked glycopeptides). The TiO_2 beads were dried in the vacuum centrifuge. The TiO_2 beads were subsequently incubated with 100 µL of pH = 11.3 ammonia solution under shaking. After incubation, the beads were pelleted, the peptides were eluted and dried by lyophilization prior to SIMAC. The peptides were redissolved in 50mM TEAB (pH = 8) and treated with PNGaseF (Roche) and Sialidase A (Prozyme, CA, USA) overnight at 37°C to remove linked glycans, the mixture was then acidified and dried. After deglycosylation, the SIMAC peptide enrichment was performed essentially as previously described [38]. Briefly, the lyophilized peptides were redissolved in 200 µL of 50% ACN, 0.1% TFA. The pH was adjusted to 1.6-1.8 using 10% TFA. A total of 70 µL of IMAC slurry (PhosSelect, Sigma-Aldrich, St. Louis, MO, USA) were washed twice with 50% ACN, 0.1% TFA prior to incubation with the peptide solution. The IMAC beads were incubated with the peptide solution for 30 min at room temperature under shaking. After incubation, the solution was introduced into a constricted 200 µL GeLoader tip and the liquid pressed through the tip using gentle air pressure. The flow through was collected (containing monophosphorylated and formerly N-sialylated peptides). The IMAC column was washed with 60 µL of the loading buffer (50% ACN, 0.1% TFA), which was collected together with the flow through. The multiply phosphorylated peptides were subsequently eluted from the IMAC material using 80 µL of pH = 11.3 ammonia solution. The IMAC flow through was adjusted to 70% ACN, 1% TFA and incubated for 10 min under continuous shaking with the same amount of TiO_2 material as used in the first TiO_2 purification. After incubation, the beads were pelleted by centrifugation, and the supernatant was collected and subsequently incubated with half the amount of TiO_2 beads for 10 min under continuous shaking. After the second incubation, the beads were pelleted by centrifugation and the supernatant was collected (sialylated N-linked glycopeptides). The two pools of TiO2 beads were washed once with 50% ACN, 0.1% TFA and the beads were pelleted. After

drying the TiO$_2$ beads in a vacuum centrifuge, the mono phosphorylated peptides were incubated with 100 µL of pH = 11.3 ammonia solution for 10 min under continuous shaking. All of peptide samples were purified using Poros Oligo R3 RP microcolumns.

Enrichment of N-linked glycopeptides - N-linked glycopeptides were enriched using an homemade HILIC micro-column. Briefly, a small plug of C$_8$ material (3M Empore) was inserted in the constricted end of a P200 tips, followed by packing of the stage tip with PolyHYDROXYETHYL A^{TM} (PolyLC, Columbia, MD), resuspended in 100% ACN, by applying a gentle pressure. The peptide samples, containing the flow though and the N-linked peptide fractions of the first TiO$_2$ pre-purification, were resuspended in 80% ACN 1% TFA, loaded onto the micro-column, washed twice with 80% ACN 0.1% TFA and N-linked glycopeptides were eluted with 0.1% TFA. Samples were dried down, redissolved in 50mM TEAB (pH = 8) and treated with PNGaseF overnight at 37°C to remove N-linked glycans. After deglycosylation, N-linked deglycosylated peptides were purified using Poros Oligo R3 RP microcolumns.

Peptide fractionation – Formerly N-sialylated deglycopeptide samples were fractionated by using hydrophilic interaction chromatography (HILIC) on an Agilent 1200 HPLC system. Samples were loaded onto a 450 µm OD x 320 µm ID x 17 cm micro-capillary column packed with TSK-gel Amide 80 (3 µm, Tosoh Bioscience, Japan). Peptides were resuspended in solvent B (90% ACN 0.1% TFA) and eluted over a gradient of 100% to 60% solvent B (solvent A = 0.1% TFA) over 35 min, followed by 60% to 0% over 7 min at a flow rate of 6 µl/min. HILIC fractions were combined into eight samples and lyophilized [44].

Reversed phase nLC-MS/MS - Dried fractions were resuspended in 0.1% FA (solvent A) and loaded onto a Ultimate 3000 RSLC nanoLC system (Thermo Fisher Scientific) coupled to a Q-Exactive Plus mass spectrometer (Thermo Fisher Scientific, Bremen, Germany). The peptides were loaded onto a two-columns setup employing an Acclaim PepMap 100 precolumn (100 µm x 2 cm, C$_{18}$, 5 µm, 100A, nanoViper) and a 20 cm long fused silica capillary column (75 µm ID) packed with Reprosil – Pur C$_{18}$ AQ 3 µm reversed-phase material (Dr. Maisch, Ammerbuch-Entrigen, Germany). In the case of formerly N-sialylated and N-linked-deglycopeptides, the HPLC gradient was 0-28% solvent B (95% ACN 0.1% FA) in 60 min at a flow rate of 250 nl/min. In the case of mono and multi-phosphorylated peptides, the HPLC gradient was 1-35% solvent B (95% ACN 0.1% FA) in 120 min at a flow rate of 250 nl/min. The mass spectrometer was operated in positive mode with a data dependent acquisition method (Top N, N = 12). A falcon tube with 5% ammonia solution was placed below the needle tip of the chromatographic column, located next to the orifice of the mass spectrometer to decrease the charge state of the ions and increase the HCD

fragmentation [45]. Briefly, MS scans (400-1400 m/z) were recorded at a resolution of 70,000. The automatic gain control (AGC) target for MS acquisitions was set to 1×10^6 with a maximum ion injection time of 120 msec. Microscans were set to 1 for both the MS and MS/MS. Dynamic exclusion was set to 15 sec. Singly charged species were rejected. Analytes of two and higher charges were fragmented into the HCD collision cell with higher-energy collisional dissociation (HCD) with a normalized collision energy (NCE) set to 32. Subsequent MS/MS scans with a target value of 2×10^4 ions were collected with a maximum injection time of 100 msec and a resolution of 17,500. All MS and MS/MS spectra were obtained in profile mode. All raw data were viewed in Xcalibur v2.2 (Thermo Fisher Scientific).

Data Analysis - The Proteome Discoverer software v.1.4.0.288 (Thermo Fisher Scientific) was used to perform database searching and peptide/protein relative quantification. The data were searched using MASCOT (v2.3, Matrix Science, London, UK) and Sequest HT (Thermo Fisher Scientific) as database searching engines with a Swiss-Prot v.3.53 human database (20, 243 entries) and the Uniprot human reference database (updated April 2014). Methionine oxidation, iTRAQ labeling (on peptide N-terminals and lysines), asparagine deamidation, serine, threonine and tyrosine phosphorylation were set as variable modifications, while cysteine carbamidomethylation was set as a fixed modification. Precursor mass tolerance was set to 10 ppm and MS/MS tolerance to 0.05 Da. During search, up to two missed cleavages were allowed. Data were filtered to a 1% false discovery rate using Proteome Discoverer's Percolator function [46]. Peptide iTRAQ ratios were log2 transformed and normalized for the average to compensate for unequal amounts of digested and labeled protein samples in the sample mixture. Before submission to significance analysis, the modified peptides were normalized to the values of the corresponding proteins (Chapter 2). One tail heteroscedastic Student's t-test (p-value < 5%) was used to assess statistical differences in peptide amount between conditions. Only putative glycosylation sites, which contain glycosylation sequon (NXS/T/C, X ≠ P), were further analyzed. Annotation and classification of the identified proteins were facilitated by using PANTHER Classification System (http://www.pantherdb.org/) [47]. Motif-X algorithm was used to predict the consensus phosphorylation site motifs. All the phosphopeptides were aligned, and their lengths were adjusted to ±12 aa from the central phosphorylation site position and submitted to the Motif-X software (http://motif-x.med.harvard.edu/) [48]; the IPI Human Proteome database was selected as background. The cutoff values were a minimum of 20 occurrences and a significance of p < 0.000001. Logo-like representations were created to graphically display each identified motif. In addition, the adjusted 13 aa phosphopeptide sequences were searched against multiple known linear protein kinase motifs (http://www.phosida.com), to obtain the kinase motifs matched with high

probability [49]. Clustering analysis was performed by using Perseus (v. 1.5.0.15, tool of MaxQuant package). Literature mining of protein-protein interactions was carried out using STRING (v. 9.1) in action view at high settings (0.7) [50].

3. RESULTS

In this study we looked into the membrane proteome of PMPs with the aim of unveiling phosporylation and glycosylation sites. We applied quantitative proteomics to investigate modified peptide changes in PMPs obtained by differentially activated platelet samples (Fig.1). ADP, thrombin and collagen were used for platelet activation as known physiological agonists. Thrombin, which is constantly used to generate PMPs *in vitro*, was set as control. PMPs were first obtained from fresh apheresis platelet, lysed in presence of Na_2CO_3 [51], membrane enriched, iTRAQ labeled and subjected to phosphorylated and glycosylated peptide enrichments (Fig.2). Modified peptides were then purified or fractionated by HILIC and analyzed by nLC-MS/MS. All experiments were performed in biological triplicates.
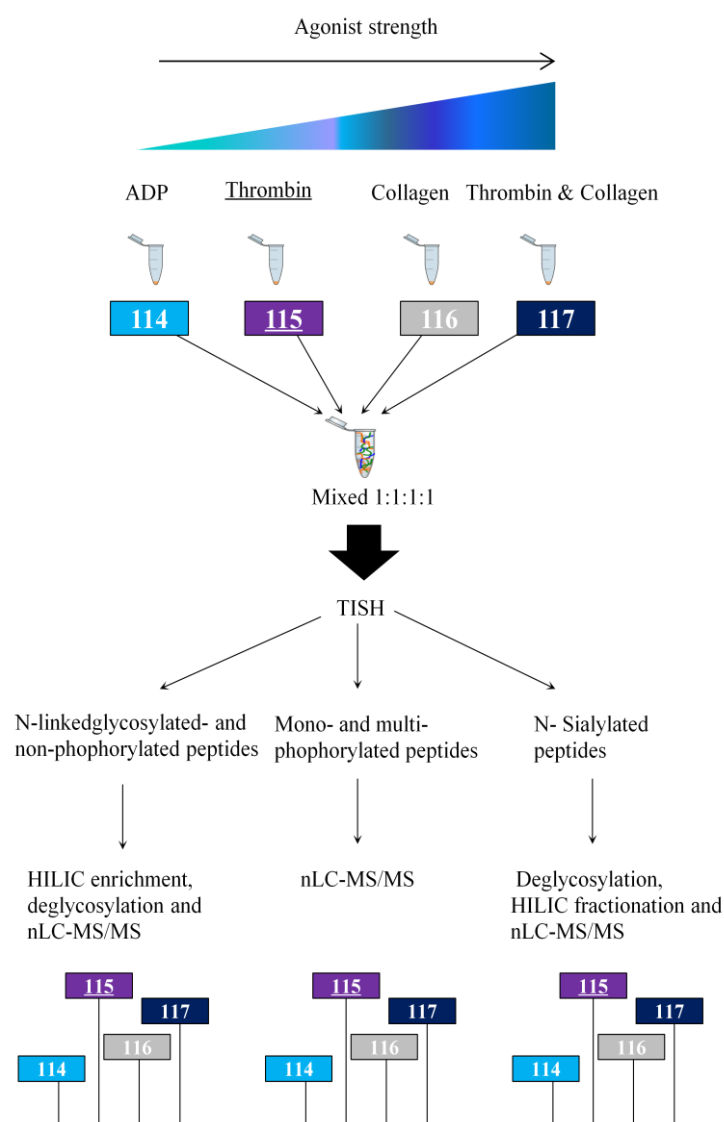
Fig. 1 Experimental scheme for the quantitative phosphoproteomics and glycoproteomics comparison of PMPs obtained from differentially activated platelet samples

Modified peptide identification and comparison analysis – A total of 1315 phosphopeptides including 1206 mono-phosphorylated peptides, 95 double phosphorylated peptides and 14 triple-phosphorylated were found. In particular, a total of 1438 phosphorylation sites including 1161 phospo-serine (pS), 205 phospho-threonine (pT) and 35 phospho-tyrosine (pY) were identified. After removing redundancy a total of 1225 unique phosphopeptides and 614 unique phospoproteins were identified (Fig. 3A). In the phosphopeptide fraction a total of 42 peptides were found to be significantly different in terms of relative abundance in the ADP induced MPs as compared to the control, which was thrombin stimulation. Thirteen proteins were significantly different in collagen induced activation and 26 peptides in thrombin and collagen co-stimulated MPs. A total of 1765 peptides were identified in the N-sialylated fraction (Fig. 3A). In this fraction 54 peptides were

found to be significantly different in terms of relative abundance in the ADP induced MPs as compared to the control, which was thrombin activation. Twenty-two proteins were significantly different in collagen induced activation and 16 peptides in thrombin and collagen co-stimulated MPs. A total of 1166 peptides were found in the N-glycosylated fraction (Fig. 3A). In this fraction a total of 46 peptides were found to be significantly different in terms of relative abundance in the ADP induced MPs as compared to the control, which was thrombin stimulation. Seven-teen proteins were significantly different in collagen induced activation and 18 peptides in thrombin and collagen co-stimulated MPs. After removing redundancy between the glycosylated fractions, a total of 481 unique N-sialylated peptides were identified and assigned to 306 unique proteins and 241 unique N-glycosylated peptides assigned to 187 proteins (Fig. 3B). Moreover, 523 peptides were identified in both of the glycosylated fractions and assigned to 234 proteins. In this work, a total of 1245 unique glycosylated peptides were identified and assigned to 533 unique glycosylated proteins.
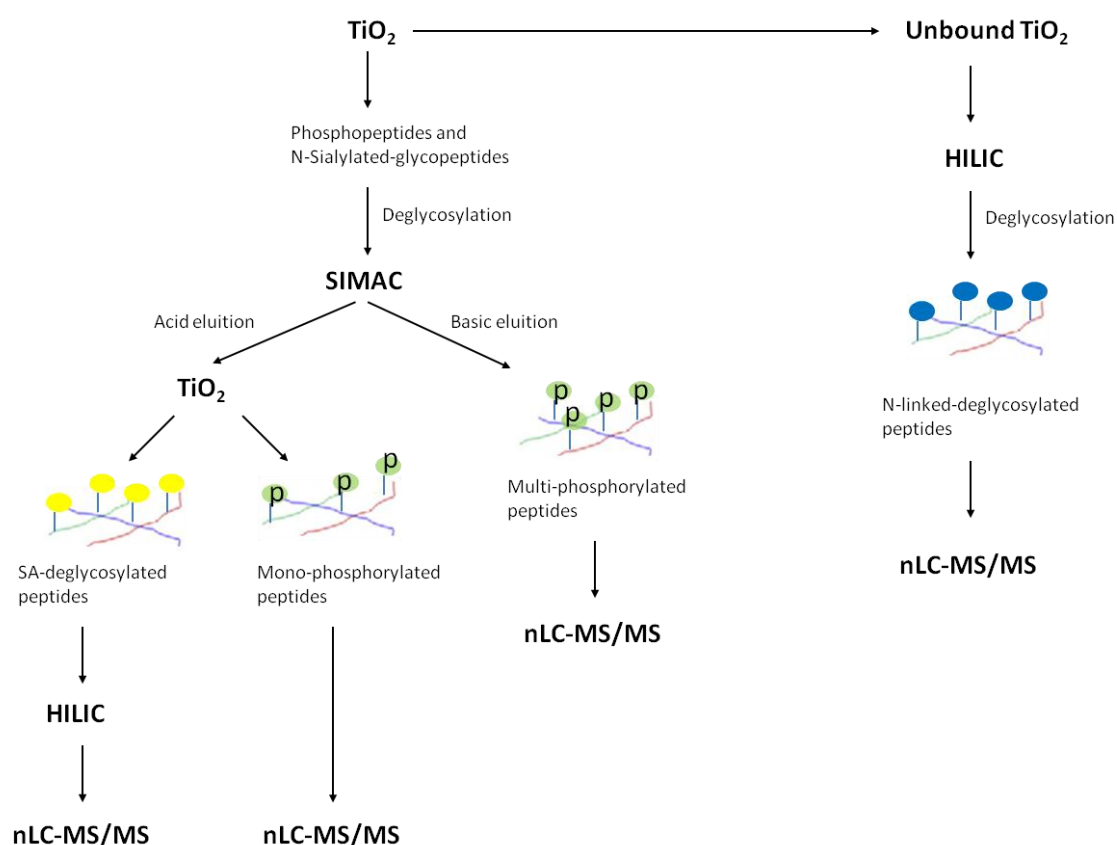
Fig. 2 Experimental scheme of the enrichment strategies used for the quantitivative phosphoproteomics and glycoproteomics analysis of PMPs
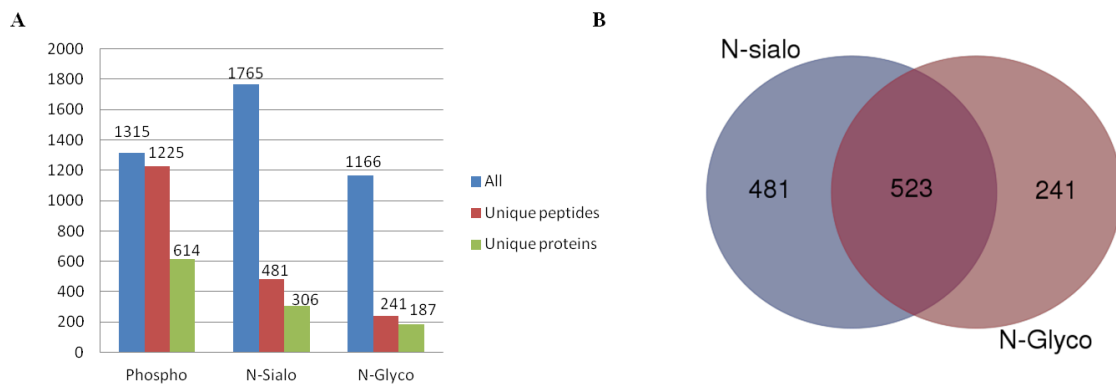
Figure 3. A) Overview of the all identified peptides, unique modified peptides and unique modified proteins. B) Overlap between the glycopeptides found in the N-sialo and in the N-Glyco fraction

Gene ontology analysis of the identified proteins – We next characterized the gene ontology of the identified proteins. Biological processes analysis showed that most of the proteins detected were involved in cellular and metabolic process (Fig. 4A). Molecular functions analysis underlined that the majority of proteins played roles in protein binding, catalytic and receptor activity (Fig. 4B). Cellular component analysis highlighted that proteins were mostly associated with cell part and organelle. Protein class analysis displayed that proteins were mainly receptors and hydrolases (especially in the sialylated fraction), enzyme modulators and cytoskeletal proteins (especially in the phosphorylated fraction).

Motif-X and kinase associated motif analysis - In order to identify possible phosphorylation and kinase related motifs in our phosphopeptide data, the frequency of particular amino acids in the proximity of phosphorylation sites was analyzed with the Motif-X software. Briefly, 9 putative motifs were identified, 2 of which were found to be associated to kinase motifs such as CAMKII (R-X-X-pS) and PKA (R-X-pS) (Fig. 4C). The identified motifs were only pS based motifs; this might be due to the low abundance of pT and pY compared to pS.
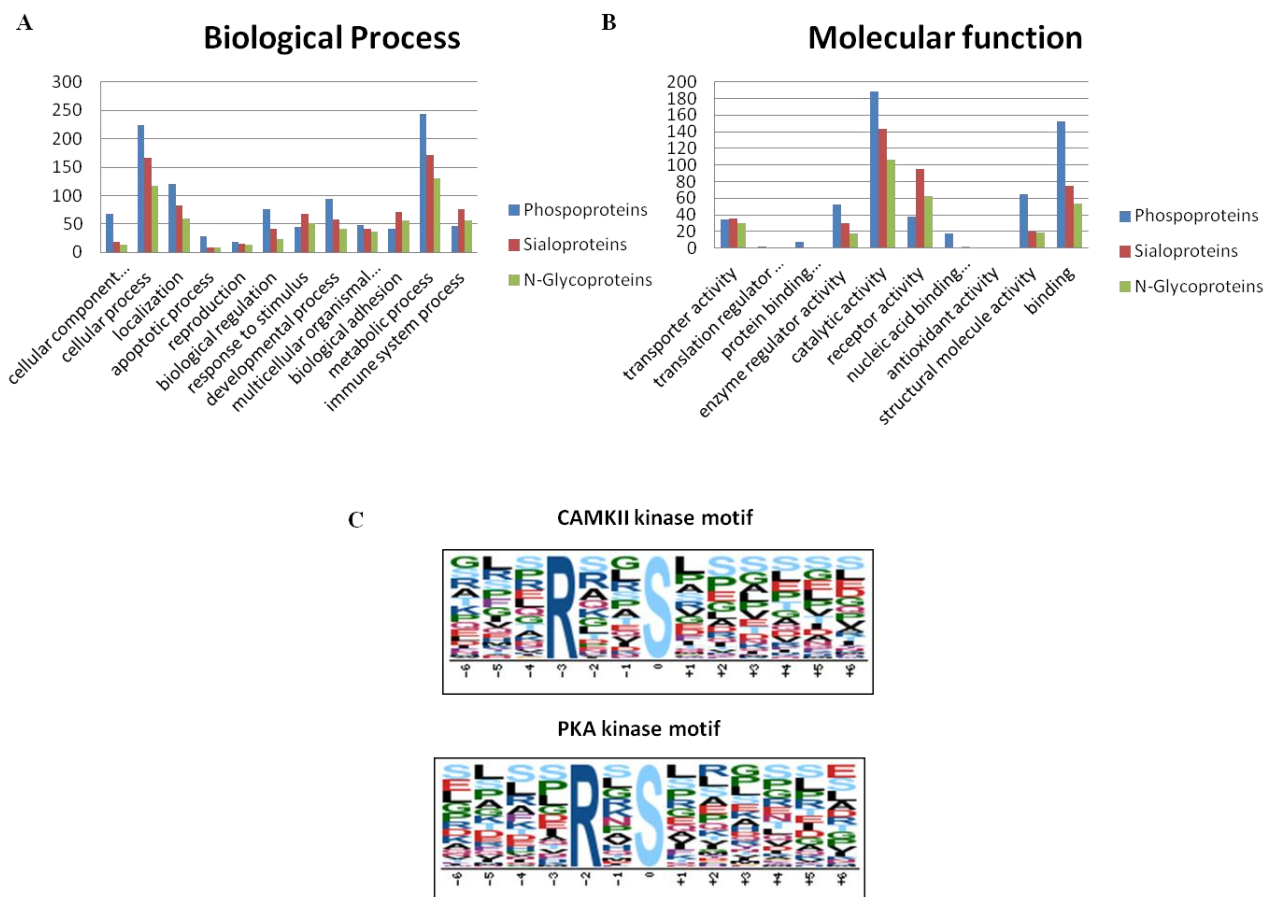
Fig. 4 GO analysis of the identified phosphoproteins, sialoproteins and glycoproteins showing A) Biological process and B) Molecular function. C) Motif-X and kinase associated motif analysis of the identified phosphopeptides

Clustering and protein-protein interaction analysis of differentially abundant proteins between treatments- We next performed cluster analysis, considering the relative abundance of a protein in the three treatments as compared to control. We divided the trends of protein abundance into four clusters for the phosporylated, four clusters for the N-sialylated and five clusters for the N-glycosylated fraction. Proteins belonging to the same cluster were subjected to STRING analysis to perform literature mining of protein-protein interactions and protein networks. Three major clusters were found to be associated to focal adhesion. A first cluster (Fig. 5A), containing 32 membrane phospoproteins mostly abundant in ADP induced microparticles (Fig. 5B), was enriched in proteins related to focal adhesion (Fig. 5C). A second cluster (Fig. 6A), including 66 membrane N-sialoproteins that were mostly abundant in thrombin and collagen co-stimulated microparticles (Fig. 6B), was enriched in proteins associated to focal adhesion (Fig. 6C) as well as a third cluster (Fig. 7A), which contains 47 N-linked glycoproteins (Fig. 7B, 7C).
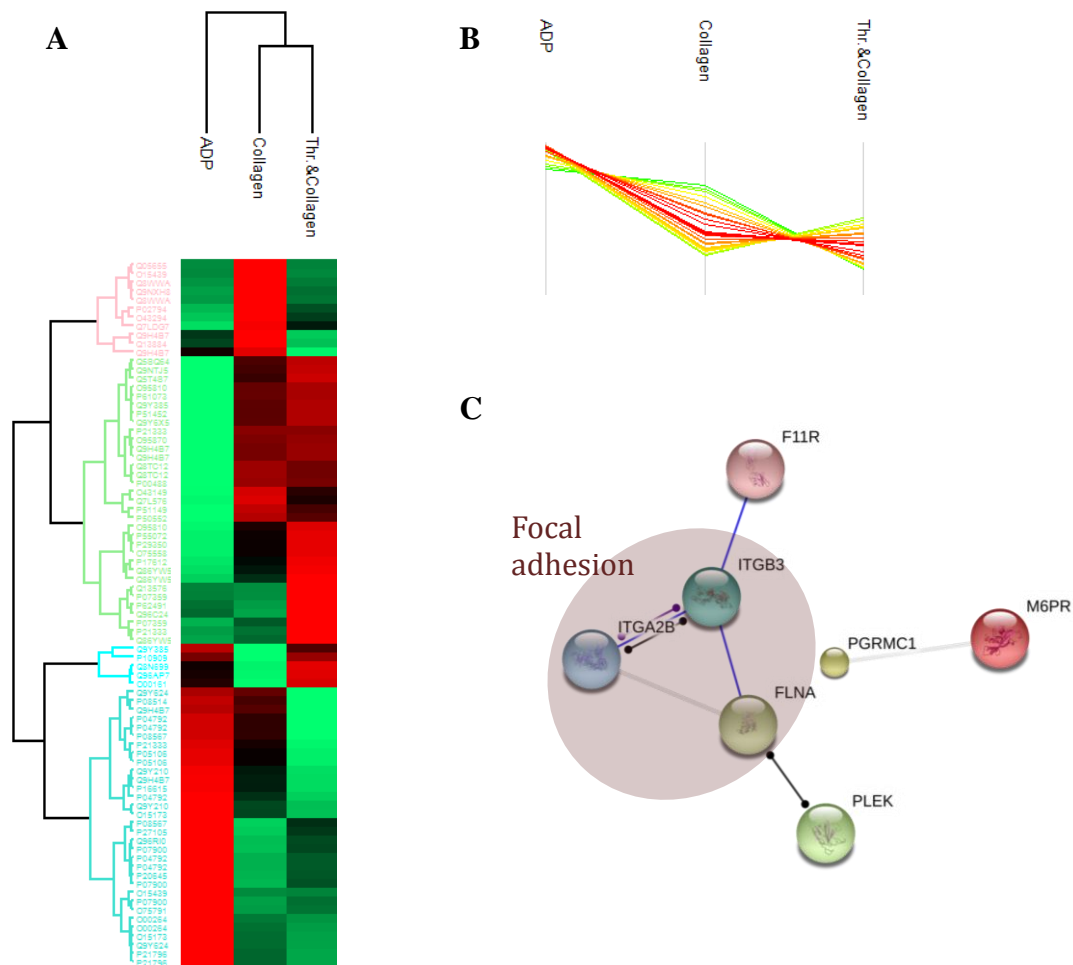
Fig. 5 A) Heat map representing log2 fold changes of the quantitative data (green-lowest abundance and red-highest abundance). B) Trends of the abundance of a specific cluster and C) protein-protein interaction analysis of the same cluster highlighting a protein network related to focal adhesion. Thicker, blue and black lines indicate more confident, binding and reaction associations, respectively.
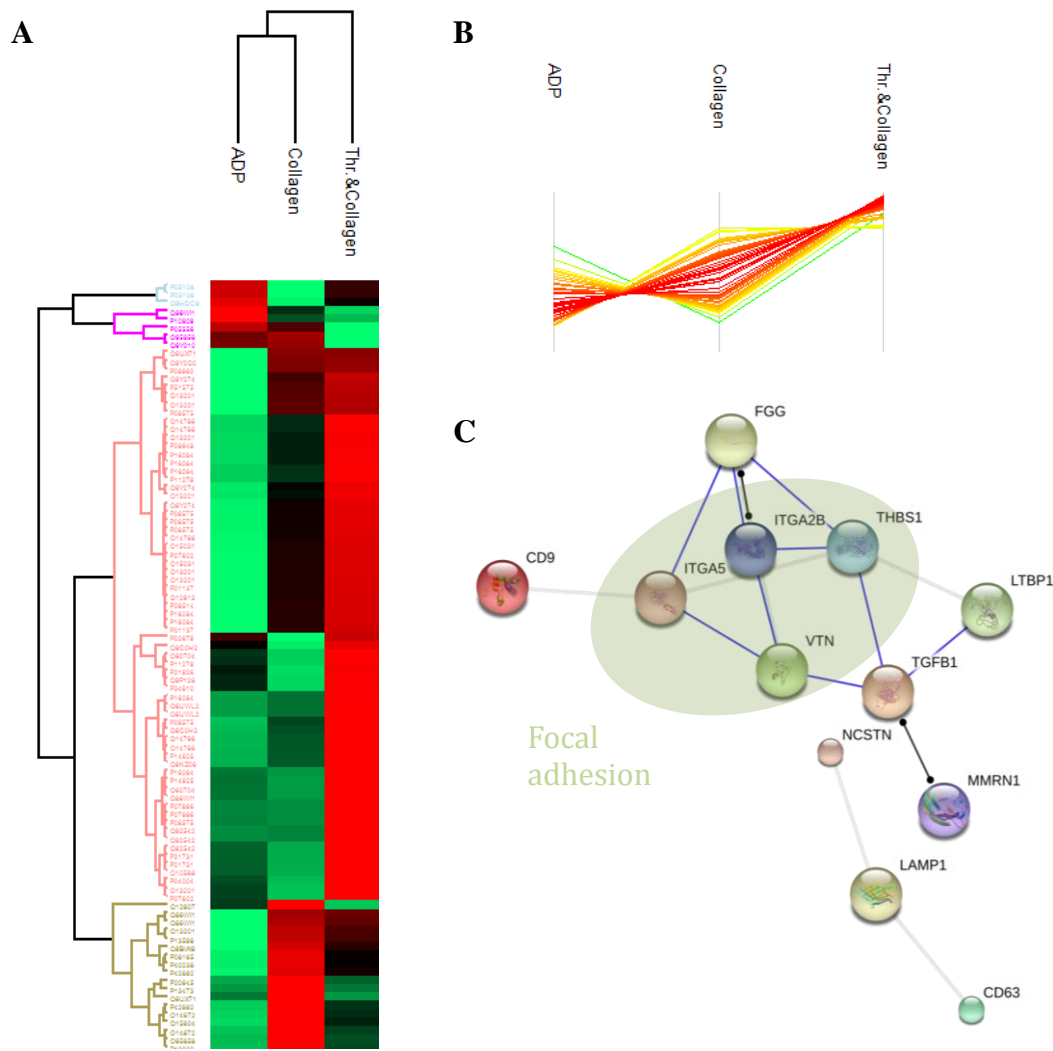
Fig. 6 A) Heat map representing log2 fold changes of the quantitative data (green-lowest abundance and red-highest abundance). B) Trends of the abundance of a specific cluster and C) protein-protein interaction analysis of the same cluster highlighting a protein network related to focal adhesion. Thicker, blue and black lines indicate more confident, binding and reaction associations, respectively.

Taken together, the list of modified proteins, that we identified and quantified, underlined many common function of phosporylated and glycosylated proteins in platelets as receptors for pledging adhesion to the subendothelial matrix and platelet-platelet cohesion [27], as motors for inside-out and outside-in signaling pathways [52] and as initiators for platelet activation [53]. In addition, we found a general enrichment of proteins implicated in cell-cell communication, which may confirm the role of microparticles as key components of the intercellular communication network [36].
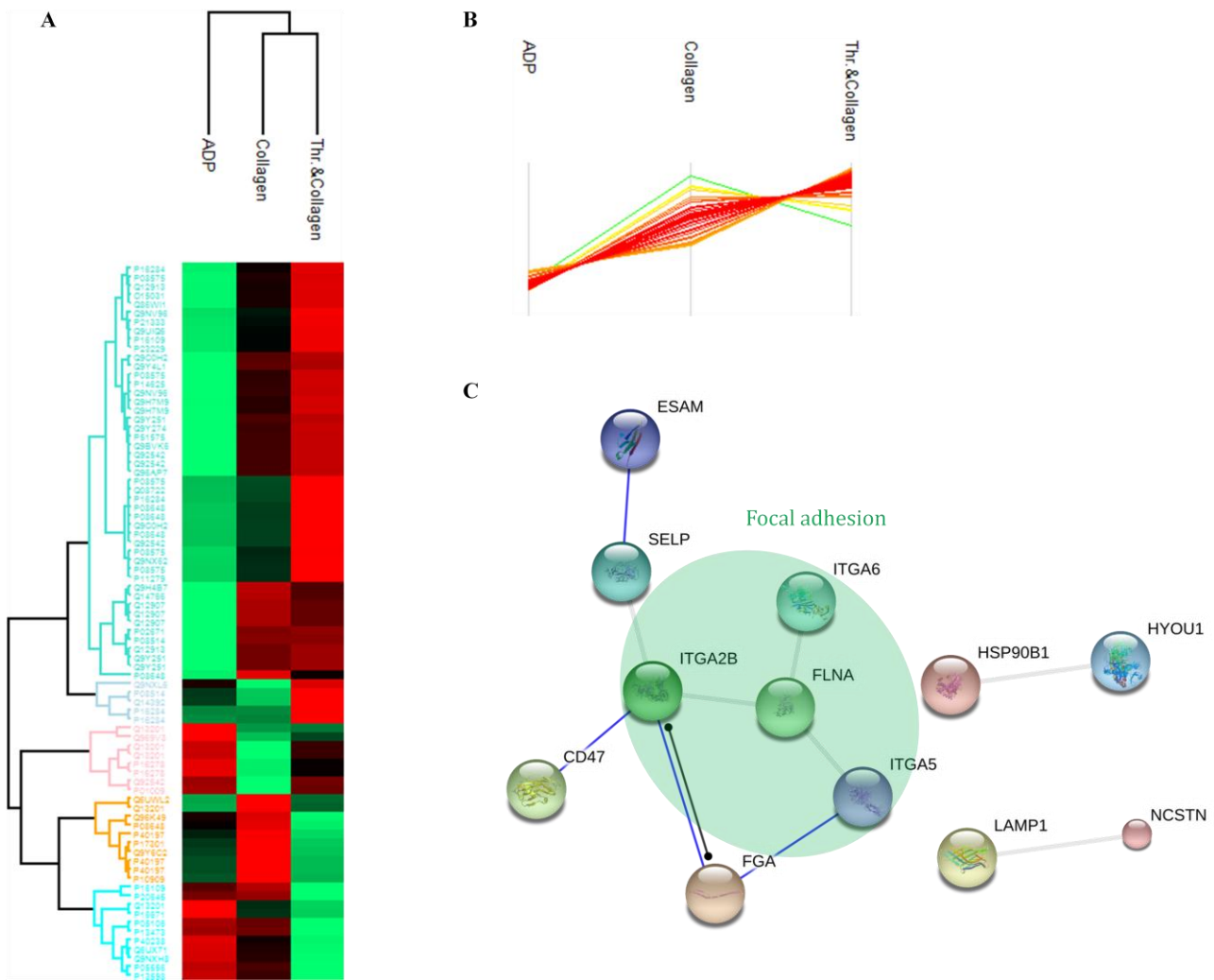
Fig. 7 A) Heat map representing log2 fold changes of the quantitative data (green-lowest abundance and red-highest abundance). B) Trends of the abundance of a specific cluster and C) protein-protein interaction analysis of the same cluster highlighting a protein network related to focal adhesion. Thicker, blue and black lines indicate more confident, binding and reaction associations, respectively.

4. DISCUSSION

In this work, we performed phosphoproteomics and glycoproteomics studies of PMPs obtained by differentially activated platelet samples. In order to reduce RBCs and leukocytes contaminations, apheresis platelets were used for PMPs generation. Activations were carried out using commonly known platelet physiological agonists following published procedures with minor modifications. An additional centrifugation step (1000 x g) was introduced to further purify PMPs from intact platelets. However, despite the supernatant was formed mainly by PMPs, we cannot exclude possible exosome contaminations in our samples. By treating with Na_2CO_3 [51], we separated and enriched membrane proteins, in which phosphorylated and glycosylated sites can normally be

found. Modified peptides were simultaneously enriched following published protocols with few modifications [38-41].

Phosphorylation in PMPs - In this study, 1438 phosphorylation sites distributed on 1225 unique phosphopeptides were identified and assigned to 614 phosphoproteins. In particular, a total of 1161 phosphoserine, 205 phosphothreonine and 35 phoshotyrosine were found. Despite the low abundance, the induction of tyrosine phosphorylation on relevant signaling molecules has emerged as a key event to stimulate signaling pathways that generate platelet activation [54]. Moreover, we found Talin-1, which was identified to be highly phosphorylated. Talin-1 was demonstrated to be post-translationally modified by phosphorylation upon platelet activation, its subcellular distribution can be regulated by its phosphorylation state [55]. Talin-1 is involved in platelet mediated processes as well as vasodilator-stimulated phosphoprotein, found to be phosphorylated in our study on Ser46, in which phosphorylation on Ser157 was discovered to be related to platelet activation [56]. This protein was shown to interact with zyxin by building actin-rich structures [57]. Zyxin was found to be highly phosphorylated as well. Vinculin, in which phosphorylation on Tyr100 and Tyr1065 was shown to affect platelet spreading [58], was identified to be highly serine phosphorylated. Vinculin was recently identified to be a possible biomarker of atherosclerotic disease [59], which is a platelet activation mediated pathological process [60]. Fibrinogen alpha chain, found to be highly serine and threonine phosphorylated, was shown to be involved with integrins in platelet spreading and adhesion [61]. However, this protein was previously identified to be phosphorylated by casein kinases [62,63]. Beta-actin, found to be phosphorylated on Ser235, was identified to be critically required for the regulation platelet nitric oxide synthase 3 activity [64]. LIM domain and actin-binding protein 1, which is also deeply involved in platelet activation, was found to be serine phosphorylated as well. In particular, this proteins was demonstrated to participate in cofilin phosphorylation mechanisms during platelet shape change and secretion [65]. Moreover, cofilin-1, which was identified to be phosphorylated on Ser156, was shown to promote actin reorganization and phosphatidylserine exposure in platelets [66]. Cofilin-1 was also shown to be regulated by Rho-associated protein kinase 2, which is required for stabilizing actin cytoskeleton [67]. Rho-associated protein kinase 2 was found phosphorylated on Ser1132 and Thr1212.

Glycosylation in PMPs – In this study, 481 unique peptides were found to be N-sialylated and assigned to 306 proteins (Fig. 8). Moreover, 241 unique peptides were identified to be N-glycosylated and assigned to 187 proteins (Fig. 9). In particular, a total of 1245 unique glycosylated peptides were found and assigned to 533 unique glycosylated proteins. In addition, glycopeptides fractionation was used in order to decrease sample complexity and improve the identification (Fig.

\10). However, coagulation factor V, which participate as cofactor with factor Xa to activate prothrombin to thrombin, was found to be highly glycosylated such as on Asn297 that is close to thrombin cleavage site Arg334 [31]. In particular, its N-linked carbohydrate moieties was shown to play a key role in activated protein C-catalyzed cleavage and inactivation of coagulation factor V. [68]. Multimerin-1, which was shown to be associated to coagulation factor V and stored within a-granules [69], was found to be heavily sialylated and glycosylated such as on Asn114, Asn120 and Asn344, Asn828, Asn1020 respectively. After factor V activation, the multimerin 1-coagulation factor V protein complex were found to be dissociated, which may suggest a role of multimerin 1 in delivering and localizing factor V on platelets prior to prothrombinase assembly [70]. Multimerin-1 was *in vitro* found to be an efficient ligand for several integrins such as integrin $\alpha_{IIb}\beta_3$ and integrin $\alpha_V\beta_3$ on activated platelets [71]. Von Willebrand factor was reported to contribute to platelet function by regulating the initiation and progression of thrombus formation at sites of vascular injury [72]. This proteins was identified to be heavily N-glycosylated such as on Asn1515, Asn1574 and Asn2585.
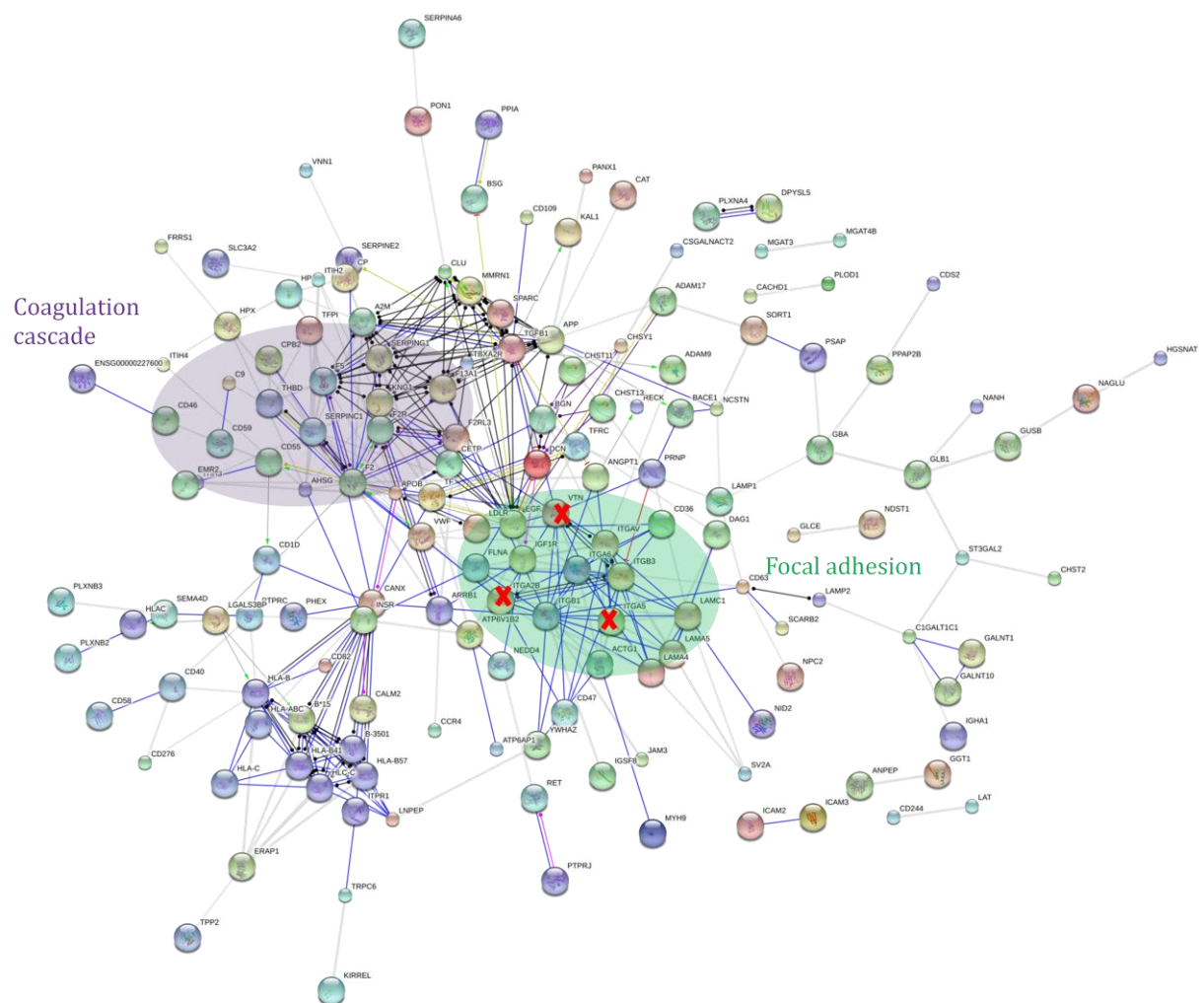
Fig. 8 Protein-protein interaction in the N-sialylated proteins identified in this study showing two different network related to coagulation cascade (purple) and focal adhesion (green).
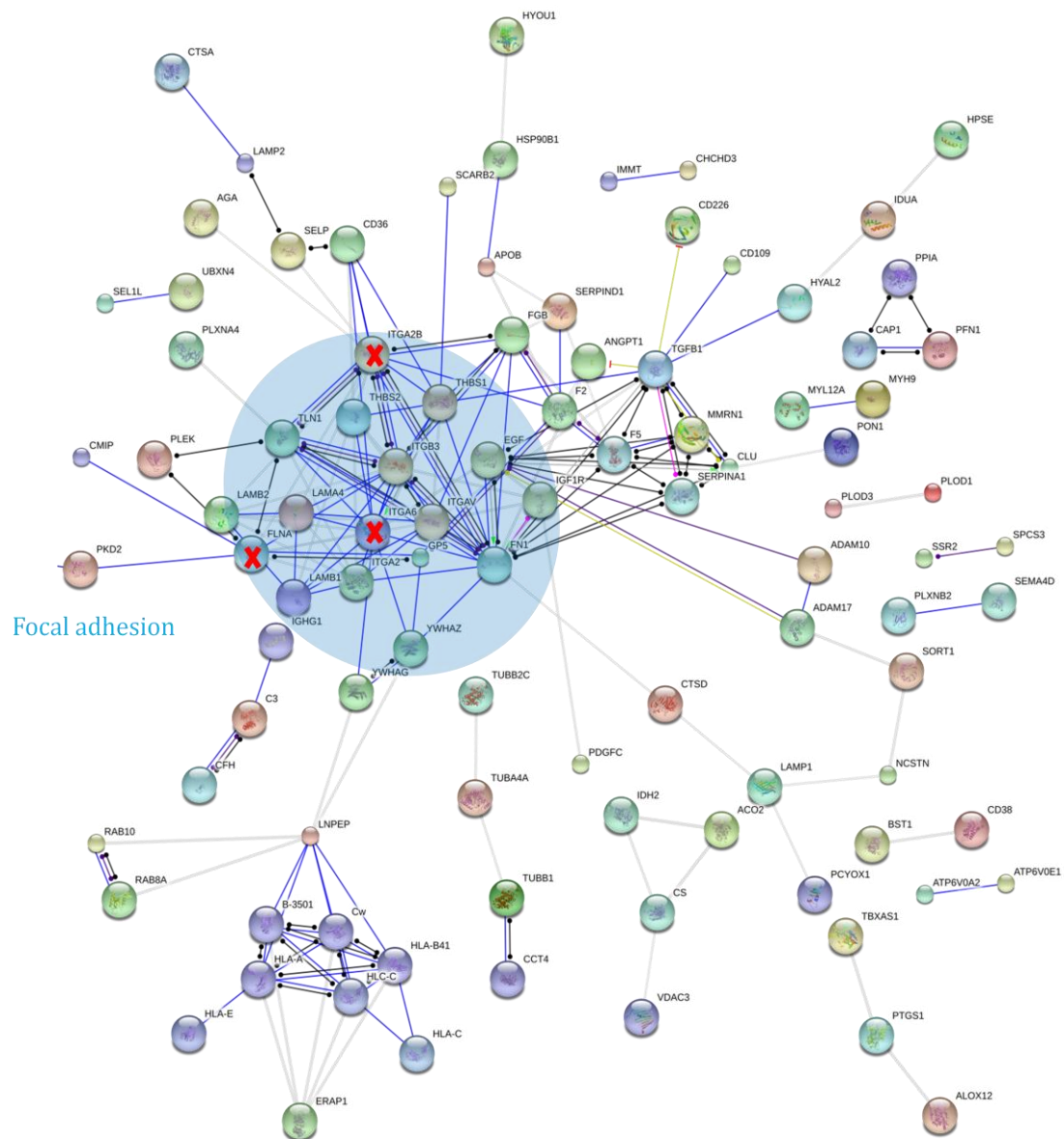
Fig. 9 Protein-protein interaction in the N-glycosylated proteins identified in this study showing a network related to focal adhesion (light blue).

Differentially expressed focal adhesion related proteins - Adhesion of cells to the extracellular matrix (focal adhesion) was shown to mediate several cellular functions such as morphology, migration, proliferation, survival, and differentiation [73]. These functions are essential during cellular development and for the maintenance of tissue architecture and the induction of tissue repair. Predominant receptors for the control of cell adhesion to the extracellular matrix are integrins [26,74]. As mentioned above, integrins are directly related to the platelet activation process. Our analysis revealed several differentially expressed modified peptides within focal adhesion related proteins and integrins. In addition, for the abundance of glycosylated significantly changed peptides in focal adhesion related proteins, we observed a decrease in the ADP and collagen induced MPs and an increase in the thrombin and collagen co-stimulated MPs. On the other hand, we found an increase in the ADP induced activation and a decrease in thrombin/collagen co-stimulated MPs in the phosphorylated significantly chaged sites. Interestingly, integrin $\alpha_{IIb}\beta_3$ showed 4 significantly changed modified peptides as compared to the control, which was thrombin stimulation. Integrin $\alpha_{IIb}\beta_3$ is involved in platelet activation and PMPs formation [24]. Integrin alpha-5, which showed 5 glycosylated changed sites as compared to the control, was found to be related to cell adhesion by N-glycosylation [75]. Integrin alpha-6, which contains a changed glycosylated site, was found to be involved in diverse platelet mediated processes such as adhesion, activation and arterial thrombosis. [76]. However, Integrin alpha-6 receptor activity is related to glycosylation in cell-matrix interaction [77]. Filamin-A, which contains 4 significantly changed peptides, 3 of which were phosphorylated and 1 was glycosylated, was shown to be implicated in cytoskeletal rearrangements and cell shape changes, which are related to platelet activation [78]. Moreover, differences in the degree of filamin phosphorylation were also found after platelet activation [79]. Thrombospondin-1, which showed a significantly changed glycosylated site, was demonstrated to mediate cell-cell and cell-matrix interactions by binding several active molecules such as integrins, fibronectin, laminin, type V collagen [80] and to be highly glycosylated [31]. Vitronectin, which contains a significantly changed glycosylated site as well, was found to be implicated in platelet aggregation by interacting with activated platelets [81].
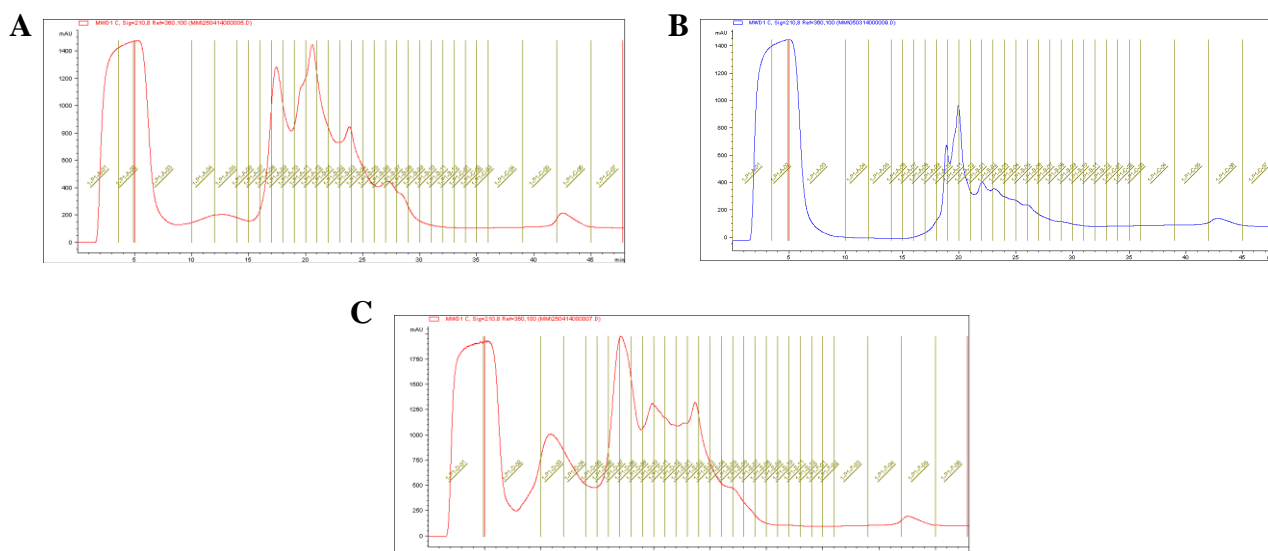
Fig. 10 HILIC chromatograms showing the fractionation of the sialopeptides respectively in the (A) first, second (B) and third (C) replicates.

5. CONCLUSIONS

In this work, the phosphoproteome and the glycoproteome of PMPs has been deeply investigated leading to the identification of 1225 unique phosphopeptides assigned to 614 phosphoproteins and to the identification of 1245 unique glycosylated peptides assigned to 533 unique glycoproteins. Our proteomics approach unveiled that glycosylation on focal adhesion related protein, in particular on integrins such as $\alpha_{IIb}\beta_3$, was directly related to the physiological agonist strength used for platelet activation. Collectively, our MS-based quantitative study provided an overview of the PTM-ome of PMPs, which can be of high interest to reveal biological insights about platelet response to stimuli.

CHAPTER REFERENCES

[1] Siljander PRM. Platelet-derived microparticles–an updated perspective. Thromb Res 2011;127:S30-3.

[2] Aoki N, Yokoyama R, Asai N, Ohki M, Ohki Y, Kusubata K et al. Adipocyte-derived microvesicles are associated with multiple angiogenic factors and induce angiogenesis in vivo and in vitro. Endocrinology 2010;151:2567-76.

[3] Flaumenhaft R, Dilks JR, Richardson J, Alden E, Patel-Hett SR, Battinelli E et al. Megakaryocyte-derived microparticles: direct visualization and distinction from platelet-derived microparticles. Blood 2009;113:1112-21.

[4] Doeuvre L, Plawinski L, Toti F, Anglés-Cano E. Cell-derived microparticles: a new challenge in neuroscience. J Neurochem 2009;110:457-68.

[5] Diamant M, Tushuizen ME, Sturk A, Nieuwland R. Cellular microparticles: new players in the field of vascular disease?. Eur J Clin Invest 2004;34:392-401.

[6] Heijnen HF, Schiel AE, Fijnheer R, Geuze HJ, Sixma, J. J. Activated platelets release two types of membrane vesicles: microvesicles by surface shedding and exosomes derived from exocytosis of multivesicular bodies and alpha granules. Blood 1999;94:3791-9.

[7] Nomura S, Shouzu A, Nishikawa M, Kokawa T, Yasunaga K. Significance of platelet-derived microparticles in uremia. Nephron 1993;63:485

[8] Nomura S, Kagawa H, Ozaki Y, Nagahama M, Yoshimura C, Fukuhara S. Relationship between platelet activation and cytokines in systemic inflammatory response syndrome patients with hematological malignancies. Thromb Res 1999;95:205-13.

[9] Nieuwland R, Berckmans RJ, McGregor S, Böing AN, Romijn FPTM., Westendorp RG et al. Cellular origin and procoagulant properties of microparticles in meningococcal sepsis. Blood 2000;95:930-5.

[10] Katopodis JN, Kolodny L, Jy W, Horstman LL, De Marchena EJ, Tao JG et al. Platelet microparticles and calcium homeostasis in acute coronary ischemias. Am J Hematol 1997;54:95-101.

[11] Lee YJ, Jy W, Horstman LL, Janania J, Reyes Y, Kelley RE et al. Elevated platelet microparticles in transient ischemic attacks, lacunar infarcts, and multiinfarct dementias. Thromb Res 1993;72:295-304.

[12] Jy W, Horstman LL, Arce M, Ahn YS. Clinical significance of platelet microparticles in autoimmune thrombocytopenias. J Lab Clin Med 1992;119:334-45.

[13] Nomura S, Suzuki M, Katsura K, Xie GL, Miyazaki Y, Miyake T et al. Platelet-derived microparticles may influence the development of atherosclerosis in diabetes mellitus. Atherosclerosis 1995;116:235-40.

[14] Kim HK, Song KS, Park YS, Kang YH, Lee YJ, Lee KR et al. Elevated levels of circulating platelet microparticles, VEGF, IL-6 and RANTES in patients with gastric cancer: possible role of a metastasis predictor. Eur J Cancer 2003;39:184-91.

[15] Janowska-Wieczorek A, Wysoczynski M, Kijowski J, Marquez-Curtis L, Machalinski B, Ratajczak, J et al. Microvesicles derived from activated platelets induce metastasis and angiogenesis in lung cancer. Int J Cancer 2005;113:752-60.

[16] Janowska-Wieczorek A, Majka M, Kijowski J, Baj-Krzyworzeka M, Reca R, Turner AR et al. Platelet-derived microparticles bind to hematopoietic stem/progenitor cells and enhance their engraftment. Blood 2001;98:3143-9.

[17] Kim HK, Song KS, Chung JH, Lee KR, Lee SN. Platelet microparticles induce angiogenesis in vitro. Br J Haematol 2004;124:376-84.

[18] Nomura S, Tandon NN, Nakamura T, Cone J, Fukuhara S, Kambayashi J. High-shear-stress-induced activation of platelets and microparticles enhances expression of cell adhesion molecules in THP-1 and endothelial cells. Atherosclerosis 2001;158:277-87.

[19] Kahn ML, Zheng YW, Huang W, Bigornia V, Zeng D, Moff S. A dual thrombin receptor system for platelet activation. Nature 1998;394:690-4.

[20] Davì G, Patrono C. Platelet activation and atherothrombosis. N Eng J Med 2007;357:2482-94.

[21] Varga-Szabo D, Pleines I, Nieswandt B. Cell adhesion mechanisms in platelets. Arterioscler Thromb Vasc Biol 2008:28:403-12.

[22] Offermanns S. Activation of platelet function through G protein-coupled receptors. Circ Res 2006;99:1293-304.

[23] Cranmer SL, Ashworth KJ, Yao Y, Berndt MC, Ruggeri ZM, Andrews RK et al. High shear-dependent loss of membrane integrity and defective platelet adhesion following disruption of the GPIbα-filamin interaction. Blood 2011;117:2718-27.

[24] Gemmell CH, Sefton MV, Yeo EL. Platelet-derived microparticle formation involves glycoprotein IIb-IIIa. Inhibition by RGDS and a Glanzmann's thrombasthenia defect. J Biol Chem 1993;268:14586-9.

[25] Morel O, Jesel L, Freyssinet JM, Toti F. Cellular mechanisms underlying the formation of circulating microparticles. Arterioscler Thromb Vasc Biol 2011;31:15-26.

[26] Nieswandt B, Varga-Szabo D, Elvers M. Integrins in platelet activation. J Thromb Haemost 2009;7:206-9.

[27] Kunicki TJ. Platelet membrane glycoproteins and their function: an overview. Blut 1989;59:30-4.

[28] Clemetson KJ, McGregor JL, James E, Dechavanne M, Lüscher EF. Characterization of the platelet membrane glycoprotein abnormalities in Bernard-Soulier syndrome and comparison with normal by surface-labeling techniques and high-resolution two-dimensional gel electrophoresis. J Clin Invest 1982;70:304-11.

[29] Gawaz M, Neumann FJ, Schömig A. Evaluation of Platelet Membrane Glycoproteins in Coronary Artery Disease Consequences for Diagnosis and Therapy. Circulation 1999;99:e1-e11.

[30] Gawaz MP, Dobos G, Späth M, Schollmeyer P, Gurland HJ, Mujais SK. Impaired function of platelet membrane glycoprotein IIb-IIIa in end-stage renal disease. J Am Soc Nephrol 1994;5:36-46.

[31] Lewandrowski U, Moebius J, Walter U, Sickmann A. Elucidation of N-glycosylation sites on human platelet proteins a glycoproteomic approach. Mol Cell Proteomics 2006;5:226-33.

[32] Lewandrowski U, Lohrig K, Zahedi RP, Wolters D, Sickmann A. Glycosylation site analysis of human platelets by electrostatic repulsion hydrophilic interaction chromatography. Clinical Proteomics 2008;4:25-36.

[33] Marcus K, Moebius J, Meyer HE. Differential analysis of phosphorylated proteins in resting and thrombin-stimulated human platelets. Anal Bioanal Chem 2003;376:973-93.

[34] Zahedi RP, Lewandrowski U, Wiesner J, Wortelkamp S, Moebius J, Schütz C et al. Phosphoproteome of resting human platelets. J Proteome Res 2008;7:526-34.

[35] Qureshi AH, Chaoji V, Maiguel D, Faridi MH, Barth CJ, Salem S et al. Proteomic and phospho-proteomic profile of human platelets in basal, resting state: insights into integrin signaling. PLoS One 2009;4:e7627.

[36] Aatonen M, Grönholm M, Siljander P, Platelet-Derived Microvesicles: Multitalented Participants in Intercellular Communication. Semin Thromb Hemost 2012;38:102-13.

[37] Shai E, Parguiña AF, Motahedeh S, Varon D, Garcia A. Comparative analysis of platelet-derived microparticles reveals differences in their amount and proteome depending on the platelet stimulus. J Proteomics 2012;76:287-96

[38] Thingholm TE, Jensen ON, Robinson PJ, Larsen MR. SIMAC (sequential elution from IMAC), a phosphoproteomics strategy for the rapid separation of monophosphorylated from multiply phosphorylated peptides. Mol Cell Proteomics 2008;7:661-71.

[39] Palmisano G, Parker BL, Engholm-Keller K, Lendal SE, Kulej K, Schulz M et al. A novel method for the simultaneous enrichment, identification, and quantification of phosphopeptides and sialylated glycopeptides applied to a temporal profile of mouse brain development. Mol Cell Proteomics 2012;11:1191-1202

[40] Engholm-Keller K, Birck P, Størling J, Pociot F, Mandrup-Poulsen T, Larsen MR. TiSH-a robust and sensitive global phosphoproteomics strategy employing a combination of TiO$_2$, SIMAC, and HILIC. J Proteomics 2012;75:5749-61.

[41] Thaysen-Andersen M, Mysling S, Højrup P. Site-specific glycoprofiling of N-linked glycopeptides using MALDI-TOF MS: strong correlation between signal strength and glycoform quantities. Anal Chem 2009;81:3933-43.

[42] Biró E, Akkerman JW, Hoek FJ, Gorter G, Pronk LM, Sturk A et al. The phospholipid composition and cholesterol content of platelet-derived microparticles: a comparison with platelet membrane fractions. J Thromb Haemost 2005;3:2754-63.

[43] Capriotti AL, Caruso G, Cavaliere C, Piovesana S, Samperi R, Laganà A. Proteomic characterization of human platelet-derived microparticles. Anal Chim Acta 2013;776:57-63.

[44] Palmisano G, Lendal SE, Engholm-Keller K, Leth-Larsen R, Parker BL, Larsen MR. Selective enrichment of sialic acid-containing glycopeptides using titanium dioxide chromatography with analysis by HILIC and mass spectrometry. Nat Protoc 2010;5:1974-82

[45] Thingholm TE, Palmisano G, Kjeldsen, F, Larsen MR. Undesirable charge-enhancement of isobaric tagged phosphopeptides leads to reduced identification efficiency. J Proteome Res 2010;9: 4045-52.

[46] Brosch M, Yu L, Hubbart T, Choudhary J. Accuarate and sensitive peptide identification with Mascot Percolator. J Proteome Res 2009;8:3176-81.

[47] Mi H, Muruganujan A, Casagrande JT, Thomas PD. Large-scale gene function analysis with the PANTHER classification system. Nat Prot 2013;8:1551-66.

[48] Schwartz D, Gygi SP. An iterative statistical approach to the identification of protein phosphorylation motifs from large-scale data sets. Nature Biotechnol 2005;23:1391-8.

[49] Gnad F, Ren S, Cox J, Olsen JV, Macek B, Oroshi M et al. PHOSIDA (phosphorylation site database): management, structural and evolutionary investigation, and prediction of phosphosites. Genome biol 2007;8:R250.

[50] Franceschini A, Szklarczyk D, Frankild S, Kuhn M, Simonovic M, Roth A et al. STRING v9. 1: protein-protein interaction networks, with increased coverage and integration. Nucleic Acids Res 2013;41:D808-15.

[51] Fujiki Y, Hubbard AL, Fowler S, Lazarow PB. Isolation of intracellular membranes by means of sodium carbonate treatment: application to endoplasmic reticulum. J Cell Biol 1982;93:97-102.

[52] Shattil SJ, Newman PJ. Integrins: dynamic scaffolds for adhesion and signaling in platelets. Blood 2004;104:1606-15.

[53] Wagner CL, Mascelli MA, Neblock DS, Weisman HF, Coller BS, Jordan RE. Analysis of GPIIb/IIIa receptor number by quantification of 7E3 binding to human platelets. Blood 1996;88:907-14.

[54] Wee K, Janet L, Jackson DE. Phosphotyrosine signaling in platelets: lessons for vascular thrombosis. Curr drug targets 2006;7:1265-73.

[55] Bertagnolli ME, Locke SJ, Hensler ME, Bray PF, Beckerle MC. Talin distribution and phosphorylation in thrombin-activated platelets. Journal Cell Sci 1993;106:1189-99.

[56] Wentworth JKT, Pula G, Poole AW. Vasodilator-stimulated phosphoprotein (VASP) is phosphorylated on Ser157 by protein kinase C-dependent and -independent mechanisms in thrombin-stimulated human platelets. Biochem J. 2006;393:555-64.

[57] Reinhard M, Jouvenal K, Tripier D, Walter U. Identification, purification, and characterization of a zyxin-related protein that binds the focal adhesion and microfilament protein VASP (vasodilator-stimulated phosphoprotein). Proc Nat Acad Sci USA 1995;92:7956-60.

[58] Zhang Z, Izaguirre G, Lin SY, Lee HY, Schaefer E, Haimovich B. The phosphorylation of vinculin on tyrosine residues 100 and 1065, mediated by SRC kinases, affects cell spreading. Mol Biol Cell 2004;15:4234-47.

[59] Kristensen LP, Larsen MR, Mickley H, Saaby L, Diederichsen AC, Lambrechtsen J et al. Plasma proteome profiling of atherosclerotic disease manifestations reveals elevated levels of the cytoskeletal protein vinculin. J Proteomics 2014;101:141-53.

[60] Bigalke B, Schuster A, Sopova K, Wurster T, Stellos K. Platelets in atherothrombosis-diagnostic and prognostic value of platelet activation in patients with atherosclerotic diseases. Curr vasc pharmacol 2012;10:589-96.

[61] McCarty OJT, Zhao Y, Andrew N, Machesky LM, Staunton D, Frampton J, Watson SP. Evaluation of the role of platelet integrins in fibronectin-dependent spreading and adhesion. J Thromb Haemost 2004;2:1823-33.

[62] Itarte E, Plana M, Guasch MD, Martos C. Phosphorylation of fibrinogen by casein kinase 1. Biochem Biophys Res Comm 1983;117:631-36.

[63] Guasch MD, Plana M, Pena JM, Itarte E. Phosphorylation of fibrinogen by casein kinase 2. Biochem J 1986;234:523-26.

[64] Ji Y, Ferracci G, Warley A, Ward M, Leung KY, Samsuddin S. β-Actin regulates platelet nitric oxide synthase 3 activity through interaction with heat shock protein 90. Proc Nat Acad Sci USA 2007;104:8839-44.

[65] Pandey D, Goyal P, Bamburg JR, Siess W. Regulation of LIM-kinase 1 and cofilin in thrombin-stimulated platelets. Blood 2006;107:575-83.

[66] Dasgupta SK, Le A, Haudek S, Entman ML, Thiagarajan P. Cofilin-1-induced actin reorganization and phosphatidylserine exposure in platelets. Blood 2014;124:4153.

[67] Shi J, Wu X, Surma M, Vemula S, Zhang L, Yang Y. Distinct roles for ROCK1 and ROCK2 in the regulation of cell detachment. Cell death dis 2013;4:483.

[68] Silveira JR, Kalafatis M, Tracy PB. Carbohydrate moieties on the procofactor factor V, but not the derived cofactor factor Va, regulate its inactivation by activated protein C. Biochemistry 2002;41:1672-80.

[69] Hayward CP, Rivard GE, Kane WH, Drouin J, Zheng S, Moore JC et al. An autosomal dominant, qualitative platelet disorder associated with multimerin deficiency, abnormalities in platelet factor V, thrombospondin, von Willebrand factor, and fibrinogen and an epinephrine aggregation defect. Blood 1996;87:4967-78.

[70] Jeimy SB, Woram RA, Fuller N, Quinn-Allen MA., Nicolaes GA, Dahlbäck B. Identification of the MMRN1 binding region within the C2 domain of human factor V. J Biol Chem 2004;279:51466-71.

[71] Adam F, Zheng S, Joshi N, Kelton DS, Sandhu A, Suehiro Y et al. Analyses of cellular multimerin 1 receptors: in vitro evidence of binding mediated by alphaIIbbeta3 and alphavbeta3. Thromb Haemost 2005;94:1004.

[72] Ruggeri ZM. Von Willebrand factor, platelets and endothelial cell interactions. J Thromb Haemost 2003;1:1335-42.

[73] Gumbiner BM. Cell adhesion: the molecular basis of tissue architecture and morphogenesis. Cell 1996;84:345-57.

[74] Hynes RO. Integrins: bidirectional, allosteric signaling machines. Cell 2002;110:673-87

[75] Zheng M, Fang H, Hakomori SI. Functional role of N-glycosylation in alpha 5 beta 1 integrin receptor. De-N-glycosylation induces dissociation or altered association of alpha 5 and beta 1 subunits and concomitant loss of fibronectin binding activity. J Biol Chem 1994;269:12325-31.

[76] Schaff M, Tang C, Maurer E, Bourdon C, Receveur N, Eckly A et al. Integrin $\alpha6\beta1$ is the main receptor for vascular laminins and plays a role in platelet adhesion, activation, and arterial thrombosis. Circulation 2013;128:541-52.

[77] Chammas R, Veiga SS, Travassos LR, Brentani RR. Functionally distinct roles for glycosylation of alpha and beta integrin chains in cell-matrix interactions. Proc Nat Acad Sci 1993;90:1795-9.

[78] Van der Flier A, Sonnenberg A. Structural and functional aspects of filamins. Biochim Biophys Acta 2001;1538:99-117.

[79] Carroll RC, Gerrard, JM. Phosphorylation of platelet actin-binding protein during platelet activation. Blood 1982;59:466-71.

[80] Chen H, Herndon ME, Lawler J. The cell biology of thrombospondin-1. Matrix Biol 2000;19:597-614.

[81] Asch E, Podack E. Vitronectin binds to activated human platelets and plays a role in platelet aggregation. J Clin Invest 1990;85:1372.

6. **APPENDIX**

Table 1. Dataset of significantly changed phoshoproteins

ADP	Collagen	Thr.&Collagen	Cluster	Accessions
-0.5961741	1.154494	-0.5583196	Cluster 1	Q05655
-0.5790147	1.154699	-0.5756842	Cluster 1	O15439
-0.6272953	1.153216	-0.525921	Cluster 1	Q8WWA1
-0.6772734	1.14856	-0.4712865	Cluster 1	Q9NXH8
-0.6539287	1.151151	-0.4972219	Cluster 1	Q8WWA1
-0.7844507	1.126036	-0.3415852	Cluster 1	P02794
-0.8447746	1.104125	-0.2593509	Cluster 1	O43294
-0.9417709	1.049505	-0.1077342	Cluster 1	Q7LDG7
-0.2340707	1.096274	-0.8622032	Cluster 1	Q9H4B7
-0.2956866	1.114501	-0.8188144	Cluster 1	Q13884
0.0763157	0.9596557	-1.035971	Cluster 1	Q9H4B7
-1.120209	0.3175181	0.8026913	Cluster 2	Q5SQ64
-1.110837	0.2824157	0.8284215	Cluster 2	Q9NTJ5
-1.095715	0.2323309	0.8633838	Cluster 2	Q5T4S7
-1.142475	0.4261051	0.7163697	Cluster 2	O95810
-1.143032	0.4297151	0.7133173	Cluster 2	P61073
-1.136602	0.391945	0.7446573	Cluster 2	Q9Y385
-1.135654	0.3869497	0.7487048	Cluster 2	P51452
-1.136056	0.38905	0.7470056	Cluster 2	Q9Y6X5
-1.1547	0.5763887	0.5783113	Cluster 2	P21333
-1.153429	0.5297903	0.6236383	Cluster 2	O95870
-1.151748	0.5044125	0.6473358	Cluster 2	Q9H4B7
-1.151748	0.5044125	0.6473358	Cluster 2	Q9H4B7

-1.149693	0.6678793	0.4818133	Cluster 2	Q8TC12
-1.149693	0.6678793	0.4818133	Cluster 2	Q8TC12
-1.151841	0.6462522	0.5055889	Cluster 2	P00488
-1.075371	0.901942	0.173429	Cluster 2	O43149
-1.05277	0.9371848	0.1155853	Cluster 2	Q7L576
-1.114771	0.8180835	0.2966881	Cluster 2	P51149
-1.132144	0.7627645	0.3693793	Cluster 2	P50552
-1.055686	0.1226937	0.932992	Cluster 2	O95810
-1.023478	0.048738	0.9747398	Cluster 2	P55072
-1.021595	0.0446874	0.9769072	Cluster 2	P29350
-1.021937	0.0454224	0.9765148	Cluster 2	O75558
-0.9815561	-0.0359199	1.017476	Cluster 2	P17612
-0.9485215	-0.0960288	1.04455	Cluster 2	Q86YW5
-0.889893	-0.192288	1.082181	Cluster 2	Q86YW5
-0.5544647	-0.5999374	1.154402	Cluster 2	Q13576
-0.5465915	-0.6075722	1.154164	Cluster 2	P07359
-0.4799636	-0.669538	1.149502	Cluster 2	P62491
-0.4458545	-0.6995208	1.145375	Cluster 2	Q96C24
-0.7564744	-0.3772824	1.133757	Cluster 2	P07359
-0.665898	-0.4840178	1.149916	Cluster 2	P21333
-0.7033418	-0.4414133	1.144755	Cluster 2	Q86YW5
0.7928807	-1.123424	0.3305432	Cluster 3	Q9Y385
0.5030736	-1.151641	0.6485675	Cluster 3	P10909
0.0649006	-1.030869	0.9659689	Cluster 3	Q8N699
0.0906364	-1.042233	0.9515964	Cluster 3	Q96AP7
0.1477147	-1.065641	0.9179265	Cluster 3	O00161
0.7198238	0.4220026	-1.141826	Cluster 4	Q9Y624
0.8176042	0.2973441	-1.114948	Cluster 4	P08514
0.7718096	0.3578912	-1.129701	Cluster 4	Q9H4B7
0.8850541	0.1997419	-1.084796	Cluster 4	P04792
0.8850541	0.1997419	-1.084796	Cluster 4	P04792
0.8841661	0.2011026	-1.085269	Cluster 4	P08567
0.9485448	0.0959881	-1.044533	Cluster 4	P21333
0.9826832	0.0337777	-1.016461	Cluster 4	P05106
0.9826832	0.0337777	-1.016461	Cluster 4	P05106
1.046393	-0.1003532	-0.9460397	Cluster 4	Q9Y210
1.057038	-0.1260226	-0.9310153	Cluster 4	Q9H4B7
1.055927	-0.1232863	-0.9326407	Cluster 4	P16615
1.086123	-0.2035714	-0.8825511	Cluster 4	P04792
1.116326	-0.3025041	-0.8138223	Cluster 4	Q9Y210
1.113385	-0.291588	-0.821797	Cluster 4	O15173
1.082329	-0.8896226	-0.1927062	Cluster 4	P08567
1.096624	-0.861461	-0.2351627	Cluster 4	P27105
1.119025	-0.8061644	-0.3128607	Cluster 4	Q96RI0
1.115565	-0.8159218	-0.2996434	Cluster 4	P07900

			Cluster 4	P04792
1.135045	-0.7512471	-0.3837978	Cluster 4	P04792
1.135045	-0.7512471	-0.3837978	Cluster 4	P04792
1.131985	-0.7633684	-0.3686168	Cluster 4	P20645
1.126339	-0.783443	-0.3428959	Cluster 4	P07900
1.154576	-0.5919492	-0.5626273	Cluster 4	O15439
1.148404	-0.6784948	-0.4699087	Cluster 4	P07900
1.150443	-0.6610183	-0.4894245	Cluster 4	O75791
1.152833	-0.5195587	-0.6332738	Cluster 4	O00264
1.149454	-0.4795059	-0.6699479	Cluster 4	O00264
1.147222	-0.4599862	-0.6872362	Cluster 4	O15173
1.146865	-0.4571369	-0.6897286	Cluster 4	Q9Y624
1.143626	-0.4336475	-0.7099785	Cluster 4	P21796
1.143626	-0.4336475	-0.7099785	Cluster 4	P21796

Table 2. Dataset of significantly changed sialoproteins

ADP	Collagen	Thr.&Collagen	Cluster	Accessions
0.8669646	-1.093997	0.2270321	Cluster 1	P05106
0.8669646	-1.093997	0.2270321	Cluster 1	P05106
0.9658112	-1.030999	0.065188	Cluster 1	Q9HDC9
1.078065	-0.1807975	-0.8972673	Cluster 2	Q86WI1
1.125487	-0.3392278	-0.7862592	Cluster 2	P10909
0.7879565	0.3370098	-1.124966	Cluster 2	P05556
0.466007	0.6819436	-1.147951	Cluster 2	O95858
0.5045524	0.6472071	-1.15176	Cluster 2	Q9Y210
-1.154701	0.5776709	0.5770296	Cluster 3	Q6UX71
-1.153916	0.5401104	0.6138059	Cluster 3	Q9Y2Q0
-1.153121	0.5242693	0.6288514	Cluster 3	P08962
-1.109707	0.2784234	0.8312832	Cluster 3	Q9Y274
-1.124769	0.3361727	0.7885959	Cluster 3	P51575
-1.129485	0.3569	0.7725846	Cluster 3	Q13201
-1.133766	0.37733	0.7564363	Cluster 3	Q13201
-1.137774	0.3982928	0.7394814	Cluster 3	P08575
-0.9038765	-0.1703603	1.074237	Cluster 3	Q14766
-0.9038765	-0.1703603	1.074237	Cluster 3	Q14766
-0.9319314	-0.1244815	1.056413	Cluster 3	Q13201
-0.9300988	-0.1275612	1.05766	Cluster 3	P08648
-0.9254878	-0.1352562	1.060744	Cluster 3	P16284
-0.9254878	-0.1352562	1.060744	Cluster 3	P16284
-0.8801501	-0.2072285	1.087379	Cluster 3	P16284
-0.8715028	-0.2202685	1.091771	Cluster 3	P11279
-0.9905474	-0.0186446	1.009192	Cluster 3	Q9Y274
-0.9692178	-0.0589559	1.028174	Cluster 3	Q13201
-1.024289	0.0504908	0.9737982	Cluster 3	Q9Y274

-1.036452	0.0774027	0.9590494	Cluster 3	P08575
-1.036452	0.0774027	0.9590494	Cluster 3	P08575
-1.036452	0.0774027	0.9590494	Cluster 3	P08575
-1.041275	0.0884226	0.9528524	Cluster 3	Q14766
-1.055248	0.12162	0.9336277	Cluster 3	O15031
-1.057923	0.1282131	0.9297099	Cluster 3	P07602
-1.057032	0.1260077	0.9310241	Cluster 3	O15031
-1.05687	0.1256086	0.9312615	Cluster 3	Q13201
-1.057353	0.1268018	0.9305514	Cluster 3	Q13201
-1.061054	0.1360368	0.9250176	Cluster 3	P01137
-1.059451	0.1320155	0.9274352	Cluster 3	Q12913
-1.071741	0.1636773	0.908064	Cluster 3	P08514
-1.069477	0.1576927	0.9117846	Cluster 3	P16284
-1.069544	0.157869	0.9116754	Cluster 3	P16284
-1.075407	0.1735262	0.9018807	Cluster 3	P01137
0.2651565	-1.105856	0.8406992	Cluster 3	P02679
0.0211656	-1.010415	0.9892492	Cluster 3	Q9C0H2
-0.2216313	-0.8705913	1.092223	Cluster 3	O60704
-0.1951923	-0.8880128	1.083205	Cluster 3	P11279
-0.1086421	-0.9412429	1.049885	Cluster 3	P21926
-0.1606852	-0.9099277	1.070613	Cluster 3	Q9P126
-0.1541864	-0.9139517	1.068138	Cluster 3	P34810
-0.6709062	-0.4784348	1.149341	Cluster 3	P16284
-0.6688158	-0.4807694	1.149585	Cluster 3	Q6UWL2
-0.6688158	-0.4807694	1.149585	Cluster 3	Q6UWL2
-0.8199301	-0.2941557	1.114086	Cluster 3	P08575
-0.7908673	-0.333193	1.12406	Cluster 3	Q9C0H2
-0.7640859	-0.36771	1.131796	Cluster 3	Q14766
-0.7640859	-0.36771	1.131796	Cluster 3	Q14766
-0.7546077	-0.3796145	1.134222	Cluster 3	P14625
-0.7567936	-0.3768831	1.133677	Cluster 3	Q9NZ08
-0.5159518	-0.6366443	1.152596	Cluster 3	P16284
-0.479403	-0.67004	1.149443	Cluster 3	P14625
-0.4938923	-0.6569636	1.150856	Cluster 3	O60704
-0.4918929	-0.6587806	1.150674	Cluster 3	Q86WI1
-0.5578957	-0.5965887	1.154484	Cluster 3	P07996
-0.5578957	-0.5965887	1.154484	Cluster 3	P07996
-0.550312	-0.6039729	1.154285	Cluster 3	P08575
-0.5933443	-0.5612072	1.154552	Cluster 3	Q92542
-0.5933443	-0.5612072	1.154552	Cluster 3	Q92542
-0.4245703	-0.7176638	1.142234	Cluster 3	Q92542
-0.4073716	-0.7320152	1.139387	Cluster 3	P21731
-0.4073716	-0.7320152	1.139387	Cluster 3	P21731
-0.3987146	-0.7391362	1.137851	Cluster 3	Q10588
-0.3302462	-0.7931061	1.123352	Cluster 3	P04004

-0.2872919	-0.8249084	1.1122	Cluster 3	Q13201
-0.2816584	-0.8289653	1.110624	Cluster 3	P07602
-0.2551104	1.102844	-0.847734	Cluster 4	Q12907
-1.147365	0.6862228	0.4611421	Cluster 4	Q86WI1
-1.140792	0.7251367	0.4156556	Cluster 4	Q86WI1
-1.118906	0.8065102	0.3123956	Cluster 4	Q13201
-1.114473	0.8188908	0.2955818	Cluster 4	P13598
-1.075536	0.9016591	0.1738769	Cluster 4	Q9BVK6
-1.015513	0.9837292	0.0317837	Cluster 4	P08195
-1.006891	0.992963	0.0139285	Cluster 4	P40238
-1.03979	0.9547829	0.0850071	Cluster 4	P42892
-0.7227056	1.141271	-0.4185654	Cluster 4	P20645
-0.6452975	1.151922	-0.506624	Cluster 4	P13473
-0.5139806	1.152461	-0.6384805	Cluster 4	Q6UX71
-0.8752056	1.089915	-0.2147095	Cluster 4	P42892
-0.897352	1.078017	-0.1806645	Cluster 4	O14672
-0.9249661	1.061088	-0.1361223	Cluster 4	Q15904
-0.8325872	1.109185	-0.276598	Cluster 4	O14672
-0.7946767	1.12285	-0.328173	Cluster 4	O95858
-0.808507	1.118212	-0.3097054	Cluster 4	P10909

Table 3. Dataset of significantly changed N-glycoproteins

ADP	Collagen	Thr.&Collagen	Cluster	Accessions
-1.024631	0.0512317	0.9733995	Cluster 1	P16284
-1.056329	0.124274	0.9320546	Cluster 1	P08575
-1.043049	0.0925285	0.95052	Cluster 1	Q12913
-1.046509	0.1006259	0.9458827	Cluster 1	O15031
-1.047461	0.1028757	0.9445855	Cluster 1	Q86WI1
-0.9512662	-0.0912174	1.042484	Cluster 1	Q9NV96
-0.9710989	-0.0554914	1.02659	Cluster 1	P21333
-0.984266	-0.0307583	1.015024	Cluster 1	Q9UIQ6
-0.9916688	-0.0164592	1.008128	Cluster 1	P16109
-0.9921586	-0.0155025	1.007661	Cluster 1	P23229
-1.131449	0.3660571	0.7653921	Cluster 1	Q9C0H2
-1.138272	0.4010491	0.7372226	Cluster 1	Q9Y4L1
-1.084216	0.1980779	0.8861381	Cluster 1	P08575
-1.086278	0.2040216	0.8822561	Cluster 1	P14625
-1.093756	0.2262943	0.8674614	Cluster 1	Q9NV96
-1.073625	0.1687124	0.9049122	Cluster 1	Q9H7M9
-1.075378	0.1734481	0.90193	Cluster 1	Q9H7M9
-1.122861	0.328221	0.7946404	Cluster 1	Q9Y251
-1.104269	0.2598279	0.8444408	Cluster 1	Q9Y274

-1.107779	0.2717192	0.8360593	Cluster 1	P51575
-1.1094	0.2773502	0.8320503	Cluster 1	Q9BVK6
-1.110226	0.2802512	0.8299747	Cluster 1	Q92542
-1.110226	0.2802512	0.8299747	Cluster 1	Q92542
-1.112609	0.2887688	0.8238405	Cluster 1	Q96AP7
-0.8006408	-0.3202563	1.120897	Cluster 1	P08575
-0.8088363	-0.309261	1.118097	Cluster 1	Q08722
-0.8161944	-0.2992713	1.115466	Cluster 1	P16284
-0.8444408	-0.2598279	1.104269	Cluster 1	P08648
-0.8444408	-0.2598279	1.104269	Cluster 1	P08648
-0.8401878	-0.2658822	1.10607	Cluster 1	Q9C0H2
-0.8344417	-0.2739957	1.108437	Cluster 1	P08648
-0.8353217	-0.272758	1.10808	Cluster 1	Q92542
-0.9095055	-0.1613639	1.070869	Cluster 1	P08575
-0.8980265	-0.1796053	1.077632	Cluster 1	Q9NX62
-0.8918919	-0.1891892	1.081081	Cluster 1	P08575
-0.8926979	-0.1879364	1.080634	Cluster 1	P11279
-1.124314	0.7900583	0.3342554	Cluster 1	Q9H4B7
-1.127468	0.7796321	0.3478358	Cluster 1	Q14766
-1.142182	0.7179429	0.424239	Cluster 1	Q12907
-1.142182	0.7179429	0.424239	Cluster 1	Q12907
-1.141822	0.7198446	0.4219779	Cluster 1	Q12907
-1.154008	0.5423838	0.6116245	Cluster 1	P02671
-1.154701	0.5773503	0.5773503	Cluster 1	P08514
-1.149507	0.4800138	0.669493	Cluster 1	Q12913
-1.150205	0.4869481	0.6632569	Cluster 1	Q9Y251
-1.150205	0.4869481	0.6632569	Cluster 1	Q9Y251
-1.024631	0.9733995	0.0512315	Cluster 1	P08648
0.1227572	-1.055712	0.9329544	Cluster 2	Q9NXL6
-0.2434013	-0.8558304	1.099232	Cluster 2	P08514
-0.2598279	-0.8444408	1.104269	Cluster 2	Q14392
-0.5619564	-0.5926085	1.154565	Cluster 2	P16284
-0.5947547	-0.5597692	1.154524	Cluster 2	P16284
1.15208	-0.6433695	-0.5087108	Cluster 3	Q13201
1.115244	-0.8167987	-0.2984457	Cluster 3	Q969V3
0.8579978	-1.098237	0.2402394	Cluster 3	Q13201
0.8579978	-1.098237	0.2402394	Cluster 3	Q13201
0.9832103	-1.015984	0.0327737	Cluster 3	P16278
0.9832103	-1.015984	0.0327737	Cluster 3	P16278
0.6692498	-1.149535	0.4802852	Cluster 3	Q92542
0.6993029	-1.14541	0.446107	Cluster 3	P01009
-0.6999132	1.145313	-0.4453994	Cluster 4	Q6UWL2
-0.7258663	1.140647	-0.4147806	Cluster 4	Q13201
0.1122858	0.9391178	-1.051404	Cluster 4	Q96K49
0.0323497	0.9834327	-1.015782	Cluster 4	P08648

-0.1362954	1.061157	-0.9248617	Cluster 4	P40197
-0.2402394	1.098237	-0.8579978	Cluster 4	P17301
-0.2773501	1.1094	-0.8320503	Cluster 4	Q9Y6C2
-0.3307704	1.123479	-0.7927083	Cluster 4	P40197
-0.3307704	1.123479	-0.7927083	Cluster 4	P40197
-0.3636976	1.13095	-0.7672524	Cluster 4	P10909
0.3601721	0.7700229	-1.130195	Cluster 5	P16109
0.5145079	0.6379898	-1.152498	Cluster 5	P20645
1.077632	-0.1796053	-0.8980265	Cluster 5	Q13201
1.089008	-0.2120192	-0.8769888	Cluster 5	P16671
0.708361	0.4355464	-1.143907	Cluster 5	P05106
0.6725134	0.4766359	-1.149149	Cluster 5	P13473
0.9523641	0.0892841	-1.041648	Cluster 5	P40238
0.9250203	0.1360324	-1.061053	Cluster 5	Q6UX71
0.9049123	0.1687124	-1.073625	Cluster 5	Q9NXH8
0.8108485	0.3065403	-1.117389	Cluster 5	P05556
0.8510645	0.250313	-1.101378	Cluster 5	P13598

4. The targeted way

ABSTRACT

Different sample treatment protocols for the liquid chromatography-electrospray-tandem mass spectrometry (LC-ESI-MS/MS) analysis of potential residuals of ovalbumin and caseins added to red wines were developed. In particular, attention was paid to the simultaneous detection and quantitation of fining agent residues, i.e. ovalbumin, α- and β-casein, in wine samples. The different sample treatment methods were compared in terms of protein recovery. The use of denaturing agents combined with size exclusion concentration and purification allowed to obtain a reproducible (RDS < 20%) analytical protocol with good recoveries (73($\pm$2)-109($\pm$4)% range) for digested proteins from 12.5 mL of wine sample. Matrix-matched calibration from LC-ESI-MS/MS analysis indicated that the devised method allowed detection of target peptides in the 0.01-0.8 mg/mL range. Finally, method applicability and selectivity were demonstrated by using fining agents commonly exploited in winery industry and by analyzing 20 commercial red wine samples.

1. INTRODUCTION

The liquid chromatography-electrospray-tandem mass spectrometry (LC-ESI-MS/MS) determination of hidden allergens in foods is becoming of relevant importance because of the several advantages offered by this technique, including multi-tag detection, unambiguous allergen identification and accurate quantitative data [1,2]. The experimental workflow is generally based on the selection of targeted peptides and the use of selected reaction monitoring (SRM) acquisition mode for quantitative purposes [3-7]. Basically, quality of the final analytical results is based on the sample preparation procedure, the performance of the whole analytical method and the selection of a suitable calibration mode. Different sample treatment methods have been proposed as a function of the investigated food matrices and protein allergens [8-11], representing a crucial step of the whole procedure. The sample preparation method is usually performed manually and it is expected to extract and purify the compounds of interest in an easy, quantitative and reproducible manner. In this study our attention was focused on the LC-MS/MS analysis of potential residuals allergens in red wine. The organoleptic, antioxidants and anti-inflammatory properties of the red wine constituents are widely investigated and known. Red wine is an extremely complex matrix rich in polyphenols, tannins, anthocyanins and other molecules that can easily interact with proteins making challenging their quantitative analysis [10,12,13]. Recently, attention was paid to the putative presence of traces of exogenous proteins (i.e. caseins, albumins, lysozyme, gluten) added during wine fining process and removed before bottling. These proteins present allergen activity

and the accurate determination of their residual concentration level is desiderable to ensure consumer safety. Different analytical methods were proposed in the literature for quantitative purposes based both on immunoassay and mass spectrometry techniques [7,14-24]. Immunoassays present unique advantages of simplicity and fastness, but they are usually performed on a single target and mainly suffer of cross-reactivity reactions and poor accuracy. In this work, an LC-MS/MS method for the simultaneous determination of ovalbumin, α- and β-casein in red wine is proposed. Different sample treatments for the detection of allergen residues in wine were evaluated and compared in terms of protein recovery. Generally, the investigated processes involved the use of cut-off filters, denaturing agents, protein precipitation or size-exclusion purification cartridges. Finally, by using the most suitable and efficient sample treatment protocol, the LC-MS/MS method was validated and applied to commercial fining agents and red wine samples.

2. MATERIALS AND METHODS

Chemicals - Urea (99.8%, purity) and thiourea were purchased from Carlo Erba (Milan, Italy). Acetonitrile (HPLC purity), formic acid (analytical reagent grade), trifluoroacetic acid (TFA, >98% purity), sodium dodecyl sulfate (SDS, 99% purity), trichloroacetic acid (TCA, >99% purity), ammonium hydrogen carbonate (99% purity), trypsin from bovine pancreas, iodoacetamide (IAM, >99% purity), DL-dithiothreitol (DTT, > 99% purity), a-casein, b-casein, ovalbumin and Bradford reagent were from Sigma-Aldrich (St. Louis, Missouri, USA). Potassium caseinate (Protoclar®) and egg-white powder were purchased from a local enological store. Buffered solutions and mobile phases were obtained in HPLC-grade water prepared with a Milli-Q element A10 System (S. Francisco, CA, USA). A total of 20 Italian commercial red still wine samples from different wine-producing regions and brands were purchased from local stores. The investigated wines were produced during 2007-2011 vintages (Table 1).

Table 1. List of the analyzed red wine samples.

Sample N.	Red wine sample	Production Italian region	Vintage
1	Barbera	Piemonte	2010
2	Bonarda	Emilia Romagna	2010
3	Cannonau	Sardegna	2009
4	Cannonau	Sardegna	2010
5	Lambrusco	Emilia Romagna	2010
6	Lambrusco	Emila Romagna	2011
7	Lambrusco	Emilia Romagna	2011
8	Magliocco	Calabria	2009
9	Magliocco	Calabria	2011
10	Magliocco	Calabria	2011
11	Mamertino	Sicilia	2009
12	Montepulciano	Abruzzo	2011
13	Nebbiolo	Piemonte	2010
14	Nebbiolo	Piemonte	2011
15	Nero d'Avola	Sicilia	2007
16	Nero d'Avola	Sicilia	2008
17	Nero d'Avola	Sicilia	2009
18	Sangiovese	Emilia Romagna	2007
19	Syrah	Sicilia	2008
20	Syrah	Sicilia	2009

Bioinformatic analysis - For each targeted protein, peptides providing good ESI sensitivity and unequivocally identifying the target protein were selected. Thereby, a tryptic digest of a standard mixture of the three proteins (200 mg/mL) in NH_4HCO_3 50 mM pH 8 was analyzed by LC-MS/MS under data-dependent acquisition (DDA). Using this acquisition mode, the ion-trap was programmed to ignore any singly charged species acquired in the 300-1200 amu mass range and to perform MS/MS analysis (normalized collision energy: 30) only on eluting species that overcome a predefined threshold of 500 cps. For each protein two marker peptides were selected (Table 2), considering different criteria such as quality of product ion spectra matches (Bioworks 3.3 database searching software, Thermo Electron Corporation, Marietta, Ohio) signal intensity of the most abundant product ion of MS/MS spectrum, no post translational modification sites and sequence specificity (BLAST search; algorithm: blastp; MATRIX PAM 30; GAP COSTS: existence 10, extension 1; DATABASE: non-redundant protein sequences).

Table 2. SRM transitions monitored for the target peptides from the allergen proteins investigated

Protein	Precursor ion sequence (*m/z*; charge state)	Product ion sequence (*m/z*; charge state; fragment type)
α-casein	HQGLPQEVLNENLLR (*m/z* 587.2; +3)	HQGLPQEVLNENLL (*m/z* 793.6; +2; b_{14}^{+2})[a]
		HQGLPQEV (*m/z* 445.2; +2; b_8^{+2})
	YLGYLEQLLR (*m/z* 634.8; +2)	GYLEQLLR (*m/z* 991.8; +1; y_8^{+1})[a,b]
		LEQLLR (*m/z* 771.4; +1; y_6^{+1})
β-casein	VLPVPQK (*m/z* 390.9; +2)	PVPQK (*m/z* 568.4; +1; y_5^{+1})[a]
		PVPQK (*m/z* 284.6; +2; y_5^{+2})
	AVPYPQR (*m/z* 415.9; +2)	PYPQR (*m/z* 330.6; +2; y_5^{+2})[a,b]
		PYPQR (*m/z* 660.4; +1; y_5^{+1})
ovalbumin	GGLEPINFQTAADQAR (*m/z* 844.9; +2)	PINFQTAADQAR (*m/z* 666.3; +2; y_{12}^{+2})[a,b]
		PINFQTAADQAR (*m/z* 1331.7; +1; y_{12}^{+1})
	VASMASEK (*m/z* 411.9; +2)	VASMASEK (*m/z* 402.8; +2; water loss)[a]
		SMASEK (*m/z* 652.2; +1; y_6^{+1})

[a] Most intense MS/MS transition

[b] *m/z* transition monitored for the calculation of the validation parameters

Sample treatment - A volume of 12.5 mL of red wine sample was fortified with the three proteins at different amounts and the mixture was homogenized before sample treatment. Five different sample treatments were investigated (procedure 1-5). In procedure 1 the sample was centrifuged at 7000 rpm for 150 min in ultrafiltration tube with 5 kDa cut-off membrane (Sartorius Stedim Biotech, Goettingen, Germany), previously conditioned with distilled water, to obtain a concentrated final volume of 2.5 mL. Afterward, protein precipitation was performed by diluting the sample (1:8 ratio) with ethanol/TCA (15%, w/v) and keeping in ice for 2 h. The solution was centrifuged at 9000 rpm for 10 min at 4°C. The pellet was then washed with ethanol and solubilized in 1mL NH_4HCO_3 50mM to pH 8. Tryptic digestion of wine extracts was performed after protein

reduction and alkylation. Reduction was performed by addition of DDT to a final concentration of 10 mM and incubating the mixture at 30°C for 40 min. For alkylation reaction IAA was added to a final concentration of 20 mM and the mixture was left for 40 min in the dark; then DTT was added to have a final concentration of 10 mM. In the final step, enzymatic digestion was performed by adding a trypsin solution (0.5 mg/mL, in NH$_4$HCO$_3$ 50 mM pH 8) to the sample in order to obtain a trypsin:protein ratio 1:50 and incubating overnight at 37°C. Ultimately, formic acid (1%, v/v) was added to quench the digestion reaction before LC-ESI-MS/MS analysis. In the second approach (procedure 2), a treatment with urea (final concentration 6M), thiourea (final concentration 2 M) and SDS (0.2% w/v) heating in boiling water for 10 min, was performed just before the cut-off concentration step, in order to obtain proteins free from interactions with other wine components, i.e. tannins, anthocyanins, polyphenols, etc. Afterward, the sample was diluted to 5 mL with NH$_4$HCO$_3$ 50 mM at pH 8, then it was reduced, alkylated and digested as reported in the procedure 1. The tryptic digest was then purified on a C18 SPE cartridge as follows: conditioning (2 mL methanol followed by 2 mL water), sample loading (5 mL), washing (water/methanol/TFA, 89.9/10/0.1 v/v/v) and final elution (1 mL water/acetonitrile/TFA, 29.9/70/0.1, v/v/v). According to procedure 3, the addition of urea, thiourea, SDS denaturants and sample heating were carried out after centrifugation in ultrafiltration tubes. Then, the obtained 2.5 mL of sample was loaded onto a polyvinylpolypyrrolidone (PVPP)-based cartridge (Thermo Fisher Scientific, San Jose, CA, USA) to remove the phenolic compounds. NH$_4$HCO$_3$ was added to the extract to reach pH 8 and the reduction, alkylation and tryptic digestion were performed as reported in the procedure 1. Procedure 4 differs from the previous one by the fact that the purification on PVPP cartridges was performed on tryptic digest, thus after reduction, alkylation and tryptic digestion reactions. Finally, procedure 5 substitutes the use of PVPP cartridges in the procedure 3 with a size exclusion (SE)-based purification. Denaturation and heating steps were carried out on the concentrated samples before reduction and alkylation reactions. Then, a 100 mL aliquot was purified on a 6 kDa-size exclusion column Bio-Spin 6 (Bio-Rad Laboratories, Milan, Italy) as follows: conditioning for three times with 500 mL NH$_4$HCO$_3$ 50 mM pH 8, loading 100 mL of sample, and eluting by centrifugation at 1000 rpm for 4 min to collect the extract. The tryptic digestion was thus performed as described in the procedure 1. To assess recovery, a blank matrix and a wine matrix fortified with ovalbumin, α- and β-casein at two different concentration levels (10 and 100 mg/mL, five independent extractions for each level) were considered.

Liquid chromatography-tandem mass spectrometry - All LC-MS/MS analyses were performed on a Surveyor LC system (Thermo Fisher Scientific, San Jose, CA) coupled online with

a LTQ linear ion trap (LIT) (Thermo Fisher Scientific). The system was controlled by the Xcalibur software. LC separation was performed by using a 100 mm x 2.1 mm, i.d. 2.7 mm, Kinetex C18 column (Phenomenex, CA, USA) thermostated at 25 °C. A binary solvent gradient was used for the analysis of the tryptic digests; solvent A consisted of 0.1% (v/v) formic acid aqueous solution and solvent B was 0.08% (v/v) formic acid in acetonitrile. Following analytical column equilibration, each sample was loaded (30 mL) and eluted at a constant flow rate of 200 mL/min under the following optimized gradient: solvent B was initially set at 10% for 1 min, then delivered by a linear gradient from 10% to 60% in 15 min and to 95% in 2 min, then 2 min at 10% before column re-equilibration (5 min) for the next sample injection. Mass spectrometric conditions were set as follows: electrospray voltage, 3.5 kV; sheath gas, auxiliary gas and sweep gas set to 50, 20 and 5 arbitrary units, respectively; capillary temperature, 200°C; capillary voltage, 20 V; tube lens 100 V. The mass spectrometer was operated in time-scheduled "Product Ion Scan mode" and, for quantitative purposes, in Selected Reaction Monitoring (SRM) acquisition mode, by monitoring the MS/MS transitions of the peptides VLPVPQK, AVPYPQR and VASMASEK from 0 to 5.50 min (segment 1), the transitions of the peptides HQGLPQEVLNENLLR and GGLEPINFQTAADQAR from 5.50 to 8 min (segment 2), and those of the peptide YLGYLEQLLR from 8 to 25 min (segment 3). The precursor ion-product ion SRM transitions monitored for each peptide are reported in Table 2. The normalized collision energy was set to 30 for all peptides.

Method validation - Validation of the whole analytical method was performed according to Eurachem guidelines [25] on non commercial red wine subjected to fining process not involving the exploitation of the proteins under investigation. Sample treatment protocol was carried out using the procedure 5. As for the blank matrix, the absence of the proteins under investigation was previously verified. For this purpose, wine blank matrix was fortified with different amounts of standard proteins before sample treatment and measurements were carried out by monitoring the most abundant MS/MS transition for the peptide providing the best sensitivity for each protein (Table 2). The second peptide was used for confirmatory purposes. The detection (LOD) and quantification (LOQ) limits were calculated on matrix and were expressed as the concentration of analyte giving a signal that is 3s and 10s above the mean blank signal, respectively, where s is the standard deviation of the blank signal obtained from ten independent blank measurements. In particular, in order to assess the blank signal distribution, analytes were added before extraction, each in the amount proper to give the minimum integrable signal. Linearity was investigated starting from LOQ values of each peptide to 200 mg/mL (seven concentration levels, two replicates for each level and two injections for each extract). Mandel's fitting test was performed to check linearity. The significance of the intercept (α = 0.05) was established by running a t-test. Accuracy was assessed in terms of

precision and trueness. Precision was calculated as RSD% in terms of intra-day repeatability and intermediate precision on three concentration levels (LOQ value for each protein, 10 and 100 mg/mL), performing three independent replicates at each level and three LC-MS/MS injections for each extract. The intermediate precision was estimated over three days verifying homoscedasticity of the data and performing the analysis of variance (ANOVA) at the confidence level of 95%. Matrix effect was assessed by a t-test ($\alpha = 0.05$, two- tailed) between curve slopes calculated on matrix tryptic digest and on aqueous tryptic digest. Trueness was measured in terms of percent recovery on two concentration levels, i.e. LOQ of each peptide and 50 mg protein/mL matrix, by calculating the ratio of determined and added protein content.

3. RESULTS AND DISCUSSION

For method development, marker peptides were firstly selected, then their chromatographic separation was optimized, and finally different sample treatment procedures were investigated. Validation was carried out on the final selected analytical procedure.

Selection of the biomarker peptides and development of the LC-MS/MS method - The feature of this quantitative approach is the selection of the marker peptide ions, the evaluation of their CID fragmentation profile and the selection of intense and characteristic SRM transitions. As for biomarker peptide selection, different criteria were used. The selected proteins were identified with a sequence coverage average of ~75%. Transitions for SRM analysis were carefully selected by varying normalized collision energy (from 20 to 35) for each peptide. The definitive assay was performed using a series of transitions (precursor/fragment ion pairs) as reported in Table 2. As for chromatographic separation, the elution gradient was set up in order to obtain a suitable separation among peptides within 10 min (Fig. 1). SRM signals were acquired on three different time windows in order to improve LIT ion sampling and thus instrumental repeatability with complex mixtures.

Comparison of sample treatment procedures - Protein recovery was used as indication of the efficiency of the sample treatment procedure. By following the procedure 1 on five independent samples, recoveries lower than 5% and very low repeatability were observed (RSD > 60%). These findings could be explained on the basis of interactions between proteins and polyphenols, tannins and other matrix compounds that can interfere with both the protein precipitation and the tryptic digestion efficiency. In addition, strong ESI-MS signal suppression was observed. On the basis of these findings, initially, three commonly used denaturing agents (urea, thiourea and SDS) were added to the red wine samples in order to obtain proteins free from interaction with the matrix components. The use of 5 kDa cut-off filter for concentration purposes allowed to obtain extracts

with a reduced red color, suggesting a more effective separation between high-molecular weight compounds and small matrix interferents. Tryptic digestion was performed and peptides were purified on a C18 SPE cartridge with the final aim to reduce components that may cause ESI suppression. However, recovery values were lower than 10%. The protein colorimetric Bradford assay, performed after the cut-off filter step, demonstrated that the addition of the denaturing agents before this step cause a significant loss of total proteins (> 70%). This finding could be accordable to protein denaturation that reduces protein solubility due to the exposition of the hydrophobic sites. For this reason, proteins may precipitate on the filter membrane making very difficult their recovery. In order to avoid protein loss, the denaturing agents were added after centrifugation on the cut-off filter. The purification of the protein fraction from the phenolic compounds was carried out by using a PVPP cartridge. This kind of support, which is widely used for purification of red wine samples, it was used by following a standard protocol suggested by the providers. Tryptic digestion performed after purification on the PVPP cartridges provided recovery values significantly improved for both α-casein (46±10%) and ovalbumin (181±32%), whereas in the case of β-casein no signal was observed. A possible explanation could lie in the interaction or sticking of this protein on the PVPP support. When performing the tryptic digestion before PVPP treatment (procedure 4), no signals were observed for all the peptides suggesting the complete loss during the purification step. Finally, a size exclusion purification-based procedure was carried out on reduced and alkylated proteins, just before tryptic digestion. In this case, good recovery and RSD values were obtained for all proteins (ovalbumin 73±2%; α-casein 99±5%; β-casein 109±4%). After examination of the feasibility of the SPE, PVPP, and SE-based purification procedures for allergen clean-up, SE procedure was proved useful in eliminating time-consuming SPE process while maintaining the advantages of sample clean-up. In comparison with the conventionally used PVPP cartridges, the SE-based purification approach allowed to eliminate the phenolic compounds and denaturant agents without loss of proteins. The SE-based procedure provided the best performances in terms of recovery and precision. Reliability of the whole analytical procedure was thus demonstrated through validation and application to real samples.

Method validation - Method validation was carried out in terms of limits of detection and quantification, linear dynamic ranges and accuracy. Considering the complexity of the matrix, good results in terms of sensitivity were obtained, LODs and LOQs ranging from 0.01 to 0.8 mg protein/mL wine and from 0.03 to 2 mg protein/mL, respectively (Table 3). Linearity of the method was proved by matrix-matched calibration over two orders of magnitude for α-casein and ovalbumin and over three orders for β-casein (r^2 > 0.987, n = 20). Linearity was demonstrated by

variance homogeneity assessment (p > 0.05) and by applying the Mandel fitting test after calculation of linear curve equations for targeted peptide; p values greater than 0.01 allowed to confirm that the quadratic model was not significantly better than the linear one. As for method precision, good results were achieved both in terms of intra-day repeatability and intermediate precision with RSD always lower than 10% and 19%, respectively. As for intermediate precision, ANOVA performed on the data acquired over three days showed that the mean values were not significantly different (p > 0.05). To verify matrix effect, the presence of systematic proportional errors were investigated with a t-test by comparing calibration curve slopes obtained for the aqueous tryptic digests and the matrix tryptic digests. Significant signal enhancement of 67% for the AVPYPQR peptide was obtained, whereas significant ion suppression of 15 and 38% for the YLGYLEQLLR and GGLEPINFQTAADQAR peptides, respectively, were calculated. Thus, matrix effect was overcome by performing a label-free quantification using calibration curves built on matrix tryptic digests. Trueness values from 82(±3) to 105(±3)% were also calculated.

Table 3. Matrix-matched calibration curves, LOD and LOQ values of the targeted peptides obtained by using sample procedure 5 and SRM LC-ESI-MS/MS analysis.

Protein	LOD (μg/mL)	LOQ (μg/mL)	Linear range (μg/mL)	Calibration curve y=a($\pm s_a$)x+b($\pm s_b$)	r^2 (*n*)
α-Casein	0.5	1	LOQ – 100	y = (58208 ± 1183)x - (5208 ± 525)	0.997 (20)
β-Casein	0.01	0.03	LOQ – 50	y = (21684 ± 346)x	0.997 (20)
Ovalbumin	0.8	2	LOQ – 100	y = (39768 ± 1860)x - (4419 ±827)	0.987 (20)

Method application - After validation, method suitability for the determination of allergenic proteins residues in red wine samples was investigated using two commercial fining agents, i.e. Protoclar® (i.e. potassium caseinate) and egg-white powder, commonly exploited in winery industry. Taking into account the complex composition of commercial fining powders, limits for their detection in red wine were also assessed; a LOD value of 0.2 mg/mL was calculated for Protoclar®, obtained by monitoring the m/z 415.9/m/z 330.6 MS/MS transition of the peptide AVPYPQR of β-casein; a value of 1.6 mg/mL was calculated as LOD for egg-white powder, using the m/z 844.9/m/z 666.3 MS/MS transition of the peptide GGLEPINFQTAADQAR of ovalbumin. At 2.5 mg/mL concentration level of Protoclar® also α-casein was detected. In Fig. 1 is reported the

chromatogram for the analysis of a blank red wine sample fortified with the investigated commercial fining powders at 2.5 mg/mL, verifying the possibility of monitoring the SRM transitions selected for standard proteins and proving the applicability of the developed method for the analysis of red wine samples treated with commercial fining agents. The devised method was then applied to test method selectivity and to investigate the presence of allergenic fining residues in 20 commercial red wine samples. As the marker peptides are unique for each protein, false positive allergen detection is dramatically reduced. In accordance with the results of Restani *et al*. [21], no traces of the investigated fining agents were found in the samples, thus excluding any risk for allergic sensitive people, consistent with current European legislation [26-28]. Finally, method reliability was further proved by spiking all the investigated commercial red wine samples with α-, β- casein and ovalbumin at concentration levels corresponding to LOD value for each and detecting in all the cases the three allergenic proteins.
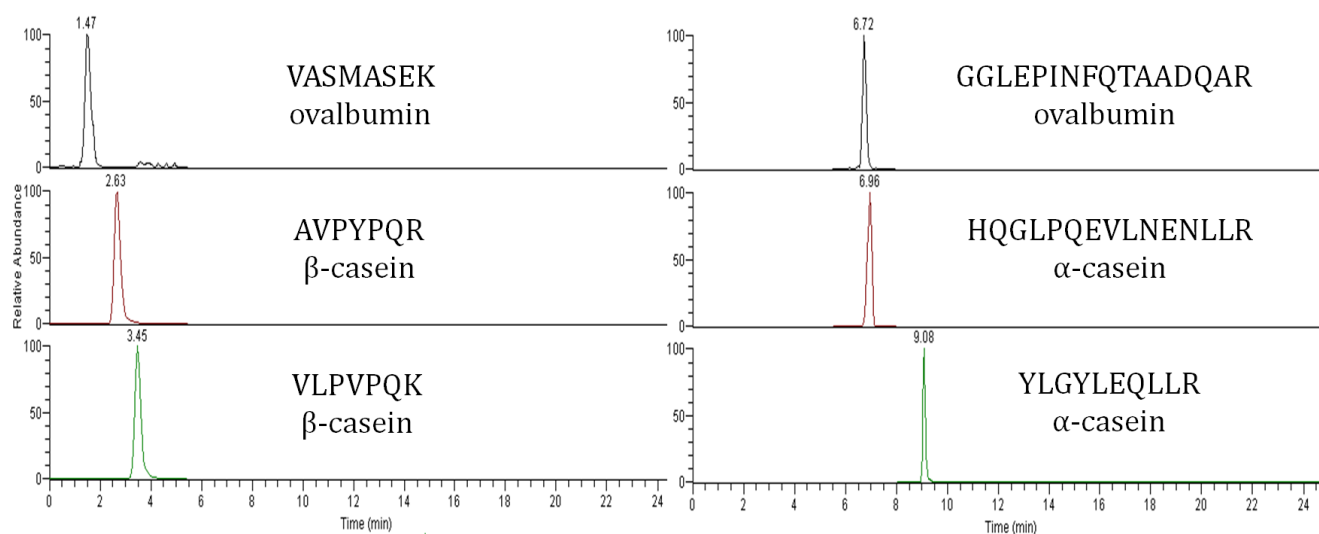
Fig. SRM LC-ESI-MS/MS chromatogram of a blank red wine sample fortified with commercial fining agents (Protoclar® and egg-white powder) at 10 µg/mL

4. CONCLUSIONS

The results described here allowed for the selection of peptide tag markers specific for the major red wine residuals allergens. The suitable selection of the biomarker peptides, the LC separation and the sample preparation protocol are crucial and constitute the basis for reliable confirmatory methods for the detection of allergens in food and beverage samples. As for red wine, an easy protein cut-off concentration protocol combined with size-exclusion-based purification was developed and proposed as reliable procedure. In comparison with a conventional PVPP, SE is able to provide improved protein recovery and extract purity. The sample workflow proposed combined with LC-MS/MS analysis was proved sensitive enough to identify and quantify allergens in red wine protein extracts at very low levels (about mg protein/mL wine), making this method useful to assist in the protection of the health of allergic consumers.

CHAPTER REFERENCES

[1] Faeste CK, Ronning HT, Christians U, Granum PE. Liquid chromatography and mass spectrometry in food allergen detection. Journal of Food Protection 2011;74:316-45.

[2] Monaci L, Visconti A. Mass spectrometry-based proteomics methods for analysis of food allergens. Trends in Analytical Chemistry 2009;28:581-91.

[3] Ansari P, Stoppacher N, Rudolf J, Schuhmacher R, Baumgartner S. Selection of possible marker peptides for the detection of major ruminant milk proteins in food by liquid chromatography-tandem mass spectrometry. Anal Bioanal Chem 2011;399:1105-15.

[4] Bignardi C, Elviri L, Penna A, Careri M, Mangia A. Particle-packed column versus silica-based monolithic column for liquid chromatographic-electrospray-linear ion trap-tandem mass spectrometry multiallergen trace analysis in foods. J Chromatogr A 2010;1217: 7579-85.

[5] Heick J, Fischer M, Popping B. First screening method for the simultaneous detection of seven allergens by liquid chromatography mass spectrometry. J Chromatogr A 2011;1218:938-43.

[6] Mattarozzi M, Bignardi C, Elviri L, Careri M. Rapid shotgun proteomic liquid chromatography-electrospray ionization-tandem mass spectrometry-based method for the lupin (Lupinus albus L.) multi-allergen determination in foods. J Agric Food Chem 2012;60:5841-6.

[7] Monaci L, Losito I, Palmisano F, Visconti A. Identification of allergenic milk proteins markers in fined white wines by capillary liquid chromatography-electrospray ionization-tandem mass spectrometry. J Chromatogr A 2010;1217:4300-5.

[8] Bignardi C, Mattarozzi M, Penna A, Sidoli S, Elviri L, Careri M et al. A rapid size-exclusion

solid-phase extraction step for enhanced sensitivity in multi-allergen determination in dark chocolate and biscuits by liquid chromatography-tandem mass spectrometry. Food Analytical Methods 2013;6:1144-52.

[9] Careri M, Elviri L, Lagos JB, Mangia A, Speroni F, Terenghi M. Selective and rapid immunomagnetic bead-based sample treatment for the liquid chromatography–electrospray ion-trap mass spectrometry detection of Ara h3/4 peanut protein in foods. J Chromatogr A 2008;1206:89-94.

[10] Le Bourse D, Jégou S, Conreux A, Villaume S, Jeandet P. Review of preparative and analytical procedures for the study of proteins in grape juice and wine. Anal Chim Acta 2010;667:33-42.

[11] Monaci L, van Hengel AJ. Development of a method for the quantification of whey allergen traces in mixed-fruit juices based on liquid chromatography with mass spectrometric detection. J Chromatogr A 2008;1192:113-20.

[12] Moreno-Arribas MV, Pueyo E, Polo MC. Analytical methods for characterization of proteins and peptides in wines. Anal Chim Acta 2002;458:63-75.

[13] Vincenzi S, Mosconi S, Zoccatelli G, Dalla Pellegrina C, Veneri G, Chignola R et al. Development of a new procedure for protein recovery and quantification in wine. American Journal of Enology and Viticulture, 2005;56:182-7.

[14] D'Amato A, Kravchuk AV, Bachi A, Righetti PG. Noah's nectar: the proteome content of a glass of red wine. J Proteomics 2010;73:2370-2377.

[15] Tolin S, Pasini G, Curioni A, Arrigoni G, Masi A, Mainente F et al. Mass spectrometry detection of egg proteins in red wines treated with egg white. Food Control 2012;23:87-94.

[16] Tolin S, Pasini G, Simonato B, Mainente F, Arrigoni G. Analysis of commercial wines by LC-MS/MS reveals the presence of residual milk and egg white allergens. Food Control 2012;28:321-6.

[17] Weber P, Steinhart H, Paschke A. Investigation of the allergenic potential of wines fined with various proteinogenic fining agents by ELISA. J Agric Food Chem 2007;55:3127-33.

[18] Lacorn M, Gosswein C, Immer U. Determination of residual egg white proteins in red wines during and after fining. American Journal of Enology and Viticulture, 2011;62:382-5.

[19] Monaci L, Losito I, De Angelis E, Pilolli R, Visconti A. Multi-allergen quantification of fining-related egg and milk proteins in white wines by high- resolution mass spectrometry. Rapid Commun Mass Spectrom 2013;27:2009-18.

[20] Monaci L, Losito I, Palmisano F, Godula M, Visconti A. Towards the quantification of residual milk allergens in caseinate-fined white wines using HPLC coupled with single-stage Orbitrap mass spectrometry. Food Addit Contam 2011;28:1304-14.

[21] Restani P, Uberti F, Danzi R, Ballabio C, Pavanello F, Tarantino C. (2012). Absence of allergenic residues in experimental and commercial wines fined with caseinates. Food Chem

2012;134:1438-45.

[22] Rolland JM, Apostolou E, De Leon MP, Stockley CS, O'Hehir RE. Specific and sensitive enzyme-linked immunosorbent assays for analysis of residual allergenic food proteins in commercial bottled wine fined with egg white, milk, and nongrape-derived tannins. J Agric Food Chem 2008;56:349-54.

[23] Simonato B, Mainente F, Tolin S, Pasini G. Immunochemical and mass spectrometry detection of residual proteins in gluten fined red wine. J Agric Food Chem 2011;59:3101-10.

[24] Weber P, Steinhart H, Paschke A. Determination of the bovine food allergen casein in white wines by quantitative indirect ELISA, SDS-PAGE, Western Blot and Immunostaining. J Agric Food Chem 2009;57:8399-405.

[25] Eurachem. Eurachem Guide. The Fitness for Purpose of Analytical Methods: A Laboratory Guide to Method Validation and Related Topics. (1st English ed.). LGC Ltd., Teddington, U.K., 1998, http://www.eurachem.org accessed on 17 October 2012.

[26] European Commission. Commission Directive 2005/26/EC of 21 March 2005 establishing a list of food ingredients or substances provisionally excluded from Annex IIIa of Directive 2000/13/EC of the European Parliament and of the Council. Official Journal of the European Union, 2005;L 75: 33-4.

[27] European Commission Commission Directive 2007/68/EC of 27 November 2007 amending Annex IIIa to Directive 2000/13/EC of the European Parliament and of the Council as regards certain food ingredients. Official Journal of the European Union 2007;L 310:11-4.

[28] European Commission. Commission Regulation (EU) No 1266/2010 of 22 December 2010 amending Directive 2007/68/EC as regards labelling requirements for wines. Official Journal of the European Union 2010;L 347:27-8.

ACKNOWLEDGMENTS

CURRICULUM VITAE

Personal data

First Name: MARCO
Surname: MILIOLI
Nationality: Italian
Birthplace: Mantova, Italia
Date of birth: 26th February 1987
Address: Via Canneti 17, 46010 Curtatone (MN), Italia
Phone: +39 3491262086
Email: marco.milioli@nemo.unipr.it
      marco.milioli@studenti.unipr.it

Education

Period: Sept. 2001- July 2006
Institute: Istituto tecnico industriale statale "E. Fermi", Mantova, Italy
Level classification: Diploma di Perito chimico industriale

Period: Oct. 2006 - Oct. 2009
Institute: University of Parma
Level classification: First Level Degree in Chemical Sciences and Technology
Semester Thesis: "A possible hydrogen bonding accepting power scale for anions"
Supervisor: Prof. Daniele Cauzzi
Final score: 100/110

Period: Oct. 2009 - Oct. 2011
Institute: University of Parma
Level classification: Second Level Degree in Chemistry
Master Thesis: "Aqueous solution preparation of nano-particles polymer embedded"
Supervisor: Prof. Daniele Cauzzi
Final score: 110/110

Languages

Mother tongue: Italian
Other languages: English

UNDERSTANDING		SPEAKING		WRITING
Listening	Reading	Spoken interaction	Spoken production	
B2	B2	B2	B2	C1

Levels: A1/2: Basic user - B1/2: Independent user - C1/2 Proficient user
Common European Framework of Reference for Languages

Working experiences

Period: Gen. 2015 – ongoing
Company: Chiesi Farmaceutici S.p.a. – R&D Unit
Main activities and responsibilities: Development of mass spectrometry-based analytical methods for screening and targeted pharmaceutical compounds analyses.

Period: Gen. 2012 – Dec. 2014
Company: University of Parma
Main activities and responsibilities: PhD. student in chemical sciences. Development and validation of mass spectrometry-based analytical methods for food and biomedical applications. Mass spectrometry analysis of small molecules and polymers.
Supervisor: Prof. Maria Careri

Period: Oct. 2013 - May 2014
Company: University of Southern Denmark
Main activities and responsibilities: Visiting PhD. student. Mass spectrometry-based proteomics analysis of blood micro-particles. Investigation of protein post-translational modifications and protein interactions. Development of new tags for large-scale proteomics.
Supervisor: Prof. Martin R. Larsen

Skills

Computing skills: Bioinformatic tools for protein analysis such as Bioworks and Proteome Discoverer (Thermo), mass spectrometry and chromatography tools such as Xcalibur (Thermo), Chromeleon (Dionex-Thermo) and Chemstation (Agilent), good command of Microsoft office tools (Word, Excel and PowerPoint) acquired through university, training, seminars and work.

Communication and organizational skills: Good communicative and team working skills gained during the period abroad, the years of university and the supervision of bachelor and master students.

Conference contributions and courses attended

Oral presentation: <u>M. Mattarozzi</u>, M. Milioli, C. Cavalieri, F. Bianchi, M. Careri, Rapid desorption electrospray ionization-high resolution mass spectrometry method for the analysis of melamine migration from melamine tableware, XXIII Congress of the Division of Analytical Chemistry (Italian Chemical Society), Biodola (LI), Italy, 16-20 September 2012

Poster presentation: <u>M. Milioli</u>, M. Ibáñez-Vea, M. Careri, M. R. Larsen, Quantitative comparison of the proteome and PTM-ome of platelet derived microparticles using different agonist stimulations, 10th Siena Meeting: From Genome to Proteome, Siena, 31 August-4 September 2014

School attendance: School of Analytical and Bioanalytical techniques in Mass Spectrometry, Parma, Italy, 14-18 Maggio 2012

Publications

- M. Mattarozzi, M. Milioli, C. Cavalieri, F. Bianchi, M. Careri, Rapid desorption electrospray ionization-high resolution mass spectrometry method for the analysis of melamine migration from melamine tableware, *Talanta, 101 (2012), 453-459*

- M. Mattarozzi, M. Milioli, C. Bignardi, L. Elviri, C. Corradini, M. Careri, Investigation of different sample pre-treatment routes for liquid chromatography–tandem mass spectrometry detection of caseins and ovalbumin in fortified red wine, *Food Control, 38 (2014), 82-87*

- M. Milioli, M. Ibanez-Vea, S. Sidoli, G. Palmisano, M. Careri, M. R. Larsen, Quantitative proteomics analysis of platelet-derived microparticles reveals distinct protein signatures when stimulated by different physiological agonists, *J. Proteomics*, Submitted

References

Prof. Maria Careri (Head of the Department, Full Professor of Analytical Chemistry, Department of Chemistry, University of Parma), careri@unipr.it

Prof. Daniele Cauzzi (Associate Professor of Inorganic Chemistry, Department of Chemistry, University of Parma), cauzzi@unipr.it